MEMORANDUM REPORT BRL-MR-3597

BLAST PARAMETRIC STUDY USING A 1:57 SCALE SINGLE DRIVER MODEL OF A LARGE BLAST SIMULATOR

GEORGE A. COULTER

JUNE 1987

US ARMY BALLISTIC RESEARCH LABORATORY
ABERDEEN PROVING GROUND, MARYLAND

Destroy this report when it is no longer needed.
Do not return it to the originator.

Additional copies of this report may be obtained from the National Technical Information Service, U. S. Department of Commerce, Springfield, Virginia 22161.

The findings in this report are not to be construed as an official Department of the Army position, unless so designated by other authorized documents.

The use of trade names or manufacturers' names in this report does not constitute indorsement of any commercial product.

REPORT DOCUMENTATION PAGE

Form Approved
OMB No. 0704-0188
Exp. Date: Jun 30, 1986

1a. REPORT SECURITY CLASSIFICATION Unclassified	1b. RESTRICTIVE MARKINGS
2a. SECURITY CLASSIFICATION AUTHORITY	3. DISTRIBUTION/AVAILABILITY OF REPORT Approved for public release; distribution is unlimited.
2b. DECLASSIFICATION/DOWNGRADING SCHEDULE	
4. PERFORMING ORGANIZATION REPORT NUMBER(S)	5. MONITORING ORGANIZATION REPORT NUMBER(S)
6a. NAME OF PERFORMING ORGANIZATION Ballistic Research Laboratory 6b. OFFICE SYMBOL (If applicable) SLCBR-TB-B	7a. NAME OF MONITORING ORGANIZATION
6c. ADDRESS (City, State, and ZIP Code) Aberdeen Proving Ground, MD 21005-5066	7b. ADDRESS (City, State, and ZIP Code)
8a. NAME OF FUNDING/SPONSORING ORGANIZATION USA Harry Diamond Laboratory 8b. OFFICE SYMBOL (If applicable) SLCHD-TI	9. PROCUREMENT INSTRUMENT IDENTIFICATION NUMBER
8c. ADDRESS (City, State, and ZIP Code) Adelphi, MD 20783-1197	10. SOURCE OF FUNDING NUMBERS PROGRAM ELEMENT NO. / PROJECT NO. 1L162120AH25 / TASK NO. / WORK UNIT ACCESSION NO.
11. TITLE (Include Security Classification) Blast Parametric Study Using a 1:57 Scale Single Driver Model of a Large Blast Simulator	
12. PERSONAL AUTHOR(S) Coulter, George A.	
13a. TYPE OF REPORT Memorandum 13b. TIME COVERED FROM Oct 85 TO Sep 86	14. DATE OF REPORT (Year, Month, Day) 15. PAGE COUNT
16. SUPPLEMENTARY NOTATION	

17. COSATI CODES		
FIELD	GROUP	SUB-GROUP
20	04	
20	14	

18. SUBJECT TERMS (Continue on reverse if necessary and identify by block number)
Air Blast, Blast Simulator, BRL-Q1D Hydrocode, Cold Gas, Driver Pressure, Impulse, Overpressure, Shock Tube Model, Scaling Techniques, Simulator Blast

19. ABSTRACT (Continue on reverse if necessary and identify by block number)

A 1:57 scale, single cold air driver model of a large blast simulator was constructed and operated in a driver overpressure range of 300-1800 kPa. Recorded overpressures were in a 10-225 kPa range for the given driver pressures. Blast parameters of overpressure, positive impulse, cold gas arrival and drag enhancement, and recompression fan arrival were measured at stations 7-28 diameters along the test section of the simulator model. The cold gas arrival at the test stations was found to enhance the dynamic drag pressure by a factor of two at the 220 kPa input level. Similar, although larger enhancement was predicted by the BRL-Q1D Code simulation. Effects of driver length, volume, and throat baffle ratio for the full-size simulator operating range are presented in tabular and graphical form. Because of the large cold gas dynamics drag enhancement at test section pressures above 100 kPa, it is recommended that a hot gas driver be used for the full-size simulator. Due to the side-on overpressure positive duration decrease caused by arrival of the throat nozzle recompression fan, a station at 20 test section diameters should be used for the full-scale simulator.

20. DISTRIBUTION/AVAILABILITY OF ABSTRACT ☐ UNCLASSIFIED/UNLIMITED ☒ SAME AS RPT. ☐ DTIC USERS	21. ABSTRACT SECURITY CLASSIFICATION Unclassified
22a. NAME OF RESPONSIBLE INDIVIDUAL George A. Coulter	22b. TELEPHONE (Include Area Code) (301) 278-6719 or 6720 22c. OFFICE SYMBOL SLCBR-TB-B

DD FORM 1473, 84 MAR

83 APR edition may be used until exhausted.
All other editions are obsolete.

The following page is blank.

ACKNOWLEDGMENTS

The author wishes to acknowledge the excellent mechanical design work on the model test section and the stagnation probe installation by Mr. Robert Peterson. Also, to thank Mr. Peter Muller, the electrical engineer in charge of the instrumentation facility, for the setup and operation of the data acquisition system. Also, Mr. Gerald Bulmash and Mr. John Simansky for their help in the data processing from analog to digital form for plotting and analysis with the BRL-Q1D code.

TABLE OF CONTENTS

LIST OF ILLUSTRATIONS

LIST OF TABLES

1. INTRODUCTION

1.1 Background. The work being reported is part of a current research task at the Ballistic Research Laboratory (BRL) to design a large blast/thermal simulator for multiservice use. The simulator is to be large enough to conduct full-size vehicle tests throughout a broad spectrum of blast/thermal effects, simulating a range of blast and thermal from nuclear environments. The simulator facility is to be similar to the French facility of Gramat (Reference 1), but is to have expanded operational capabilities, both in size and in the simulation ranges. Previous phases of the task at BRL have been reported in Reference 2, 3, and 4.

1.2 Objectives. The experiments reported here were designed to answer some questions concerning the basic shock parameters necessary to the design of the full-size blast simulator. These parameters are: the test station pressure as a function of driver pressure, the driver length/volume needed to produce the desired range of yields, the cold gas driver effect, and the effect of the recompression fan from the expansion of the divergent throat nozzle. These effects were to be examined both experimentally and by hydrocode simulation. References 2, 4, and 5 describe the BRL-Q1D hydrocode used for the computer simulation.

2. TEST PROCEDURES

The experimental parameter study task consisted first, of the design and fabrication of a 1:57 scale, single cold air driver model of the anticipated full-size blast simulator; secondly, of a selection of a range of driver/throat baffle configurations to produce the desired test pressure/yield levels, and to record the pressure-time results as a function of test section location. The model is described in the next section.

2.1 Simulator Model. The 1:57 scale for the model was chosen for the experiments, primarily because of the ready availability of the steel pipe components of the simulator model. A sketch of the shock tube model is shown in Figure 1. The drivers consisted of assorted lengths (6.05-288.0 cm) of 10.16 cm inside diameters, smooth thick-walled pipe. This was attached to the long test section (.254 I.D. by 17.14 m long - closed at end) through a converging throat or baffle to the diaphragm section. A diverging section expanded to near the inside diameter of the test section. Cold compressed air was used for the driver gas. Mylar, aluminum, and copper diaphragms were used to contain the monitored driver pressure until the diaphragm self-ruptured.

Stations for pressure transducers (side-on and stagnation probes) were located along the test section at 7, 15, 20, 24, and 28 test section diameters as noted on the drawing in Figure 1. The stations are listed on the pressure-time plots as 70-280, respectively, in the Results section.

The recording and data reduction instrumentation is described in the next section.

2.2 Instrumentation. Two separate sets of recording instrumentation were used for the experimental shots. Figures 2-A and 2-B describe the two

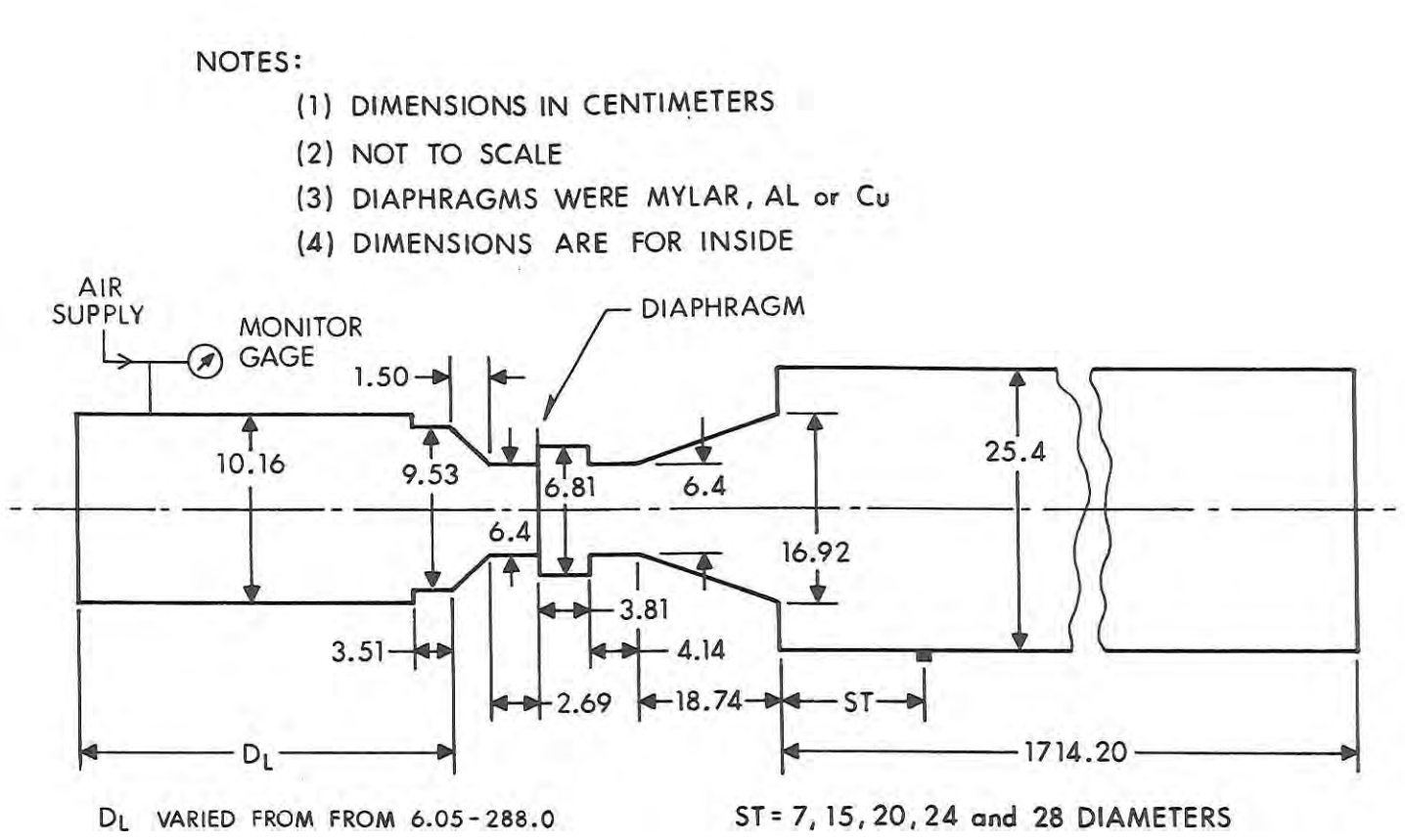

Figure 1. Sketch of 1:57 Scale Single Driver Model of Large Blast Simulator.

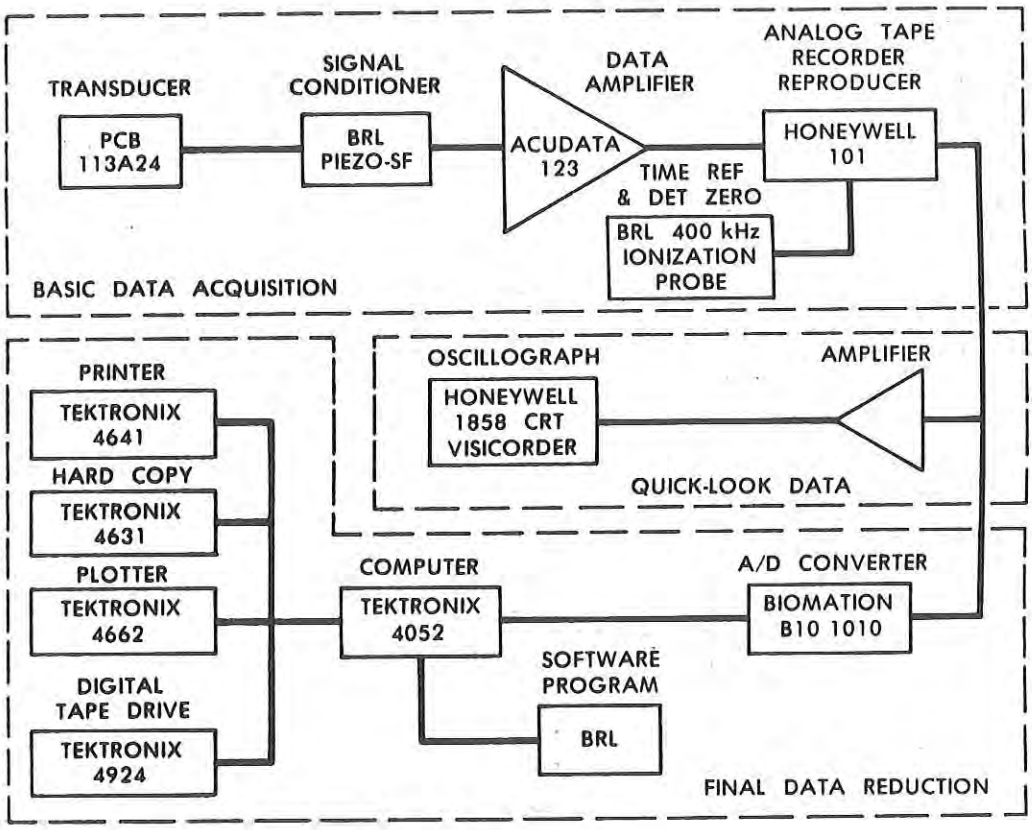

A. Tape System

Figure 2. Schematic of Data Acquisition/Reduction Systems.

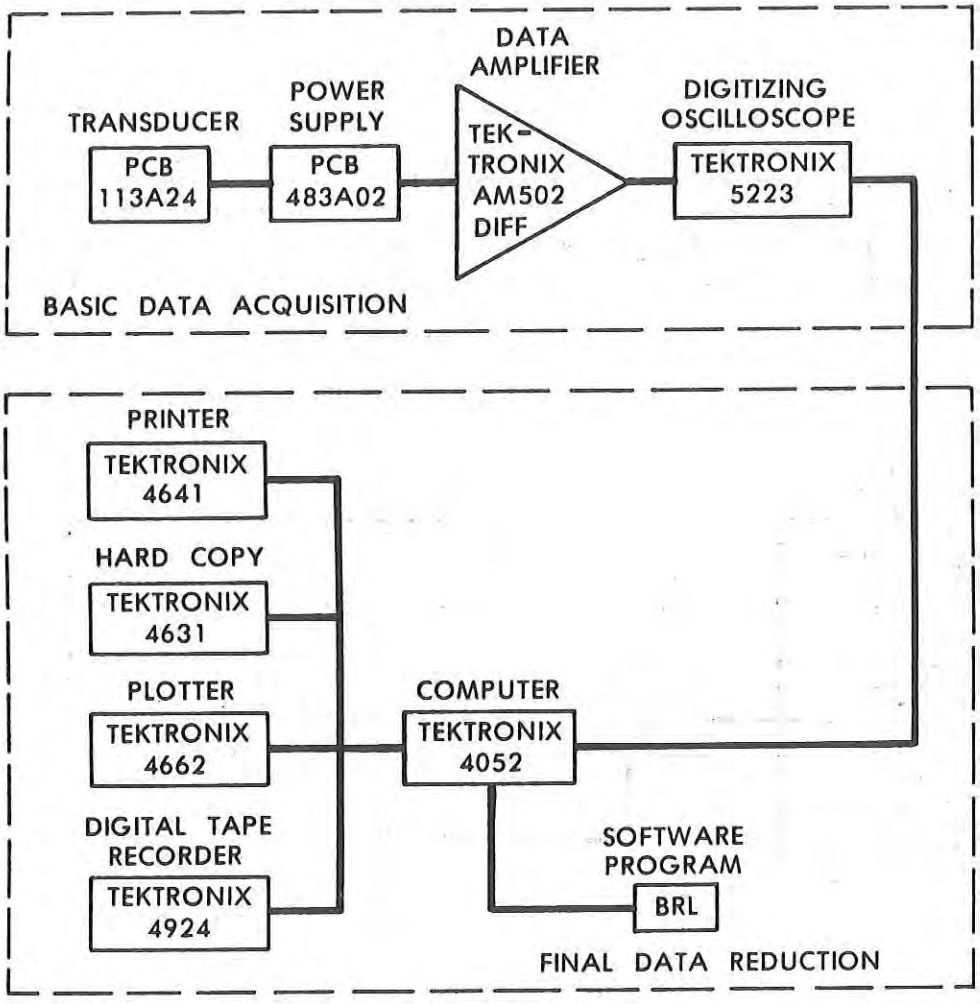

B. Oscillograph System

Figure 2. Schematic of Data Acquisition/Reduction Systems (Cont'd).

types used. Both were used to record the output generated by the PCB Model 113A24 quartz pressure transducers (Reference 6). The tape recording systems (Figure 2-A) was used for the initial multi-station recording. Later in the test program only two stations were used, so the second system (Figure 2-B) with the digitizing oscilloscope was used.

Both systems recorded the output from the transducers coupled through power supply interface cards and data amplifiers to the recorders. On-site comparisons of the pressure-time plots were made directly from the hard copies produced. Final data processing was completed with the computer, printer, and plotter. Plots of pressure-time records for various driver configurations are shown in the Results section.

2.3 Test Matrix. A variety of shots were fired with the various driver configurations. The test matrix is given in Table 1 for several shot conditions. The shots are listed by number, with driver parameters, ambient test conditions, and test section overpressure at Station 70 (7 dia.) listed for reference.

The driver lengths varied from a minimum of 6.05 cm to 288 cm for the maximum "long" driver. The inside diameter of the drivers remained constant at 10.16 cm. The pressure in the driver varied from about 300 kPa to a little over 18000 kPa. Throat baffles at the diaphragm section varied from a test section to throat baffle area ratio of 16.1 to 64:1. Sample pressure-time records and a discussion of their characteristics are given in the Results section.

3. RESULTS

The primary results from the test program are the pressure-time records and their impulses from the test stations for the various test configurations. This section will discuss the change of pressure-time records (side-on, stagnation, and dynamic) as the driver parameters were changed. Stations at 7 and 20 diameters, in particular, will be compared with computer code predictions. Both short (11.16 cm) and long (288 cm) drivers will be used for the comparisons. Finally, particular examples of cold gas/recompression fan effects will be shown.

3.1 Test Station Pressure as a Function of Driver Parameters. The first set of records shown in Figure 3-6 illustrate the decay of peak pressure along the test section for a short driver (11.12 cm) as a function of driver pressure. The driver pressure was varied within the range 314 kPa to 14479 kPa for this series of shots. These values are plotted in the graph of Figure 7. Initial test section pressures (20-225 kPa) measured at 7 diameters decay with distance along the test section to a station at 28 diameters. Decays of about 25 to 43% were measured over this distance. The hydrocode predicted similar decays, but for driver pressure above 3000-4000 kPa the predicted shock overpressure was higher than the experimental values. Below this driver range the predicted values varied both above and below the experimental values.

It can be seen from the family of curves plotted from the long driver data and shown in Figure 8, that there is very little attenuation of the

The text is continued on page 21.

TABLE 1. TEST MATRIX

Shot Number	Driver Pressure kPa	Driver Length cm	Test Section to Throat Area Ratio	Ambient Pressure kPa	Ambient Temperature ^{o}k	Shock Overpressure Station 70 kPa
4	314	11.13	16:1	102.4	294.8	20.0
5	617			102.3	295.0	32.6
6	1124			102.2	295.2	49.3
7	2055			102.1	296.6	75.0
8	3137			102.1	297.1	96.6
9	4413	Same	Same	101.9	296.0	118.2
10	5240			103.2	292.9	137.0
11	7757			103.3	294.2	169.6
12	11273			103.3	294.2	188.0
13	14479			103.3	295.4	225.0
14	5171	288	16:1	102.9	295.2	131.5
15	7481			102.2	297.9	155.0
16	3103			102.2	297.7	88.0
17	603			102.2	297.7	23.5
18	300			102.2	298.1	13.3
19	1138	Same	Same	102.0	297.7	38.0
20	2034			101.9	297.5	60.4
21	4220			102.0	297.0	106.5
22	10963			102.0	297.3	193.0
23	13169			101.7	297.7	215.0
29	1103	11.13	64:1	102.5	297.2	29.2
30	2034			102.5	297.4	39.1
31	3103			102.3	298.2	56.6
32	8618			102.5	297.5	107.0

TABLE 1. TEST MATRIX (CONT'D)

Shot Number	Driver Pressure kPa	Driver Length cm	Test Section to Throat Area Ratio	Ambient Pressure kPa	Ambient Temperature ^{o}k	Shock Overpressure kPa
33	565	11.13	33:1	102.2	297.9	26.1
34	1069			102.2	298.3	36.2
35	2027			102.2	297.5	54.3
36	3130			102.2	297.6	74.2
37	5192	Same	Same	102.2	298.1	99.6
38	8618			102.2	298.8	137.2
39	10515			102.6	298.9	156.2
40	14479			102.6	298.6	195.3
45	13617	26.36	16:1	102.1	298.6	217.9
46	13962	33.98	16:1	102.0	298.9	205.5
47	317			101.1	297.5	18.3
48	579			101.1	297.2	27.0
49	1096			101.0	296.5	43.5
50	2054			101.0	296.5	76.0
51	607	67.0	64:1	102.5	298.5	16.3
52	690	89.86	64:1	102.5	298.5	22.8
53	338		16:1	101.7	297.6	14.6
54	710		64:1	101.5	297.1	15.5
55	359	178.76	16:1	101.4	297.0	14.3
56	359	206.70		102.2	296.7	13.3
57	352	237.18		102.2	297.5	13.2
58	614	125.42	64:1	102.2	296.6	10.0
59	324		16:1	102.2	297.9	17.9
60	703		64:1	102.6	296.7	10.0
61	896		33:1	102.6	296.7	20.0
62	717		33:1	102.5	296.7	20.0
63	510		33:1	102.7	296.7	15.0

TABLE 1: TEST MATRIX (CONT'D)

Shot Number	Driver Pressure kPa	Driver Length cm	Test Section to Throat Area Ratio	Ambient Pressure kPa	Ambient Temperature °k	Shock Overpressure kPa
64	17754	33.98	16:1	102.6	296.4	262.0
65	17582	6.05		102.5	296.4	200.0
66	13962	18.74		102.2	298.0	222.7
67	13962	26.36	Same	102.1	297.9	224.8
68	14307	33.98		102.0	298.0	237.5
69	3137			102.1	298.0	106.5
70	5171			102.1	298.0	147.2
71	8446			102.2	298.1	180.0
72	11549			102.2	298.0	225.0
73	13445	102.57		103.0	298.0	220.0
74	13169	72.09		103.0	298.4	221.3
75	3137	72.09		103.0	297.9	110.0
77	3123	110.18	16:1	103.0	298.1	106.0
78	1117	110.18		102.9	297.8	47.2
79	1124	72.09		102.7	297.9	48.5
80	1145	145.74		102.6	297.6	49.5
81	483	33.99	33:1	101.8	298.4	19.3
82	1827			101.7	298.5	47.5
83	5199			101.7	298.4	103.0
84	14789			101.7	298.4	200.2
85	483	67.01	Same	101.6	298.2	20.0
86	1827			101.6	297.9	46.8
87	5240			101.6	297.9	108.0
88	14651			101.5	297.9	200.0
89	496	94.95		101.7	298.7	14.6
90	1834	94.95		101.6	297.9	40.8
91	545	145.75		101.6	298.0	15.0
92	490	11.13		101.8	297.9	19.5
93	18271	6.05		101.9	298.4	172.5
94	903	74.62	64:1	102.7	298.0	13.8

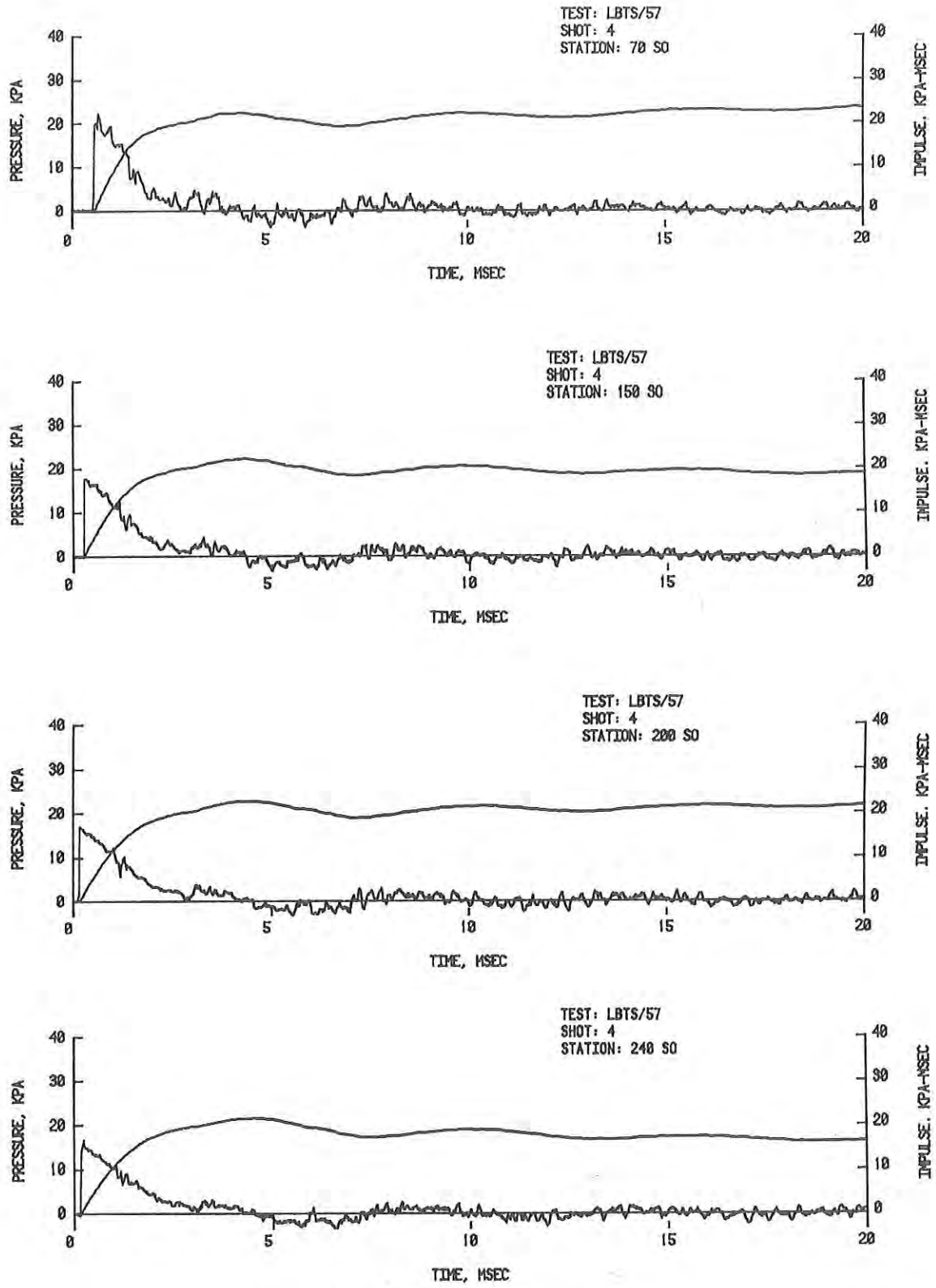

A. Side-On Overpressure

Figure 3. Pressure-Time Records from Test Section - Short Driver, 314 kPa.

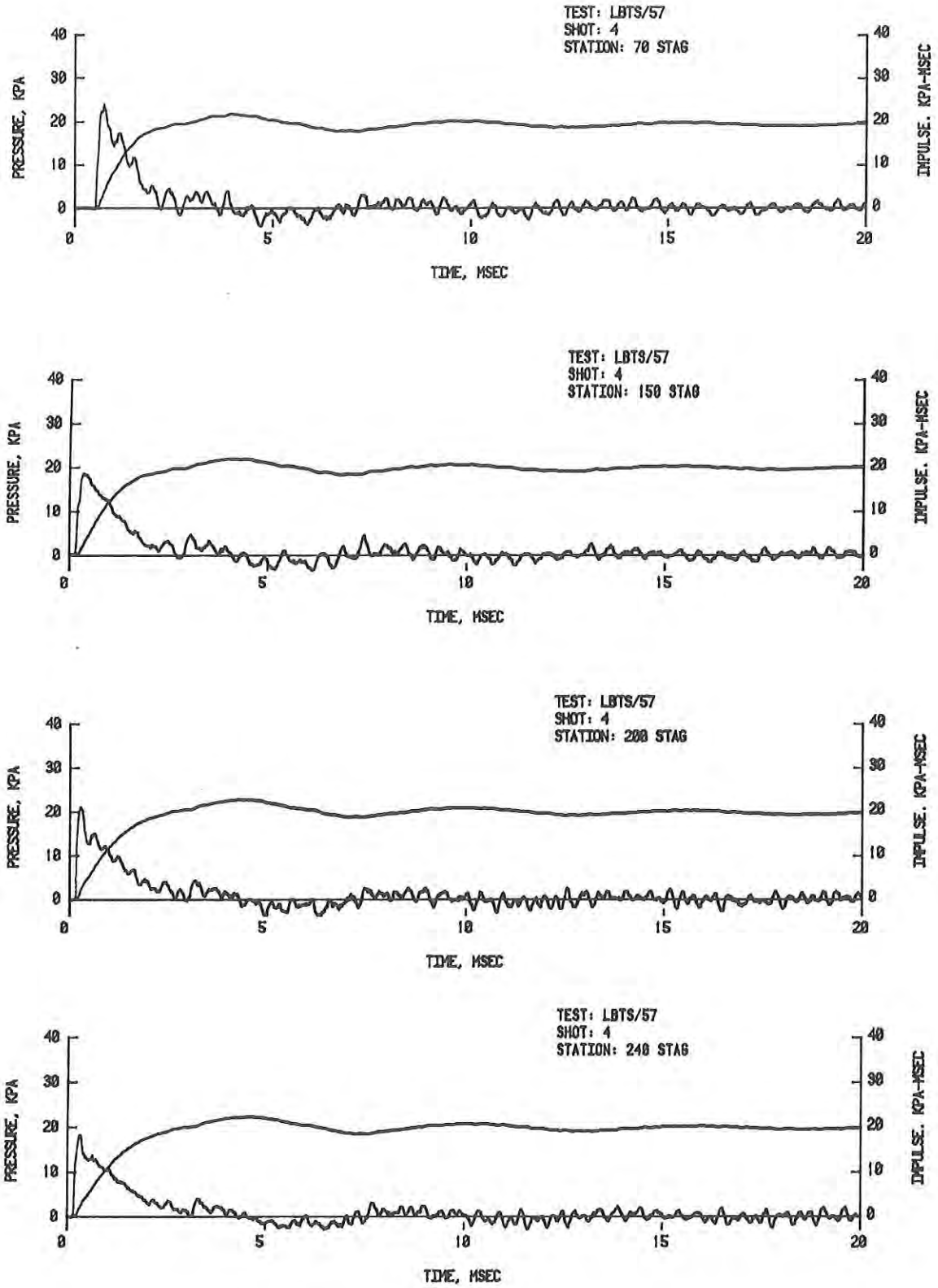

B. Stagnation Overpressure

Figure 3. Pressure-Time Records from Test Section - Short Driver, 314 kPa (Cont'd).

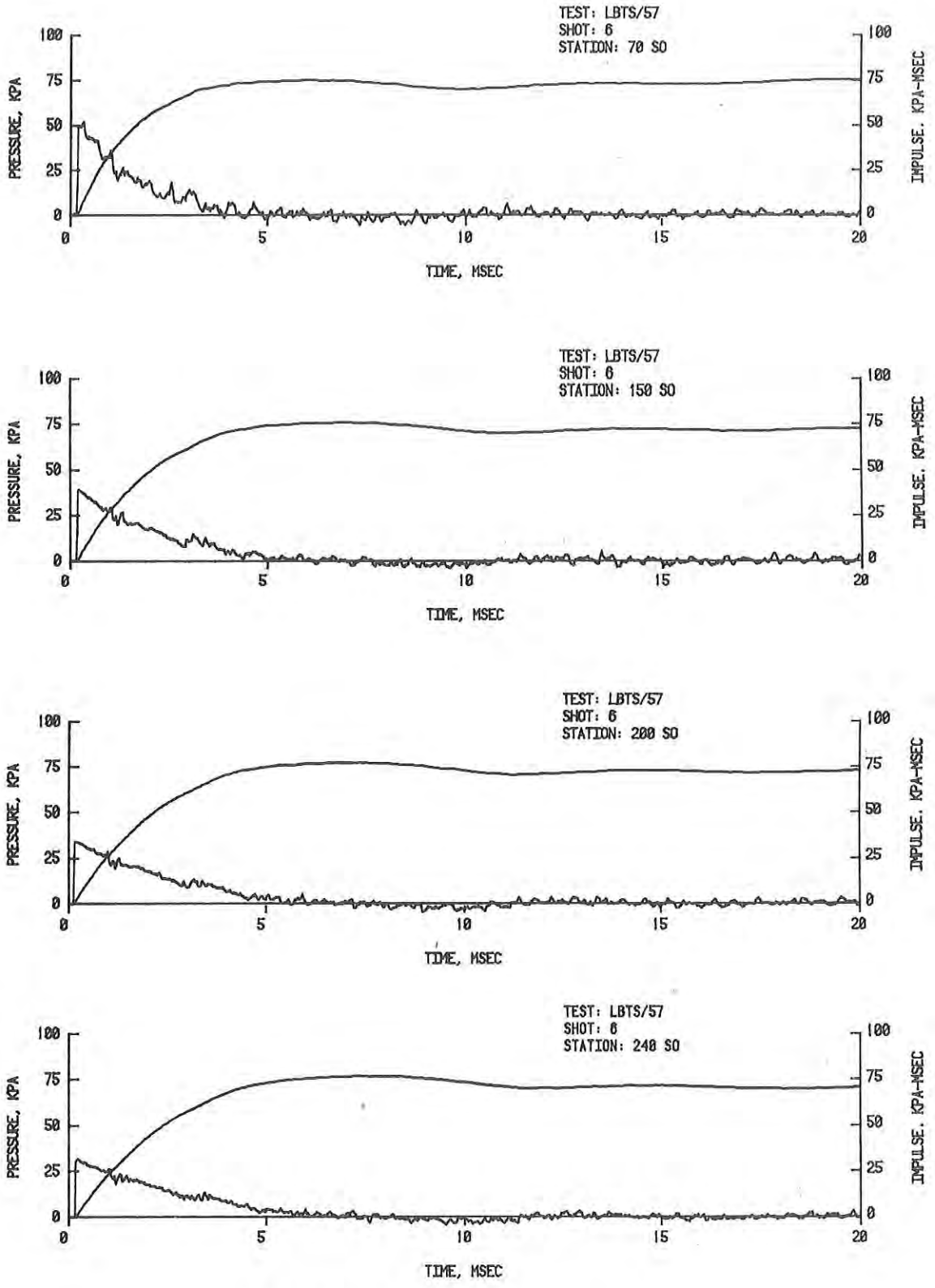

A. Side-On Overpressure

Figure 4. Pressure-Time Records from Test Section - Short Driver, 1124 kPa.

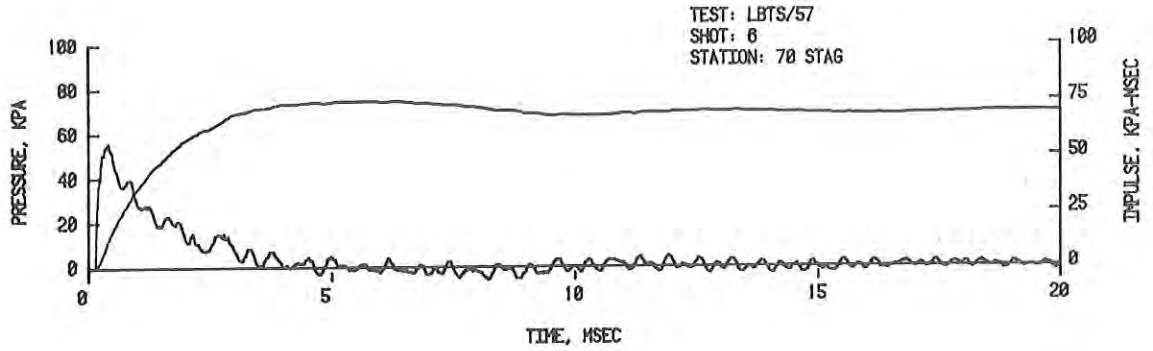

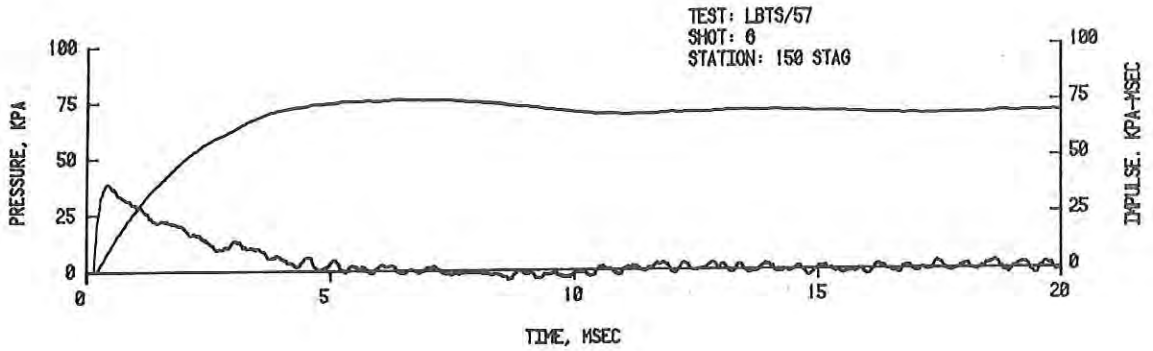

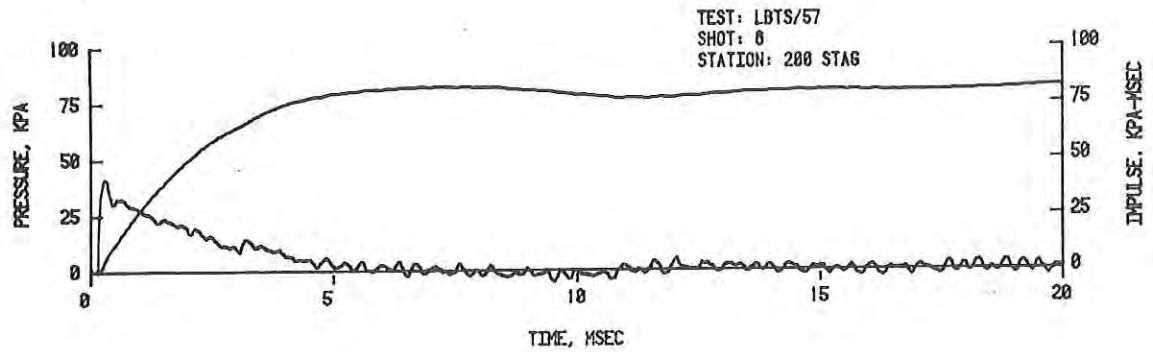

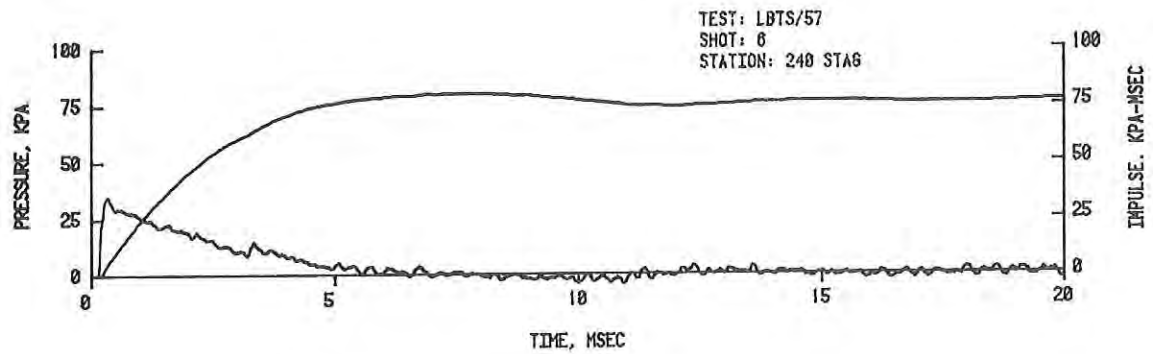

B. Stagnation Overpressure

Figure 4. Pressure-Time Records from Test Section - Short Driver, 1124 kPa (Cont'd).

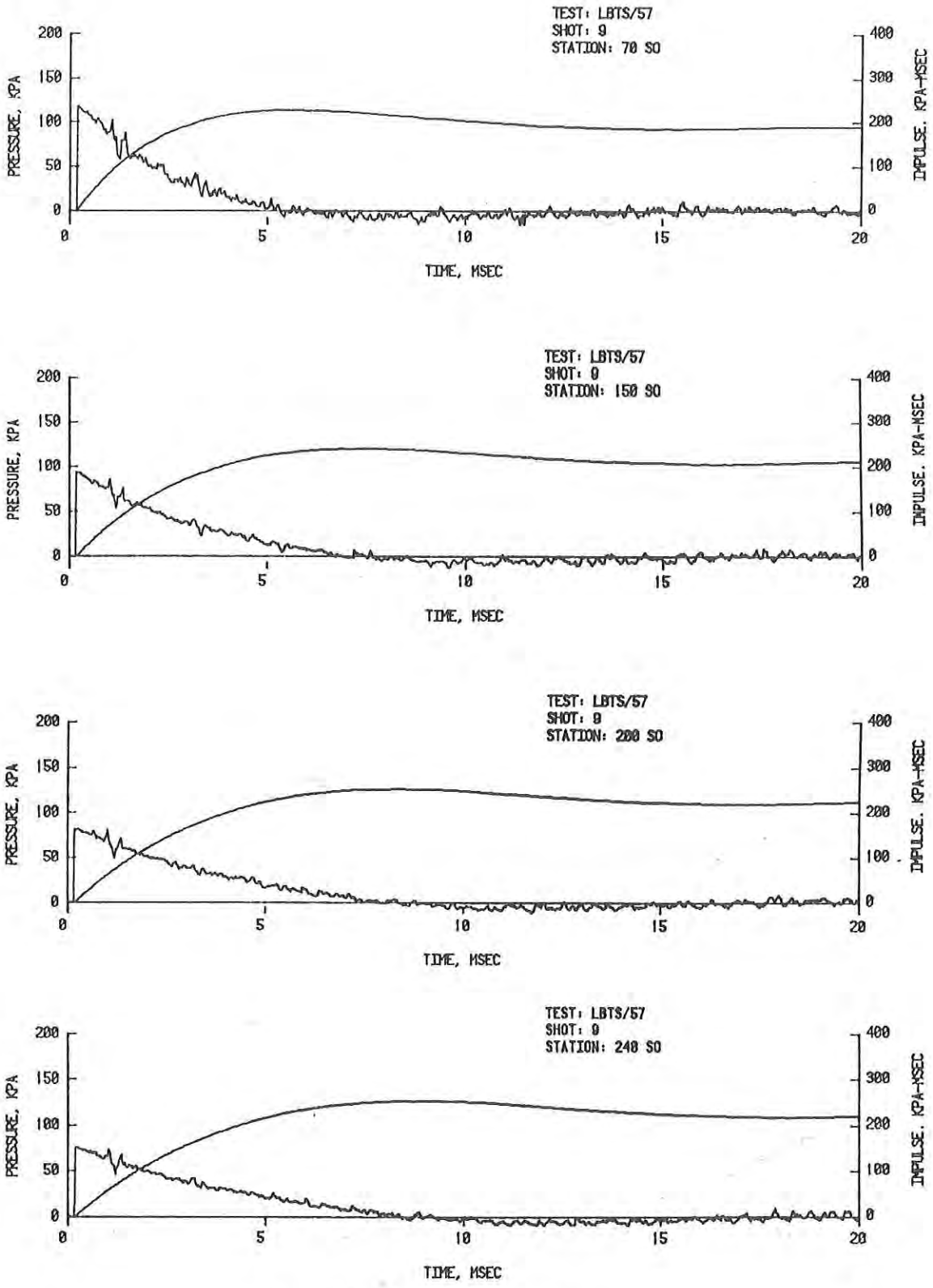

A. Side-On Overpressure

Figure 5. Pressure-Time Records from Test Section - Short Driver, 4413 kPa.

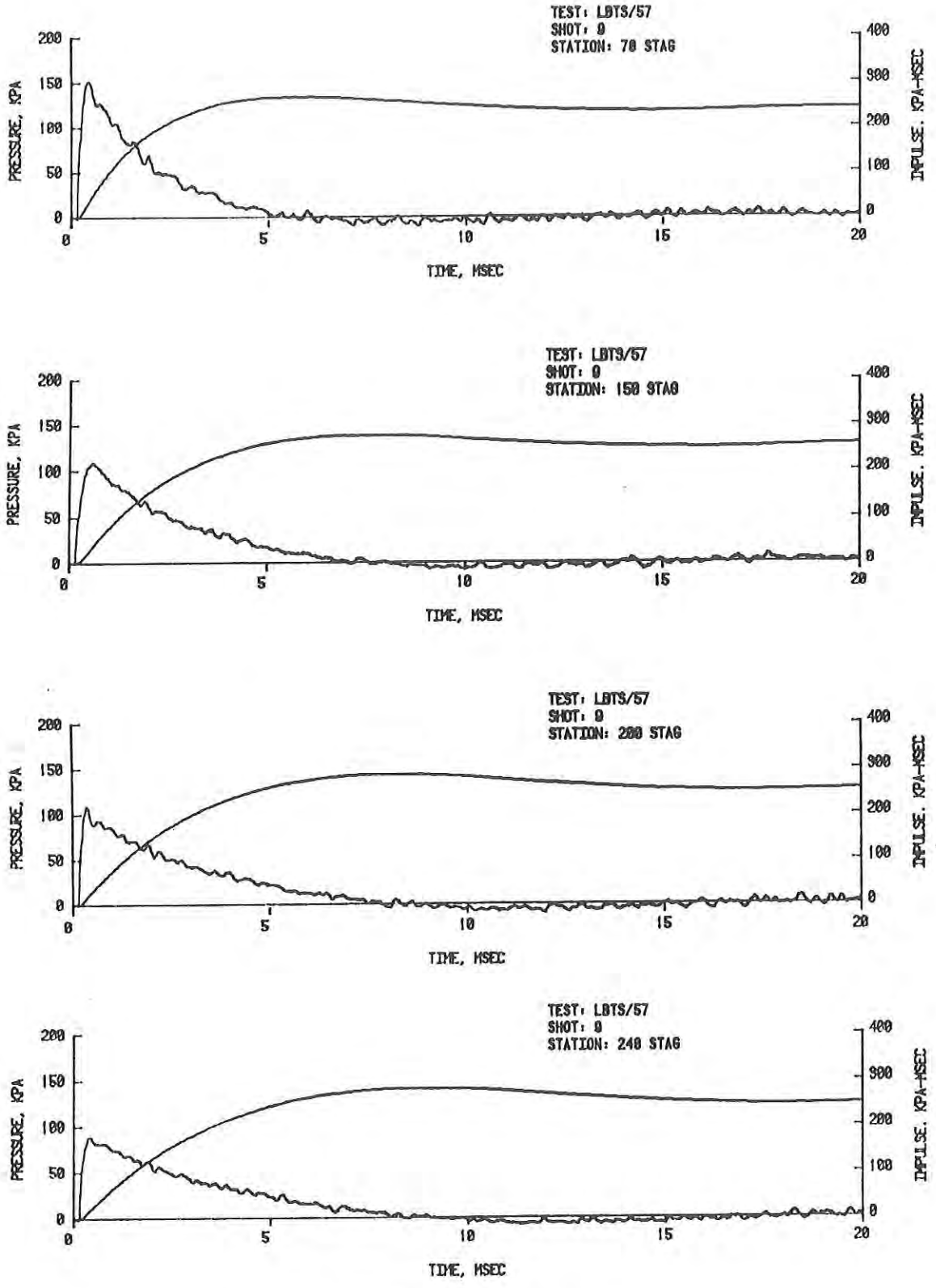

B. Stagnation Overpressure

Figure 5. Pressure-Time Records from Test Section - Short Driver, 4413 kPa (Cont'd).

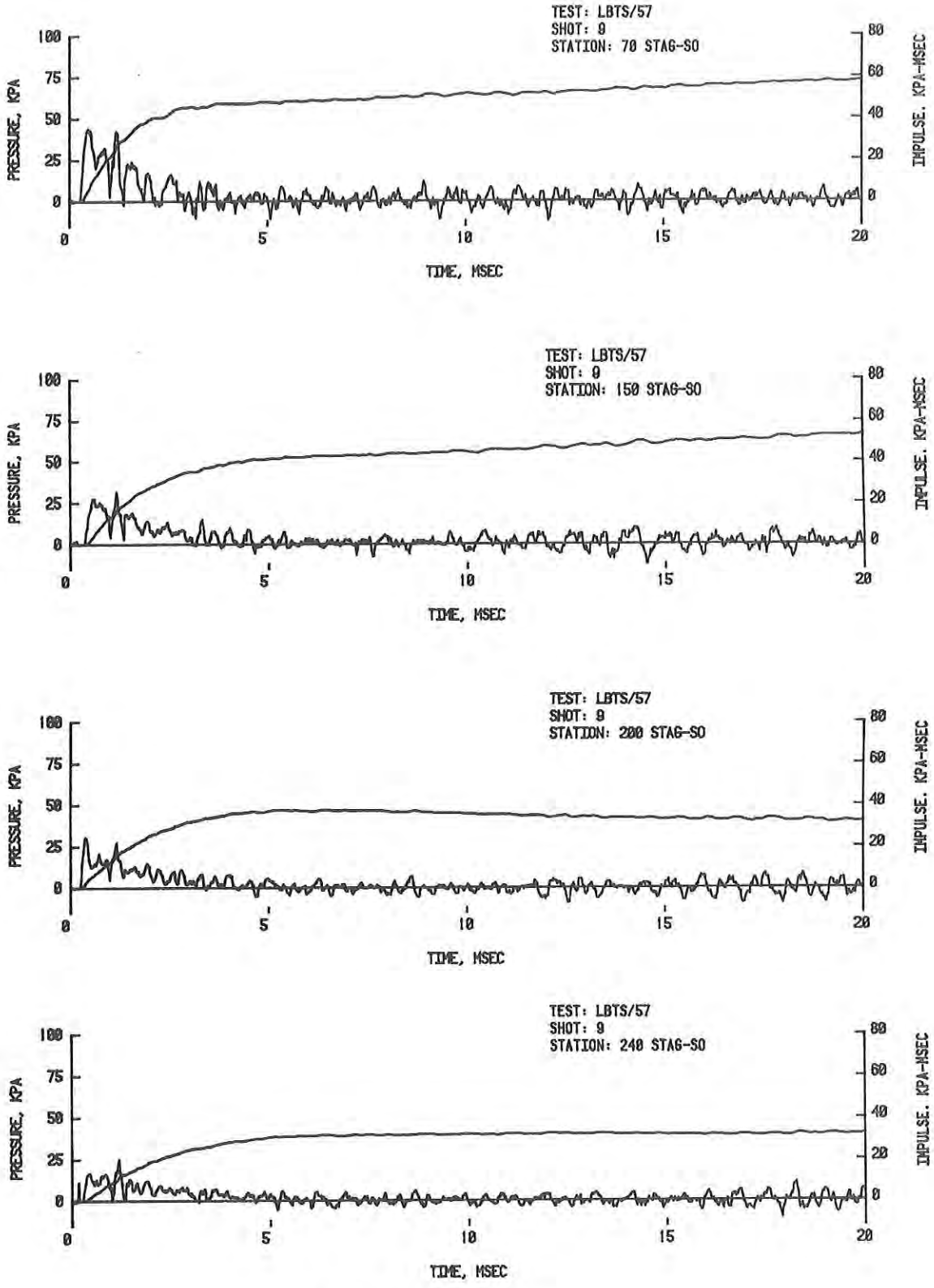

C. Dynamic Pressure

Figure 5. Pressure-Time Records from Test Section - Short Driver, 4413 kPa (Cont'd).

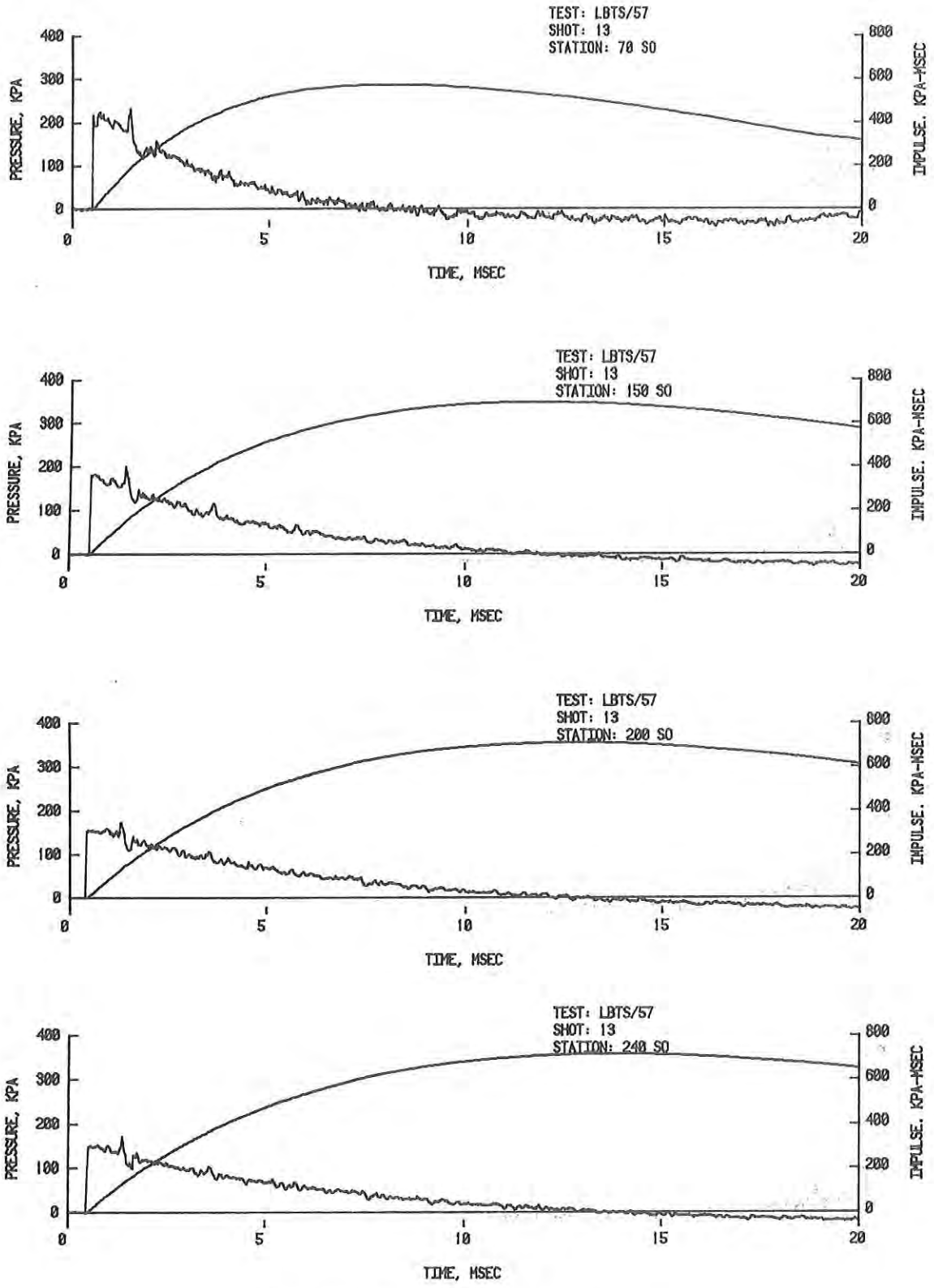

A. Side-On Overpressure

Figure 6. Pressure-Time Records from Test Section - Short Driver, 14479 kPa.

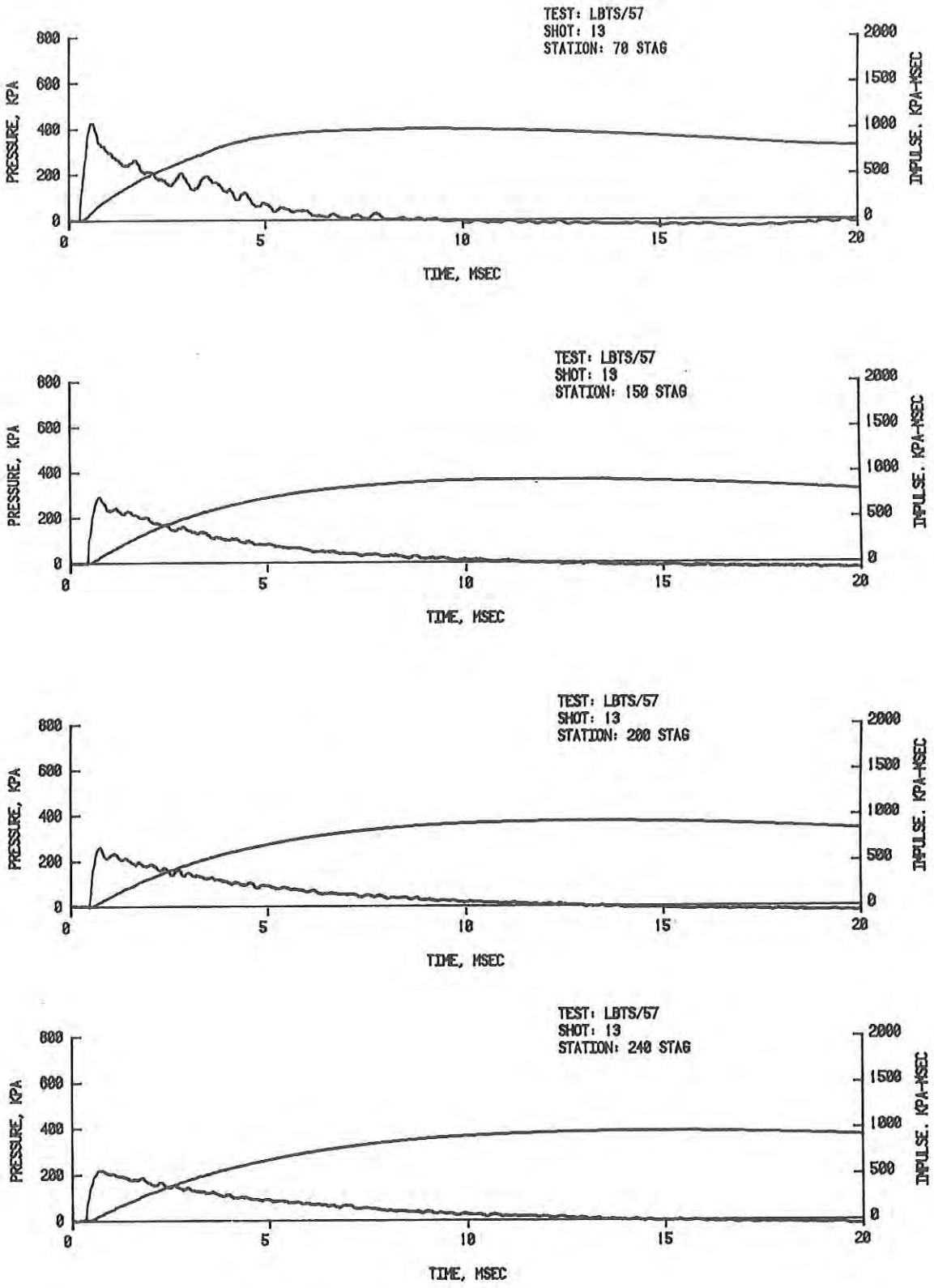

B. Stagnation Overpressure

Figure 6. Pressure-Time Records from Test Section - Short Driver, 14479 kPa (Cont'd).

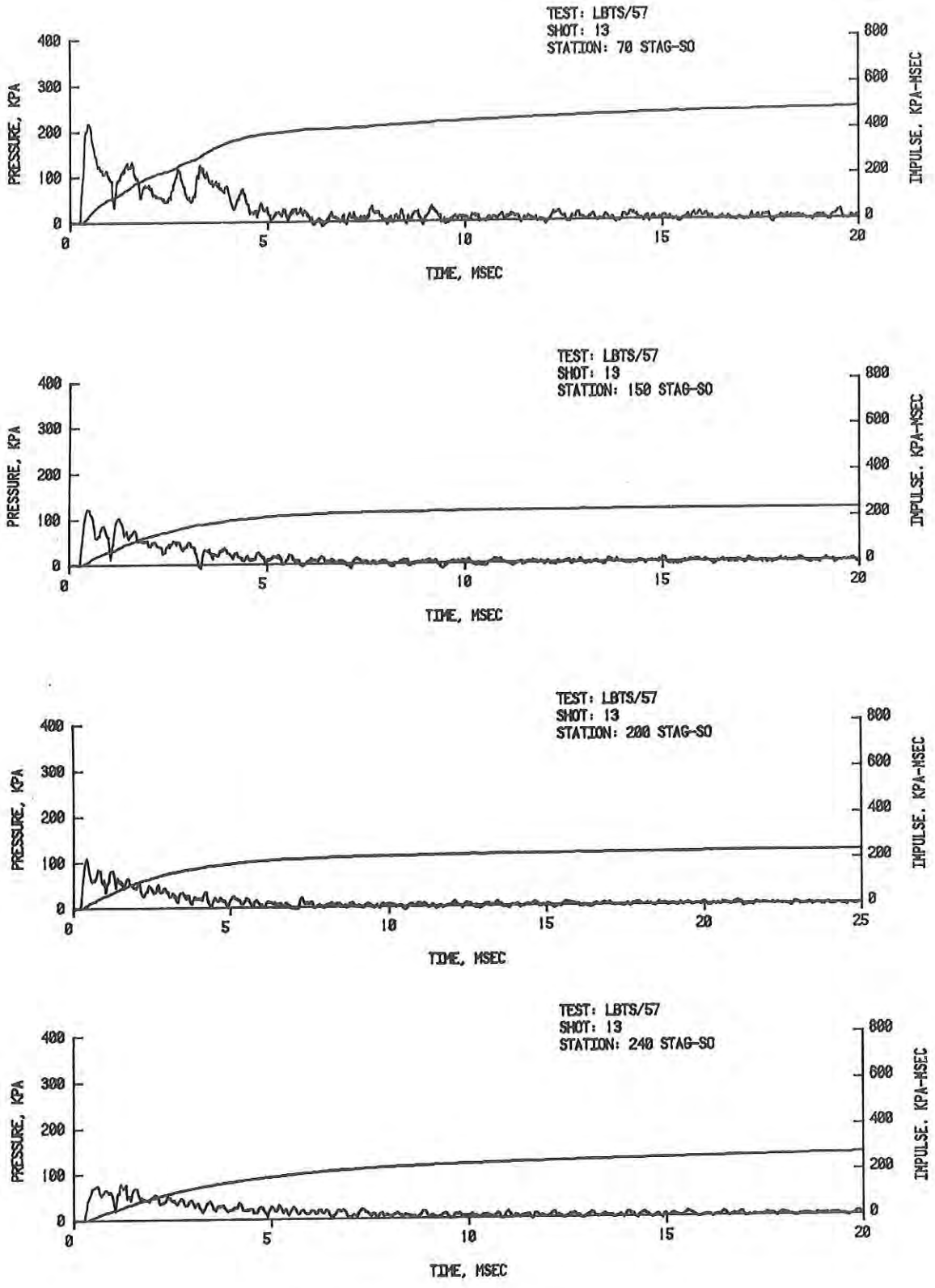

C. Dynamic Pressure

Figure 6. Pressure-Time Records from Test Section - Short Driver, 14479 kPa (Cont'd).

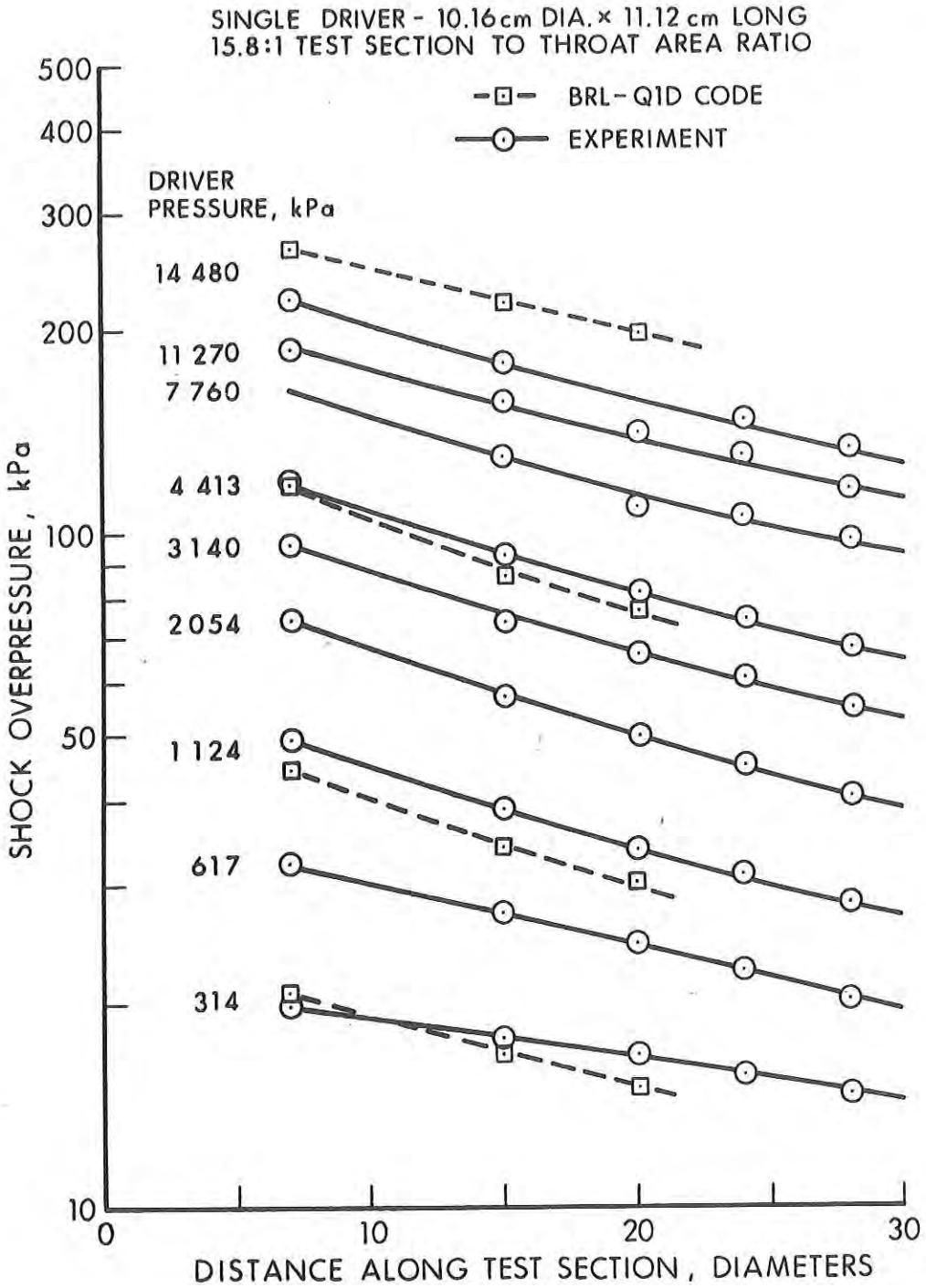

Figure 7. Side-On Shock Overpressure Along Test Section - Short Driver.

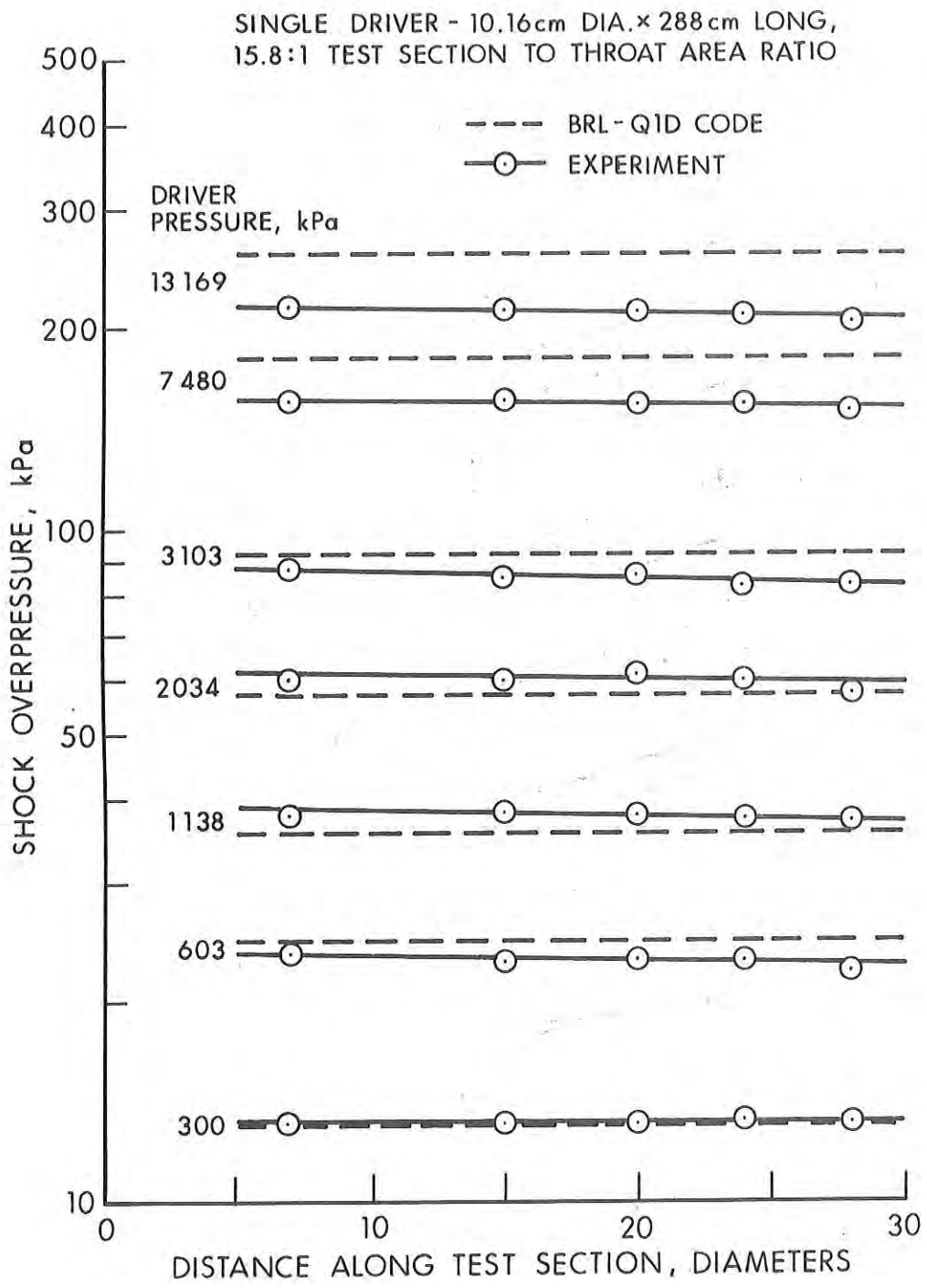

Figure 8. Side-On Shock Overpressure Along Test Section - Long Driver.

overpressure in traveling from 7 to 28 test section diameters since "flat-top" shock waves have only viscous attenuation. The hydrocode has no program for viscous attenuation and, therefore, shows no decay at all.

Figure 9 is an operating curve showing the peak overpressure to be expected at the two important stations (7 and 20 dia.) as a function of the driver pressure. The values plotted in Figures 8 and 9 were taken from the pressure-time records shown in Figures 10-13. Typical examples of pressure-time records of side-on overpessure, stagnation overpressure, and their subtraction (the dynamic pressure) are shown for the long driver of 288 cm.

Generally, between 3000 and 4000 kPa driver pressure, the predicted (computer code simulation) and experimental shock overpressures deviated. At the extreme high end for 13500 kPa, the predicted value of pressure was about 270 kPa. Experimentally, the value was 215 kPa. The lower experimental values may be explained by the thicker diaphragm needed at the higher driver pressures. Opening times are finite. Obviously, there is not a complete diaphragm removal at zero-time as was assumed by the hydrocode. Incomplete breaking of the diaphragm also occurred. All these factors tended to produce lower test section pressures than predicted from the BRL-Q1D code for the 3000-4000 kPa range. Below this range, the predicted values varied above and below the experimental values.

Tables 2-4 summarize the experimental data according to driver length and pressure. Representative values of the blast parameters are given for the two test stations at 7 and 20 diameters. Additionally, scaled-up values of the parameters for the full-size simulator are given in the last four columns of the tables. These values were obtained by multiplying by the scale factor of 57. The last column of the tables display the equivalent high explosive yield for the full-size conditions. The scaling calculations will be discussed in some detail in the Analysis section.

3.2 Hydrocode Results. One of the basic research efforts at BRL is to computationally model shock tube processes. The BRL-Q1D code used for these predictions is an adiabatic, inviscid eulerian computer algorithm adapted at BRL for this purpose. See References 2, 4, 5, and 7 for additional descriptions and uses of the code. All references to hydrocode computations refers to the BRL Quasi-one-dimensional code (BRL-Q1D).

The one-dimensional computational modeling used had the advantages that it was inexpensive to run, had capability to perform parametric studies quickly, and was useful for obtaining good engineering approximations to the simulator design. Its obvious disadvantage was that the one-dimensional analysis was necessarily an approximation. As is seen later, the BRL-Q1D code did predict appearance of the cold driver gas and the recompression fan from the diverging nozzle, but mispredicted the magnitude of both effects and their arrival after the shock front at a particular test station.

Figures 14-17 show typical records obtained for the short driver (11.13 cm). Stations 1, 2, and 3 of the computer runs correspond to Stations 70, 150, and 200 in the experimental records. As noted above in Section 3.1 of the Results, the code predicted higher peak overpressure in the test section for driver pressures in the 3000-4000 kPa range. Below this range,

 The text is continued on page 43.

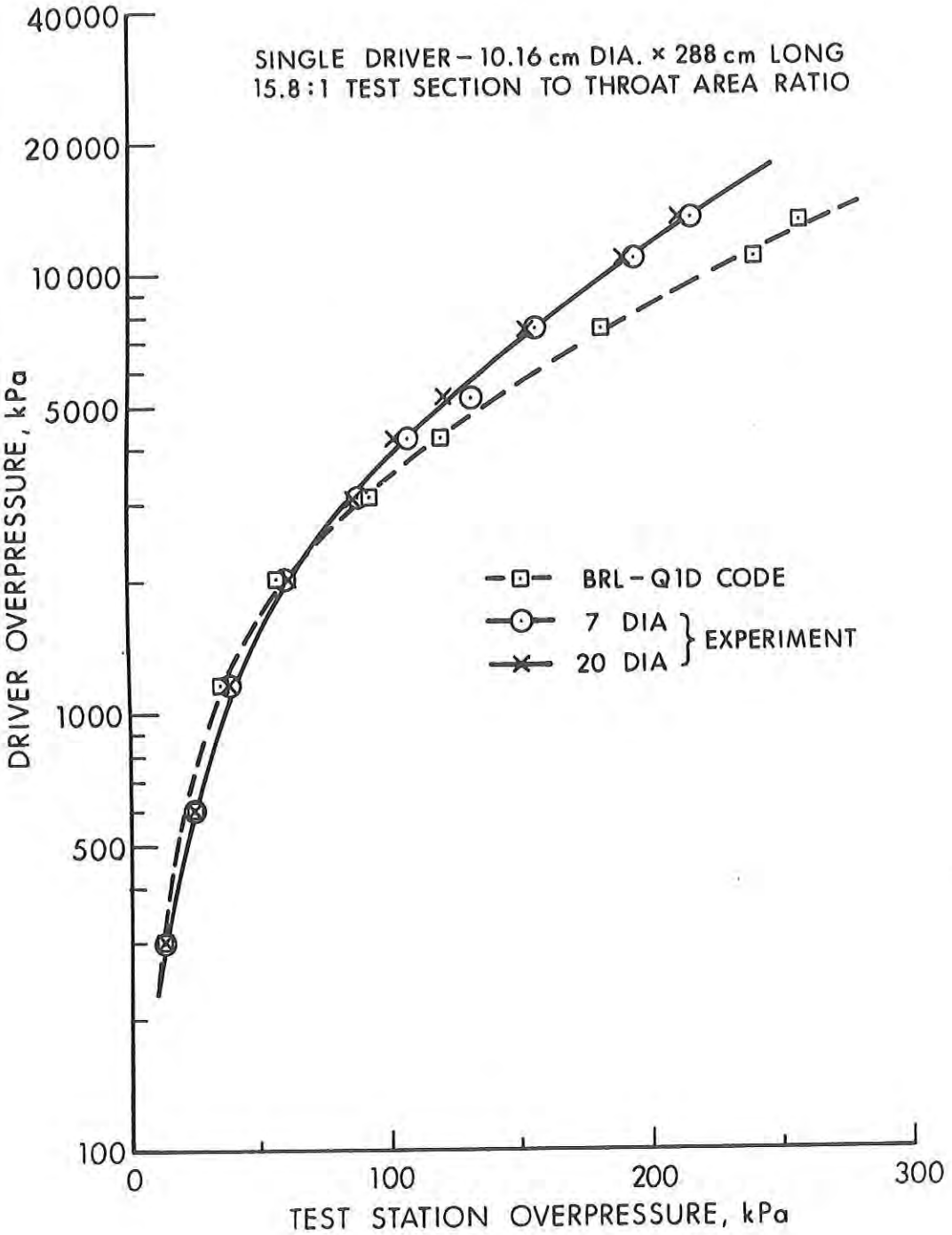

Figure 9. Test Station Overpressure as a Function of Driver Pressure.

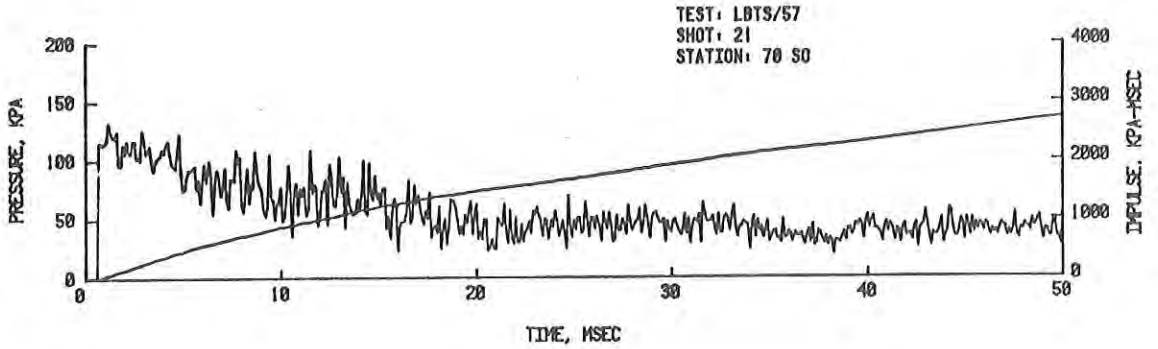

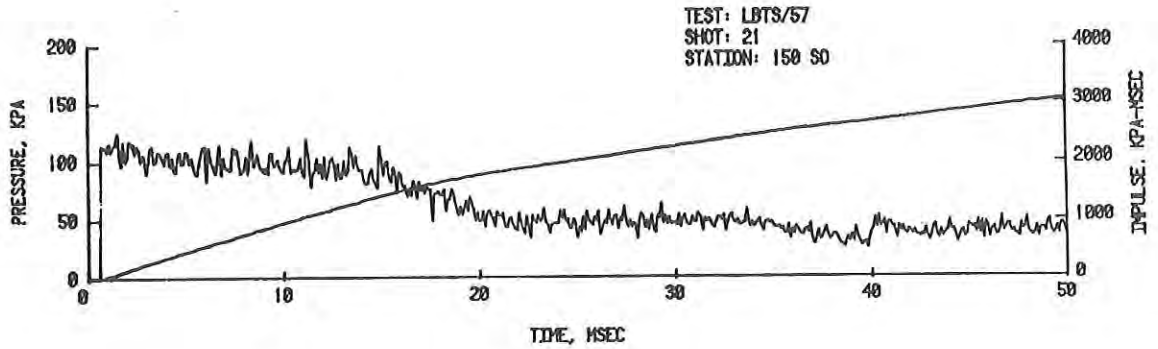

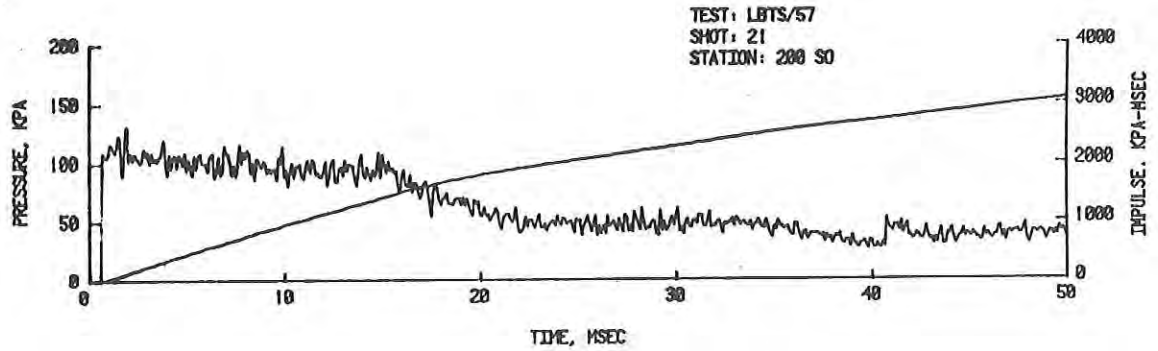

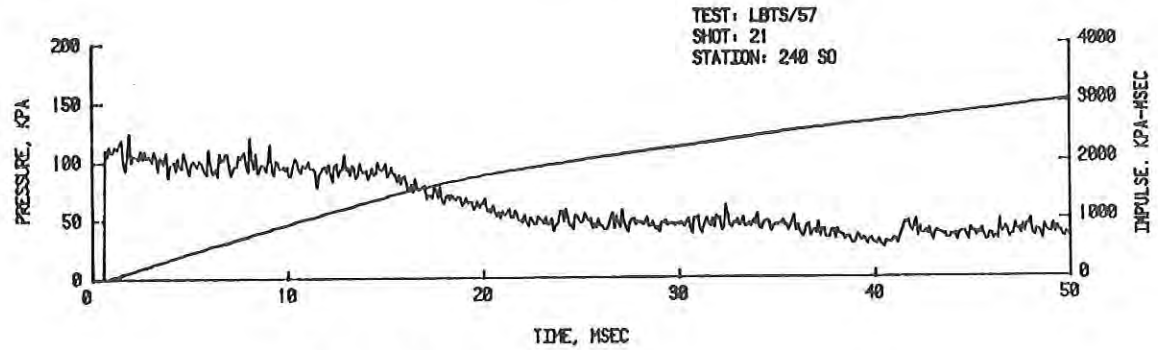

A. Side-On Overpressure

Figure 10. Pressure-Time Records from Test Section - Long Driver, 4220 kPa.

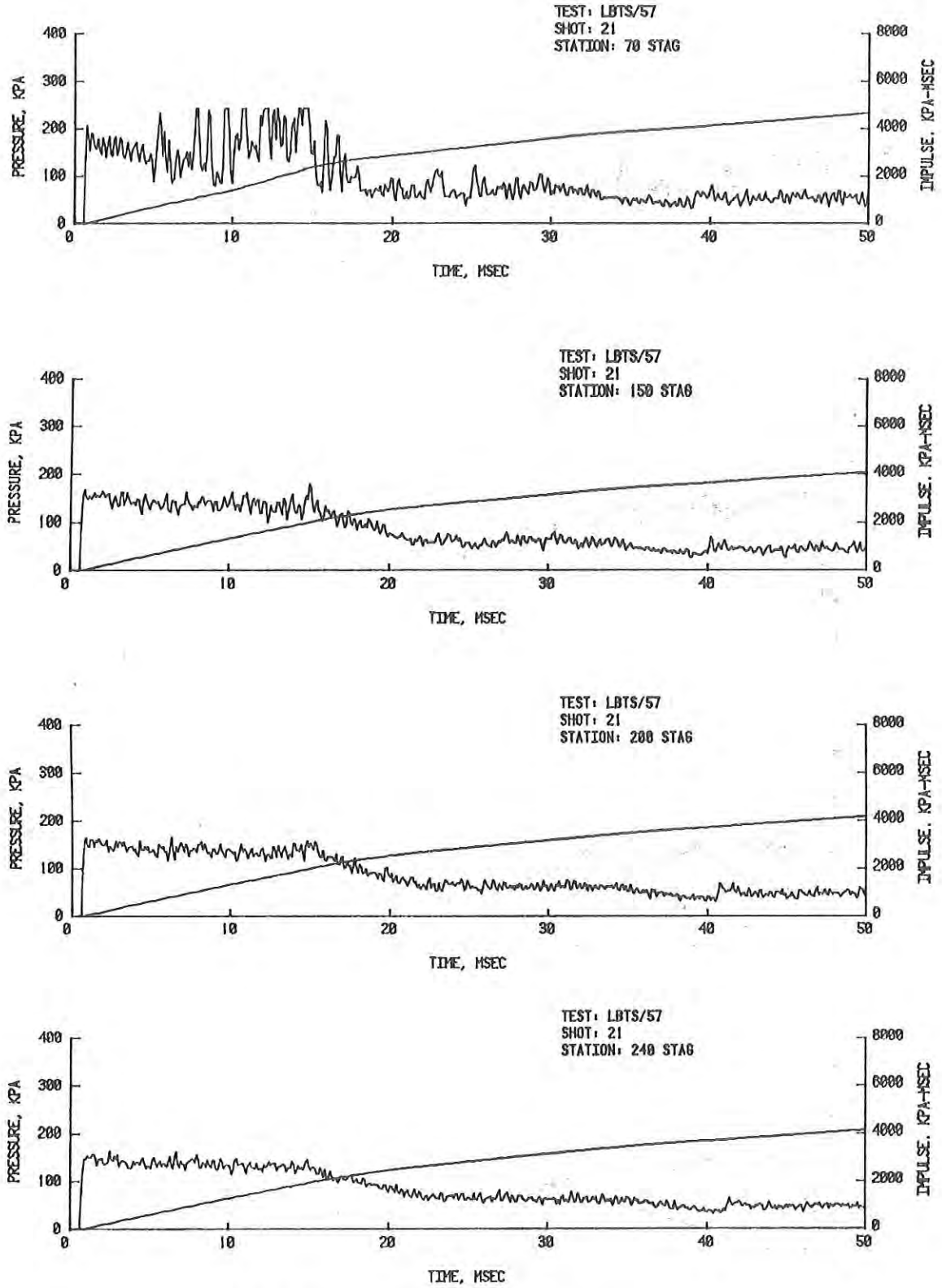

B. Stagnation Overpressure

Figure 10. Pressure-Time Records from Test Section - Long Driver, 4220 kPa (Cont'd).

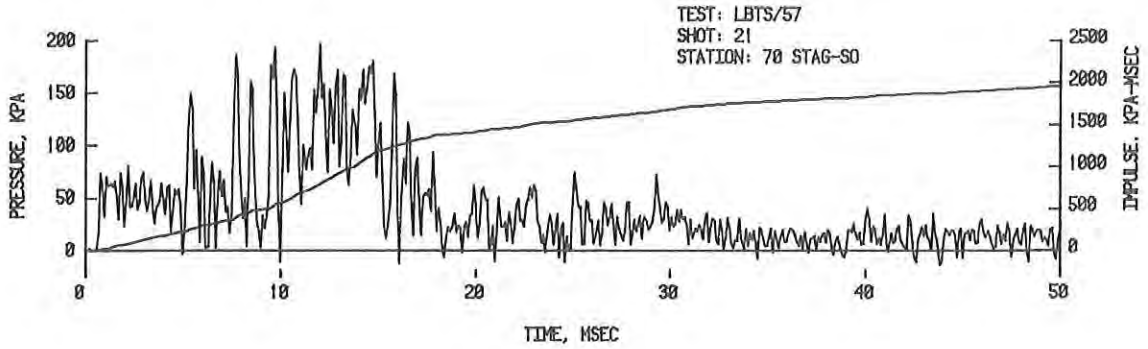

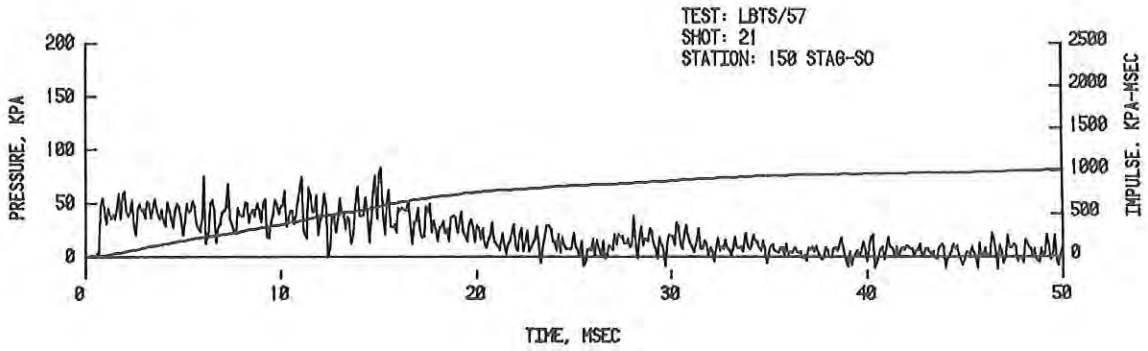

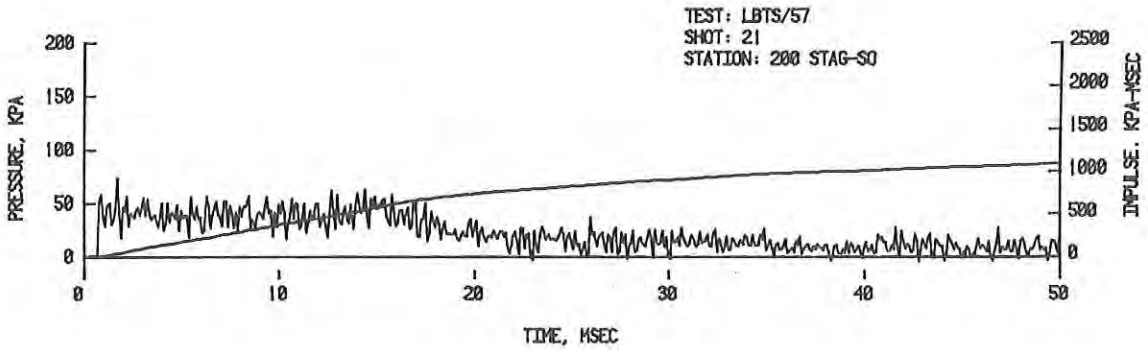

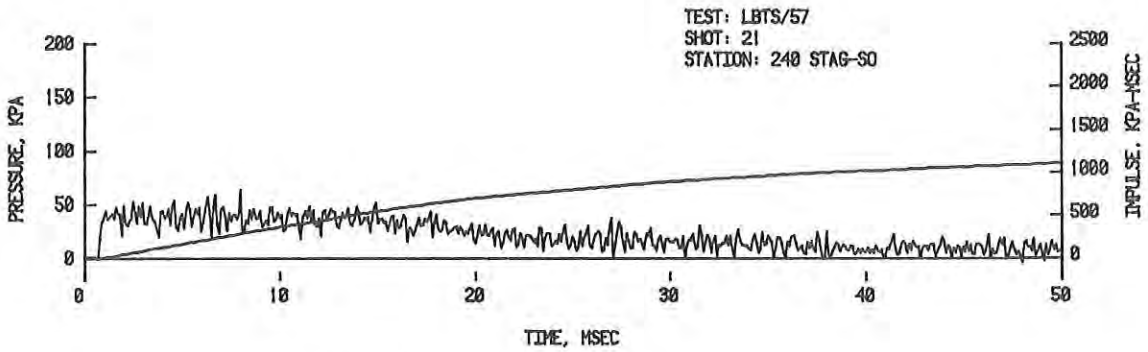

C. Dynamic Pressure

Figure 10. Pressure-Time Records from Test Section - Long Driver, 4220 kPa (Cont'd).

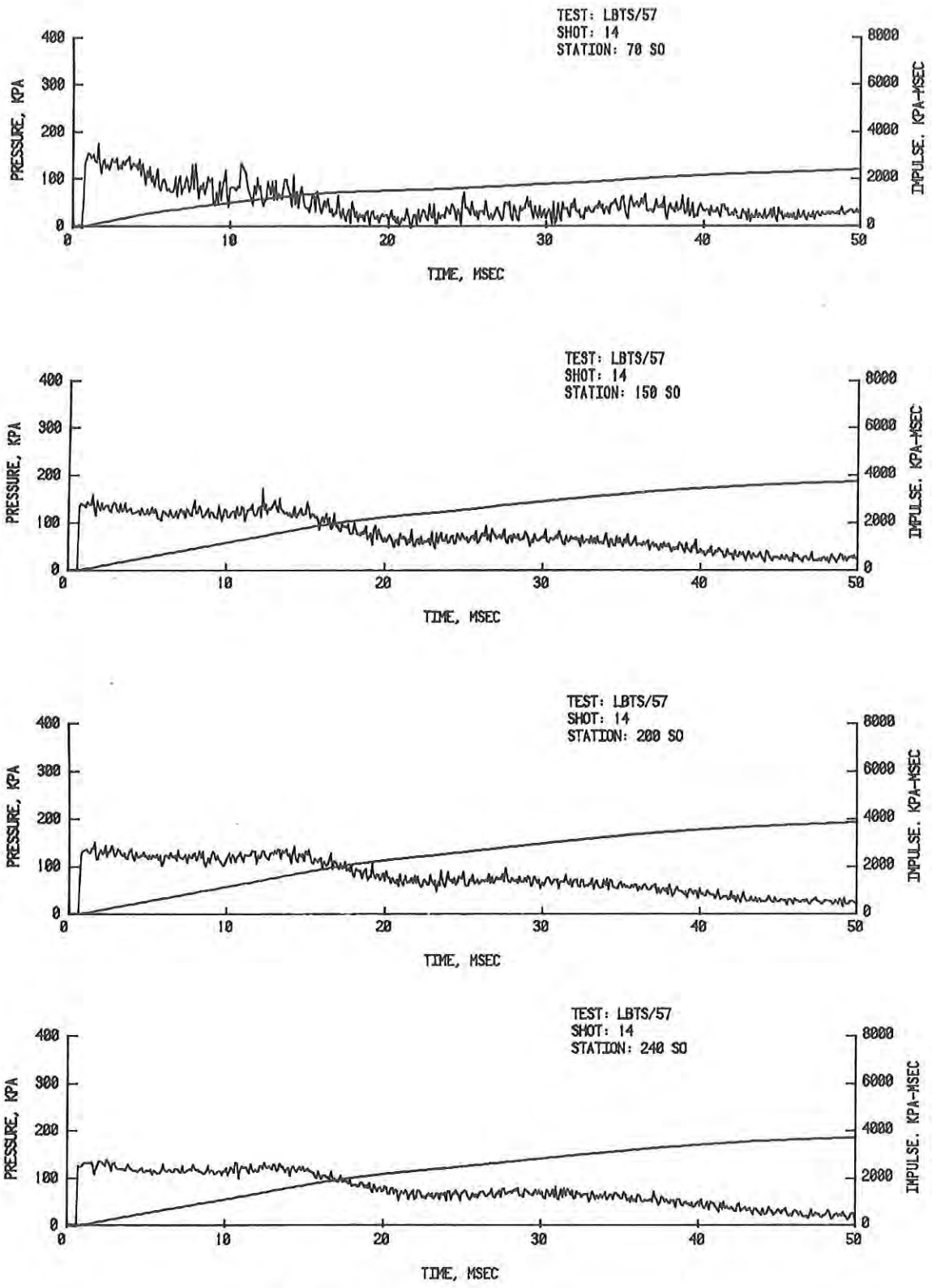

A. Side-On Overpressure

Figure 11. Pressure-Time Records from Test Section - Long Driver, 5171 kPa.

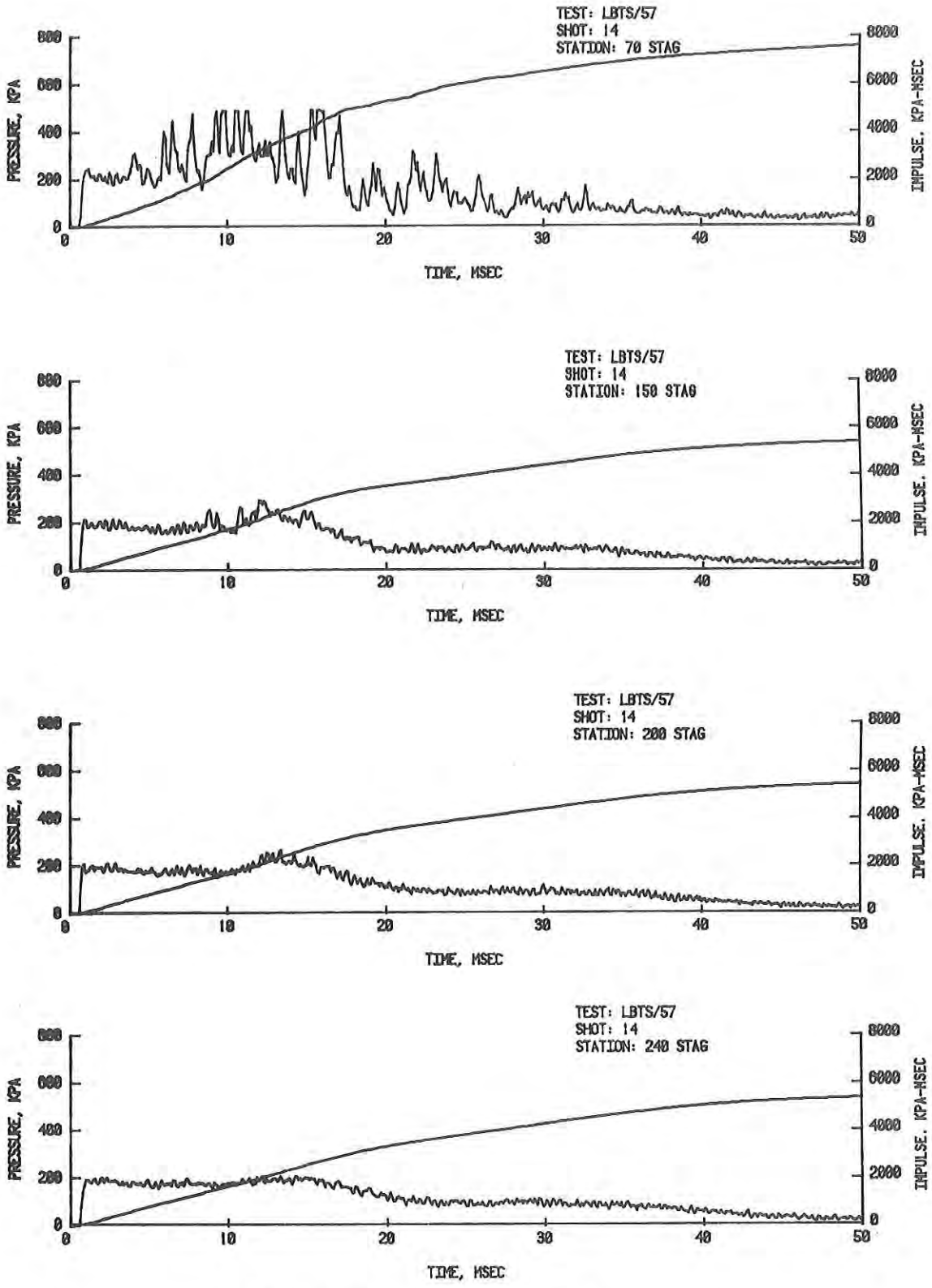

B. Stagnation Overpressure

Figure 11. Pressure-Time Records from Test Section - Long Driver, 5171 kPa (Cont'd).

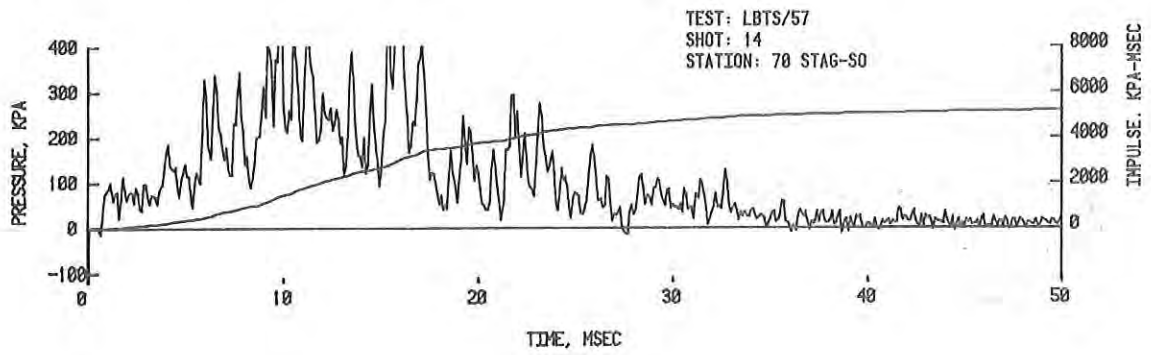

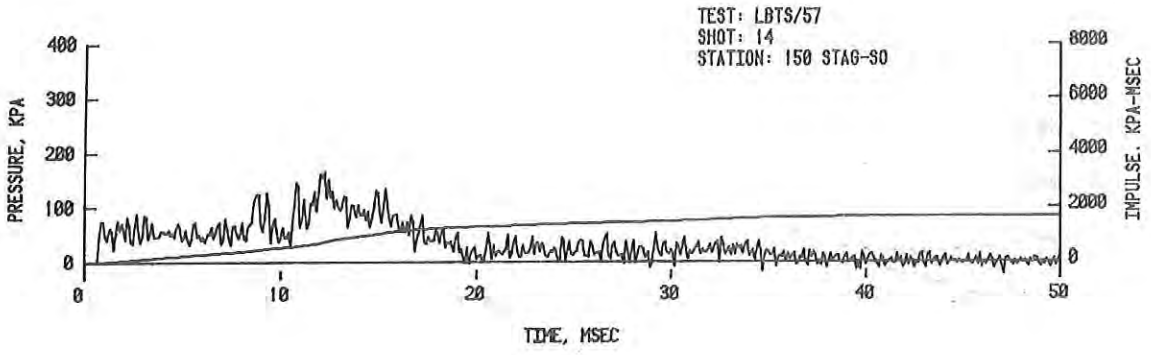

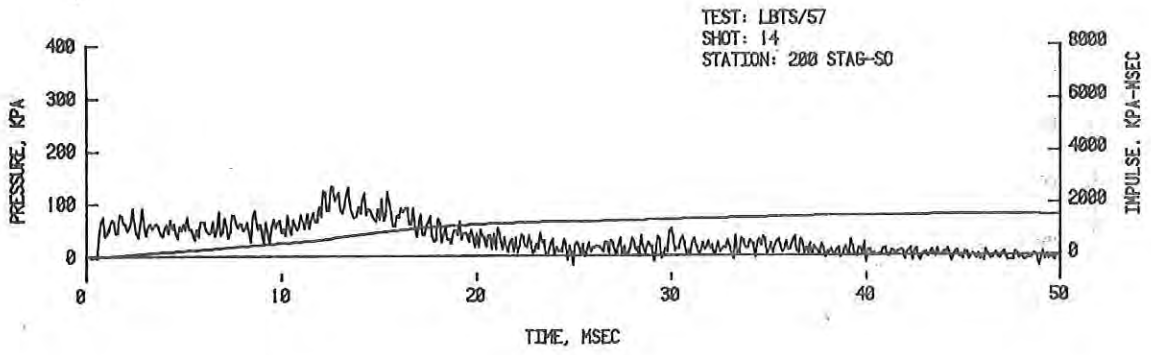

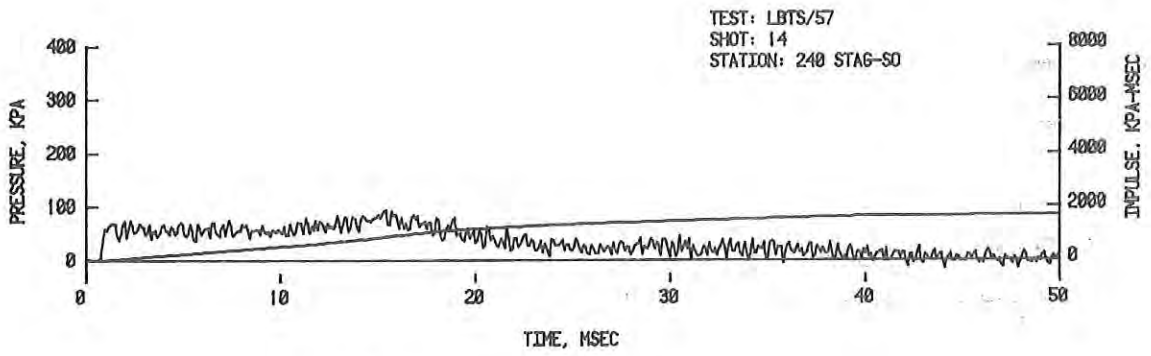

C. Dynamic Pressure

Figure 11. Pressure-Time Records from Test Section - Long Driver, 5171 kPa (Cont'd).

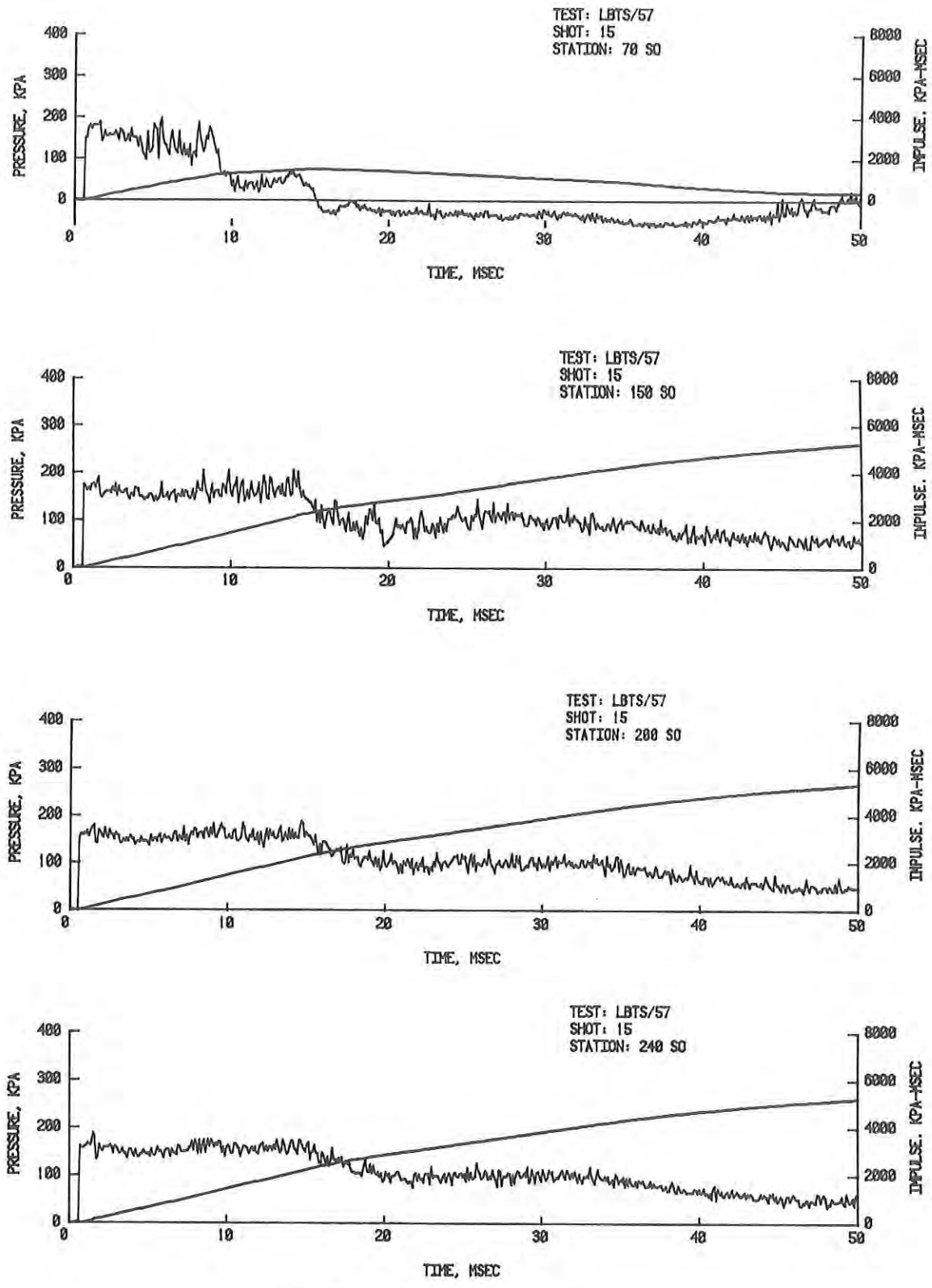

A. Side-On Overpressure

Figure 12. Pressure-Time Records from Test Section - Long Driver, 7481 kPa.

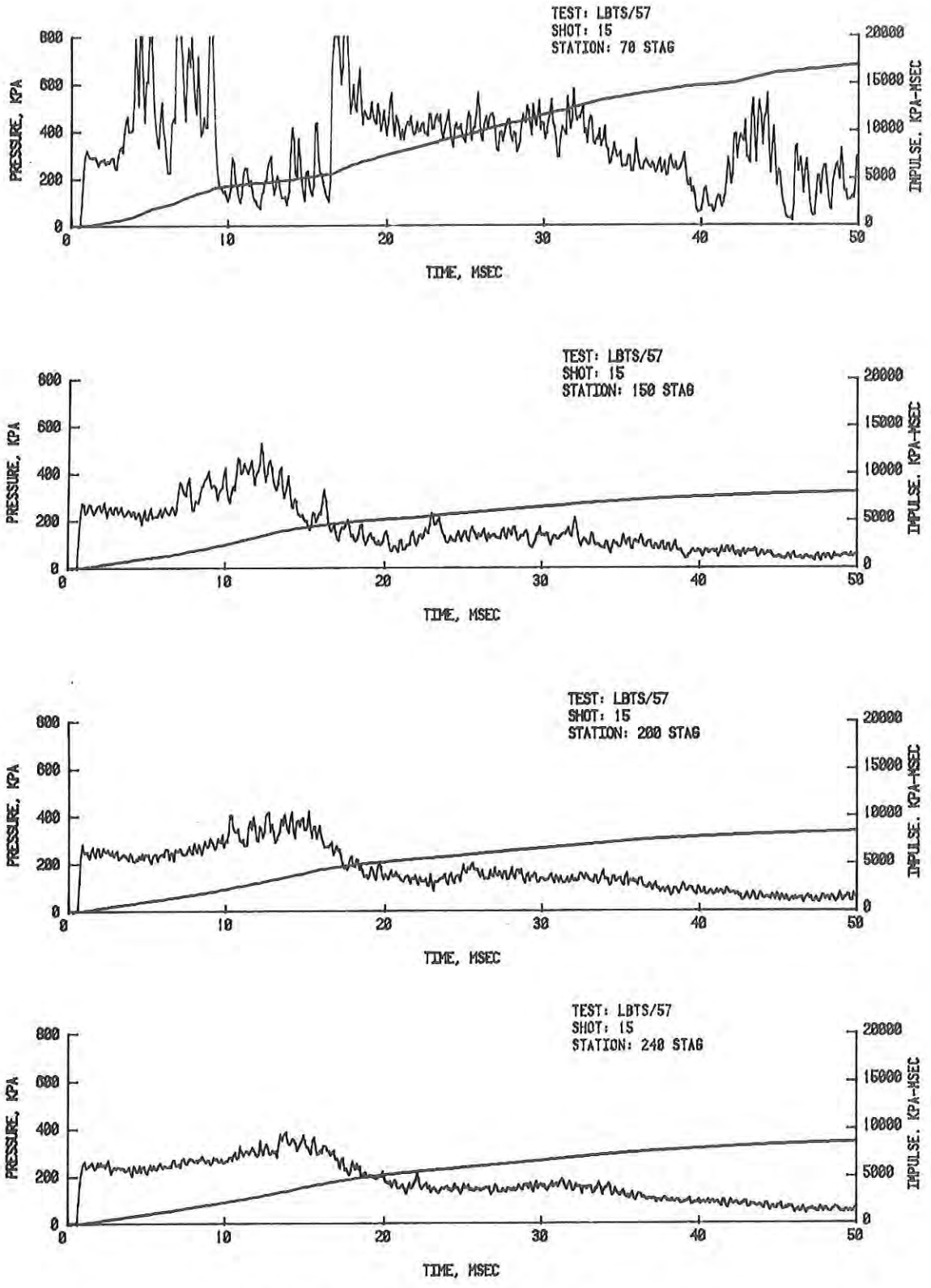

B. Stagnation Overpressure

Figure 12. Pressure-Time Records from Test Section - Long Driver, 7481 kPa (Cont'd).

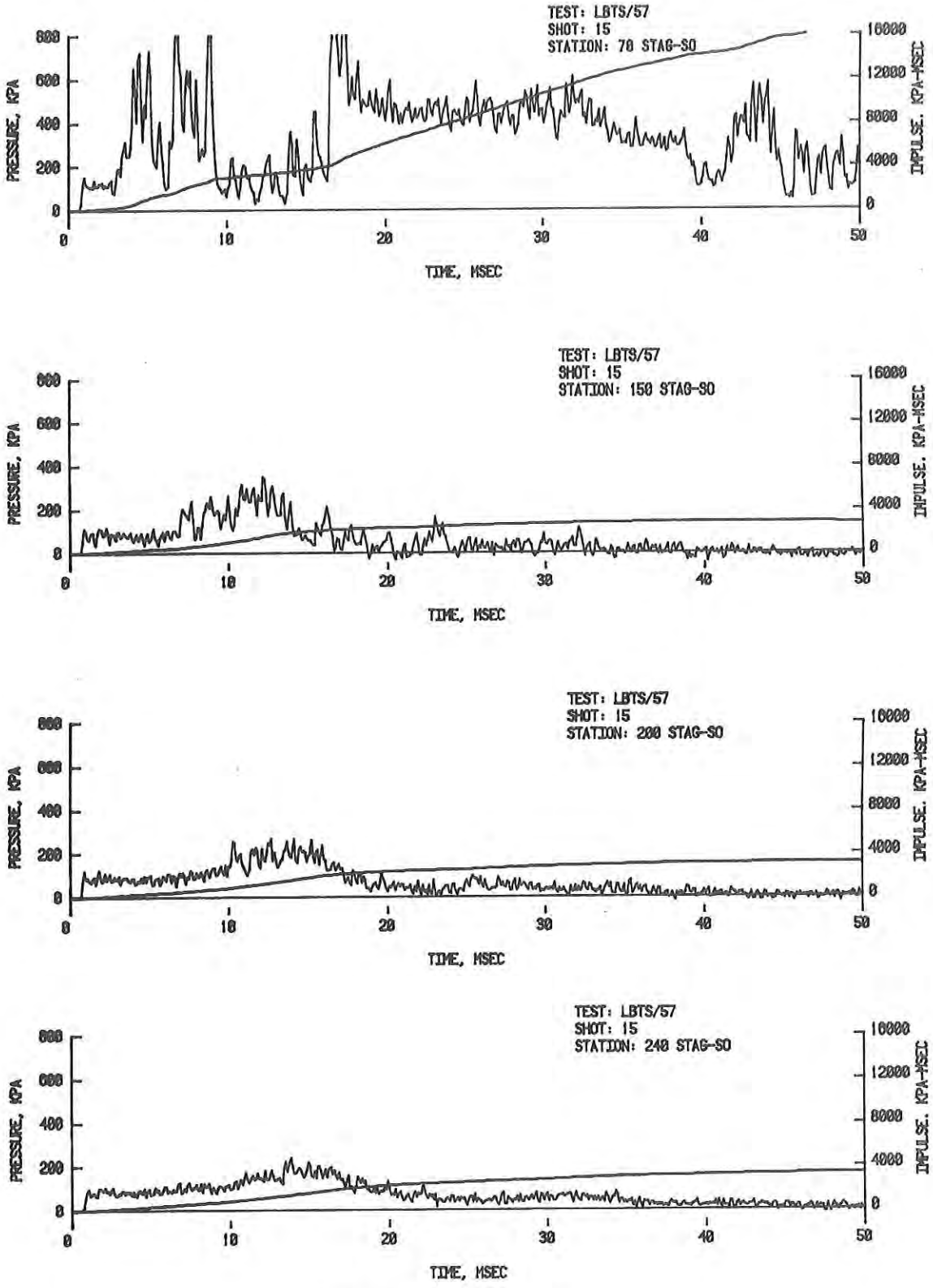

C. Dynamic Pressure

Figure 12. Pressure-Time Records from Test Section - Long Driver, 7481 kPa (Cont'd).

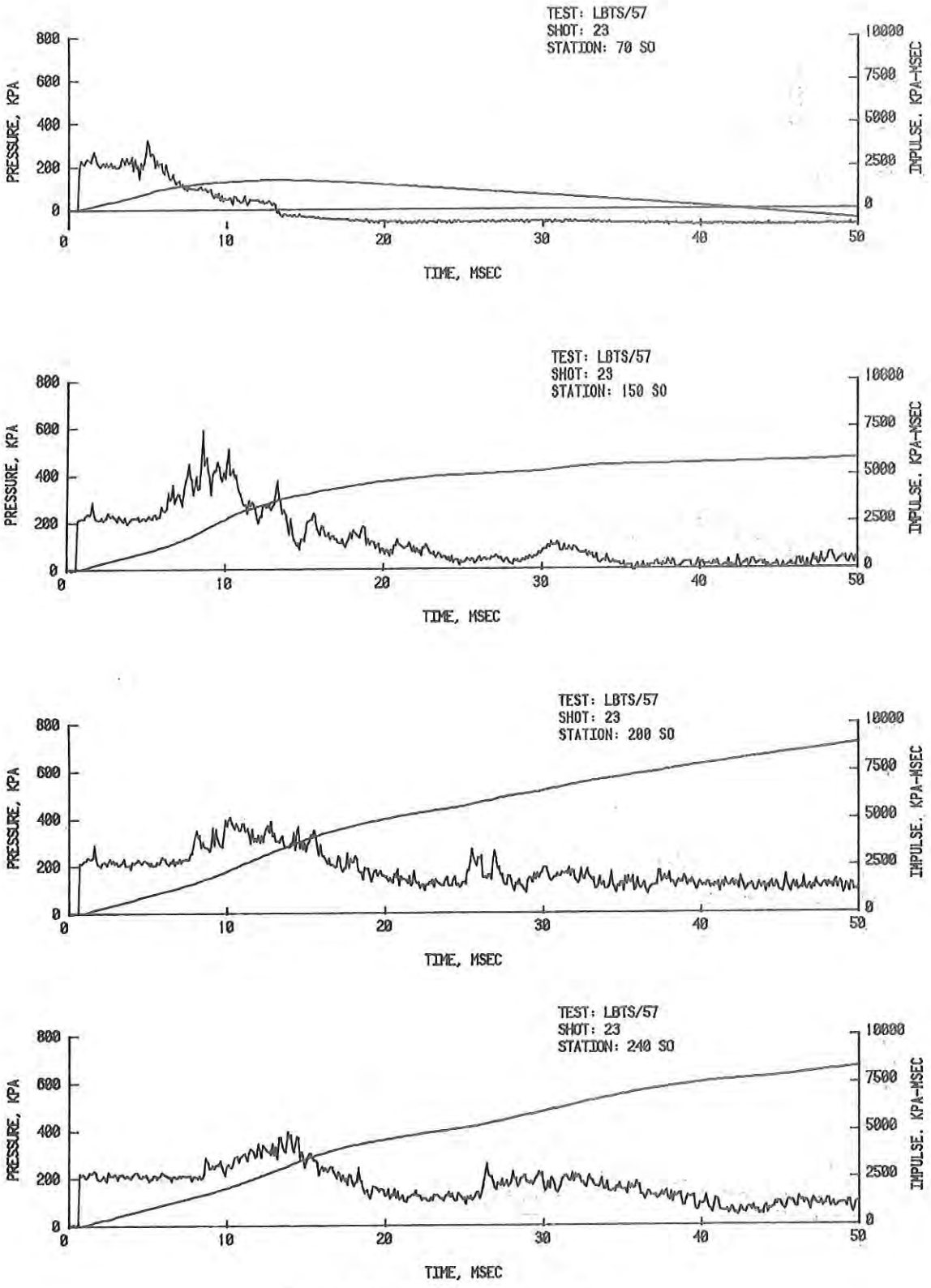

A. Side-On Overpressure

Figure 13. Pressure-Time Records from Test Section - Long Driver, 15169 kPa.

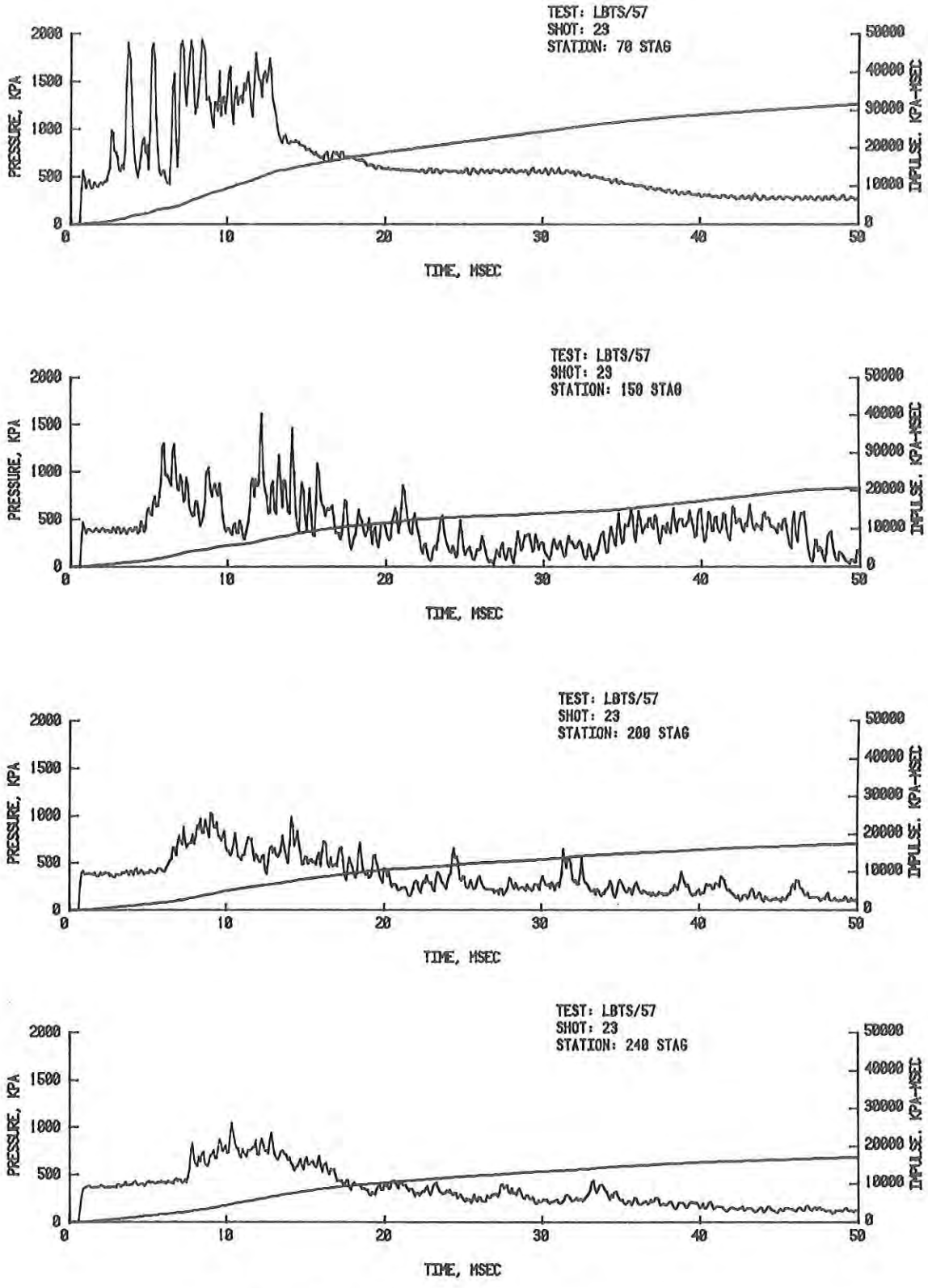

B. Stagnation Overpressure

Figure 13. Pressure-Time Records from Test Section - Long Driver, 13169 kPa (Cont'd).

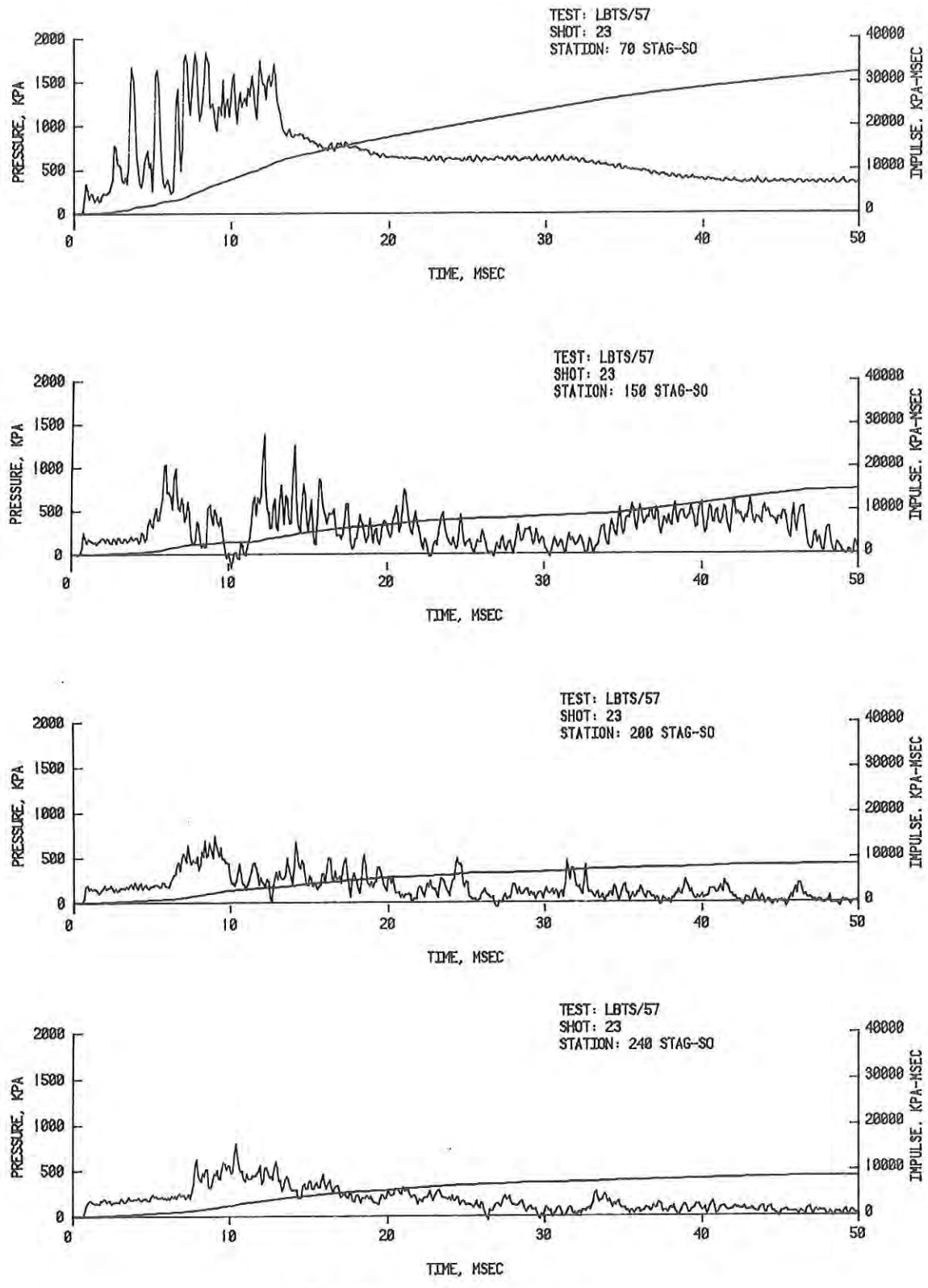

C. Dynamic Pressure

Figure 13. Pressure-Time Records from Test Section - Long Driver, 13169 kPa (Cont'd).

TABLE 2. BLAST WAVE PARAMETERS VS DRIVER PARAMETERS; TEST SECTION TO THROAT AREA RATIO OF 16:1

Shot Number-Station	Driver Pressure kPa	Driver Length cm	Side-On Overpressure kPa	Positive Duration ms	Positive Impulse kPa-ms	Driver Length m	Full Size Driver Volume m^3	Full Size Positive Impulse kPa-s	Yield* kt
4-70	314	11.13	20.0	3.7	22.5	6.34	166.93	1.28	0.08
200			17.0	4.5	22.8			1.30	0.12
5-70	617		33.1	4.7	45.0			2.57	0.27
200			24.9	5.8	45.0			2.57	0.36
6-70	1124		49.9	6.0	75.1			4.28	0.65
200		same	34.1	6.9	77.3			4.41	1.29
8-70	3137		100.1	5.1	170.1			9.70	3.0
200			66.7	7.3	185.5			10.57	6.3
13-70	14479		226.2	7.6	573.9			32.71	67.0
200			155.8	12.2	710.9			40.52	161.0
67-70	13962	26.36	224.8	8.5	803.9	15.03	395.74	45.82	185.0
200			209.6	18.0	1249.3			71.21	732.0
47-70	317	33.98	18.6	8.4	54.5	19.37	510.01	3.11	1.4
200			16.5	8.8	56.1			3.20	1.9
49-70	1096		43.4	13.8	173.5			9.89	9.9
200			49.1	16.5	168.7			9.62	7.6
69-70	3137		106.2	12.3	376.7			21.47	31.0
200			94.6	15.0	421.4			24.02	49.0
72-70	11549		224.8	12.0	830.4			47.33	205.0
200			202.5	20.3	1317.5			75.09	882.0

*Yields are based on full size driver diameter of 5.79 m, area of 26.33 m^2, and are calculated from side-on overpressure impulse. Last four columns are for full size for Tables 2-4.

TABLE 2. BLAST WAVE PARAMETERS VS DRIVER PARAMETERS; TEST SECTION TO THROAT AREA RATIO OF 16:1 (CONT.)

Shot Number-Station	Driver Pressure kPa	Driver Length cm	Side-On Overpressure kPa	Positive Duration ms	Positive Impulse kPa-ms	Full Size Driver Length m	Full Size Driver Volume m^3	Full Size Positive Impulse kPa-s	Yield kt
79-70	1124	72.09	48.5	29.0	351.7	41.09	1081.89	20.04	74.0
200			42.5	30.5	359.6			20.50	91.0
75-70	3137		110.0	----	850.6			48.48	344.0
200			94.0	----	857.5			48.88	411.0
74-70	13169		221.3	9.5	1319.5			75.21	831.0
200			233.0	30.8	2571.3			146.56	5869.0
53-70	338	89.86	13.5	19.2	118.0	51.22	1348.60	6.73	27.0
200			14.0	20.2	131.0			7.47	34.0
73-70	13445	102.57	220.0	10.3	1412.0	58.46	1539.24	80.48	1022.0
200			224.8	43.2	3800.0			216.60	19553.0
78-70	1117	110.18	47.2	41.4	512.2	62.81	1653.77	29.20	232.0
200			40.5	44.8	505.9			28.84	278.0
77-70	3123		106.0	----	1350.0			76.95	1424.0
200			99.0	57.3	1274.8			72.66	1275.0
80-70	1145	144.97	49.5	57.0	700.0	83.07	2187.20	38.18	473.0
200			45.0	56.0	720.0			41.04	677.0
59-70	324	125.42	17.9	26.0	173.1	71.49	1882.32	9.87	49.0
200			16.6	39.4	180.7			10.30	64.0
55-70	359	178.76	14.2	37.3	265.0	101.93	2683.79	15.11	275.0
200			13.0	38.5	272.8			15.55	365.0
57-70	352	237.18	13.2	48.7	328.8	135.19	3559.52	18.74	618.0
200			13.0	48.5	327.4			18.66	632.0

TABLE 3. BLAST WAVE PARAMETERS VS DRIVER PARAMETERS;
TEST SECTION TO THROAT AREA RATIO OF 33:1

Shot Number-Station	Driver Pressure kPa	Driver Length cm	Side-On Overpressure kPa	Positive Duration ms	Positive Impulse kPa-ms	Full Size Driver Length m	Full Size Driver Volume m^3	Full Size Positive Impulse kPa-s	Yield kt
93-70	18271	6.05	172.5	7.3	523.1	3.45	90.84	29.82	61.0
200			135.0	11.3	558.3			31.82	84.0
92-70	490	11.13	19.5	6.0	30.5	6.34	166.93	1.74	0.22
200			15.0	7.5	32.1			1.83	0.44
35-70	2027		54.3	11.3	120.0			6.84	2.3
200			39.0	13.8	120.0			6.84	4.0
37-70	5192		99.6	9.1	232.5			13.25	7.7
200			83.4	11.0	271.0			15.45	14.9
40-70	14479		195.3	8.3	567.9			32.37	72.0
200			142.4	14.4	636.5			36.28	121.0
81-70	483	33.99	19.3	20.8	88.0	19.37	510.01	5.02	5.5
200			15.7	18.5	84.4			4.81	7.3
82-70	1827		47.5	33.8	284.9			16.24	39.0
200			39.3	35.3	293.7			16.74	58.0
83-70	5199		103.0	43.5	686.2			39.11	192.0
200			88.9	36.3	659.6			37.60	198.0
84-70	14789		200.2	17.7	937.2			53.42	321.0
200			200.0	25.5	1525.6			89.96	1386.0
85-70	483	67.01	20.0	34.2	153.1	38.19	1005.53	8.73	27.0
200			15.7	34.3	159.5			9.09	51.0
86-70	1827		46.8	80.5	560.0			31.92	304.0
200			40.6	63.3	550.0			31.35	356.0
87-70	5240		108.0	----	1275.0			72.68	1181.0
200			94.9	----	1300.0			74.10	1415.0
88-70	14651		191.7	15.0	1450.0			82.65	1218.0
200			200.0	41.0	2640.0			150.48	7180.0
89-70	496	94.95	14.6	47.0	200.0	54.12	1424.97	11.40	114.0
200			13.5	47.5	202.0			11.51	138.0
90-70	1834		40.8	80.0	726.0			41.38	804.0
200			39.8	----	720.0			41.04	771.0
63-70	510	125.42	15.0	39.4	277.9	71.49	1882.32	15.84	288.0
200			13.8	67.3	314.9			17.95	508.0
91-70	545	145.75	15.2	69.0	315.0	83.07	2187.21	17.96	414.0
200			15.0	72.3	363.0			20.69	641.0

TABLE 4. BLAST WAVE PARAMETERS VS DRIVER PARAMETERS;
TEST SECTION TO THROAT AREA RATIO OF 64:1

Shot Number-Station	Driver Pressure kPa	Driver Length cm	Side-On Overpressure kPa	Positive Duration ms	Positive Impulse kPa-ms	Driver Length m	Full Size Driver Volume m^3	Full Size Positive Impulse kPa-s	Yield kt
29-70	1103	11.13	29.2	28.5	76.8	6.34	166.93	4.38	1.8
200			21.8	33.8	84.0			4.79	4.1
30-70	2034		39.1	21.6	112.8			6.53	3.6
200			28.8	33.2	134.0			7.64	9.7
31-70	3103		56.6	25.8	187.5			10.69	10.4
200			39.6	34.0	177.0			10.09	13.1
32-70	8618		107.0	42.1	418.4			23.85	62.8
200			86.9	35.1	451.7			25.75	94.7
94-70	903	74.62	13.8	>85.0	300.0	42.54	1120.07	17.10	444.0
200			13.0	>85.0	329.9			18.80	681.0
54-70	710	89.86	15.5	86.0	257.0	51.22	1348.61	14.65	224.0
200			13.8	86.0	283.5			16.16	371.0

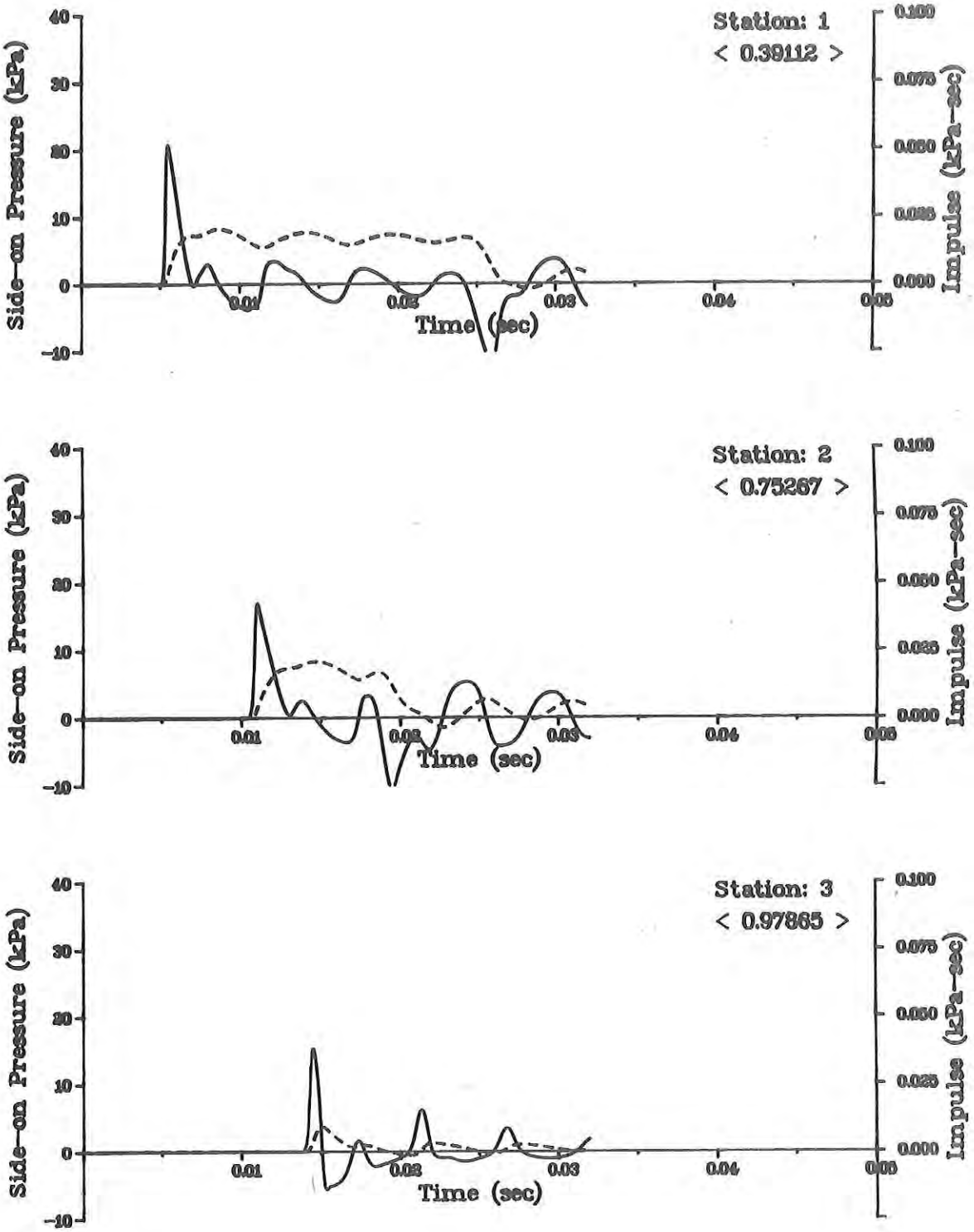

Figure 14. Hydrocode Predictions - Short Driver, 314 kPa.

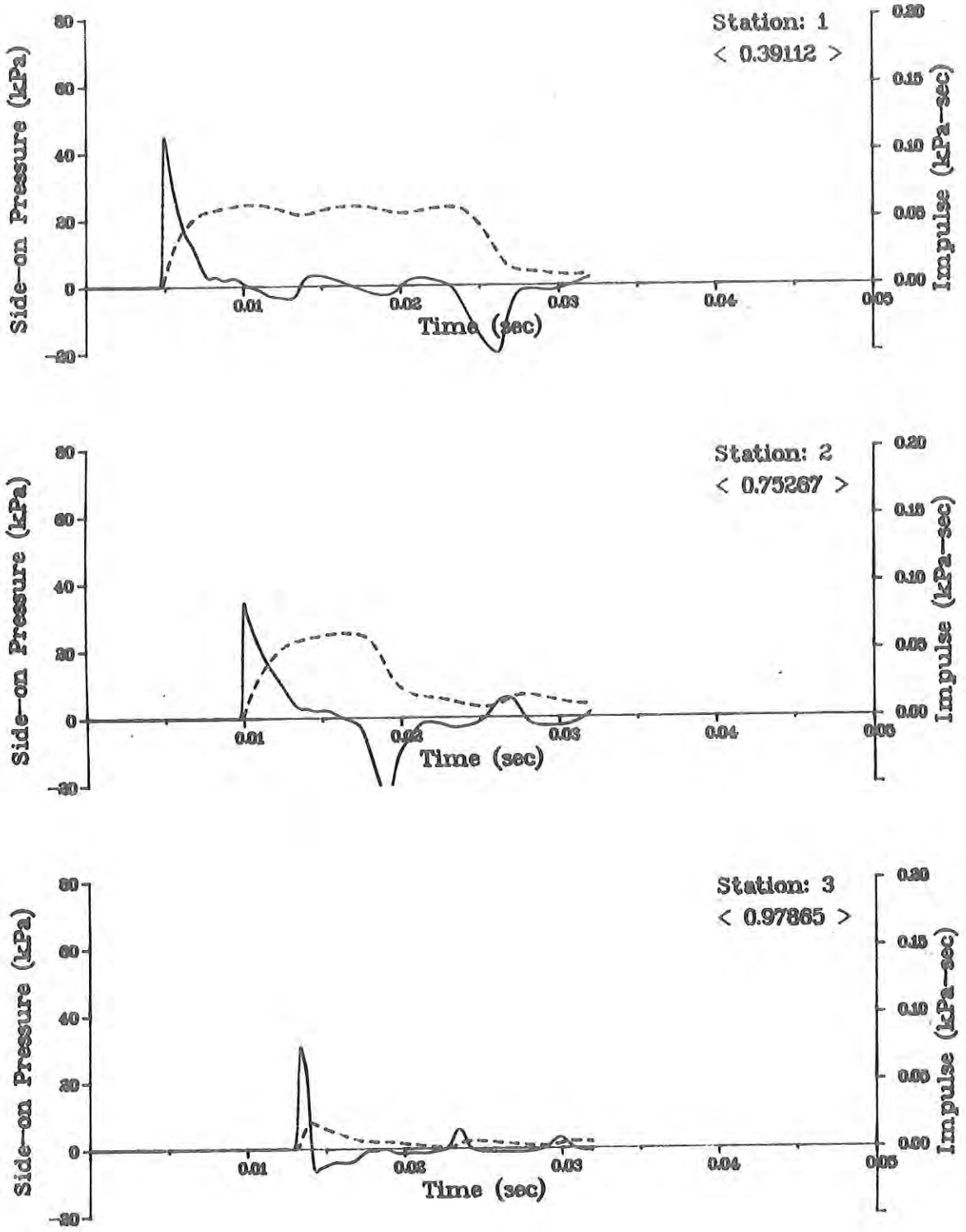

Figure 15. Hydrocode Predictions - Short Driver, 1124 kPa.

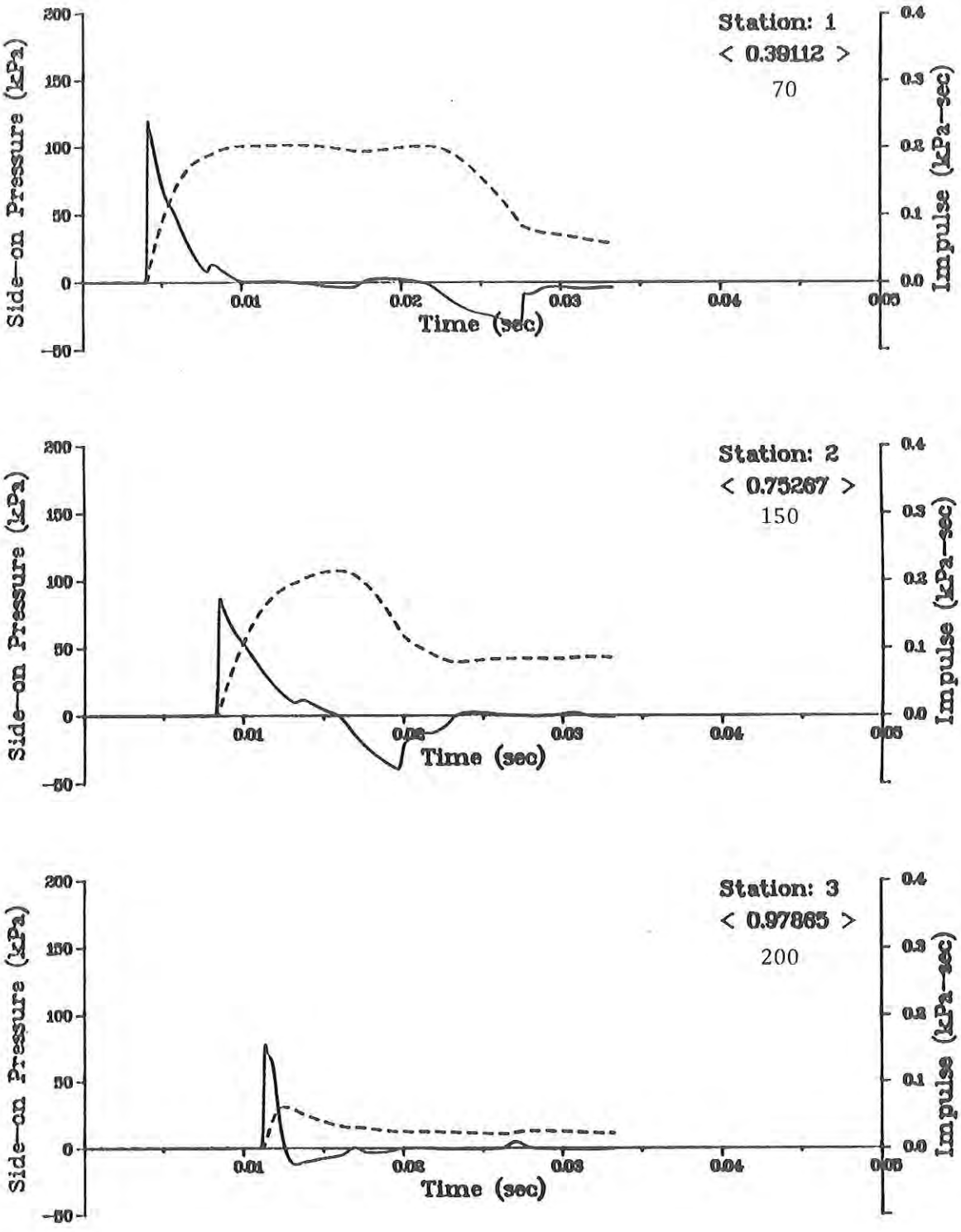

Figure 16. Hydrocode Predictions - Short Driver, 4413 kPa.

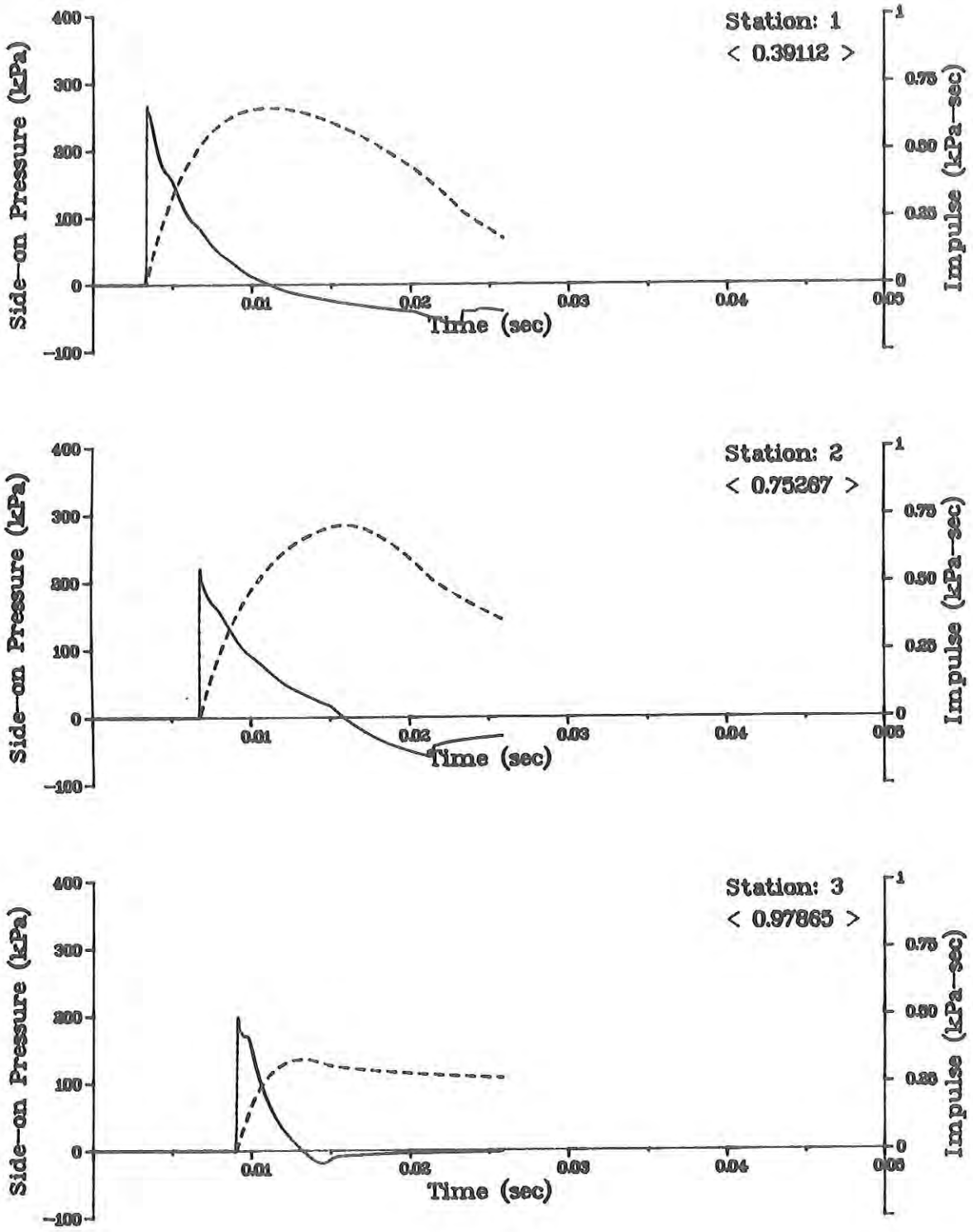

Figure 17. Hydrocode Predictions - Short Driver, 14480 kPa.

the predicted pressures from the code varied both above and below the experimental values. The general decay along the test section was similar to the measured experimental values.

The positive durations predicted were 5 to 10 percent smaller than the experimental records showed. Station 3 should not be compared here (except for peak pressure) since it was near the open end of the computational shock tube. The rarefaction from the open end shortened the positive duration. The experiments used a long test section with a closed end so no rarefactions could occur.

The agreement in negative phase between the code and experimental values was not nearly as close. The code values of negative pressure were anywhere from 30 to 100% lower (Station 1, 7 diameters; before open end rarefaction arrived at station) than was actually measured. Overall, the code predictions were quite useful to predict the general pressure-time waveforms from the various driver configurations, given the limitations discussed.

3.3 Cold Gas/Recompression Fan Effects. Figures 18-22 show some of the code predictions of pressure-time records for the long driver. As was noted earlier, side-on overpressure begins to be predicted too high for driver pressures of about 3000 kPa. Both the cold gas and recompression fan (backward facing shock) arrival are very apparent. Table 5 summarizes and compares the code results with that of the test data. Figures 23-25 display these comparisons in graphical form.

Theoretically, the cold gas should not appear on side-on overpressure records at all. It does, however, appear on the experimental records although the code cannot predict it for the side-on records. It does, of course, predict it for the stagnation records. See Figure 21. Experimentally, the cold gas region tends to diffuse and be quite turbulent in nature. The code, instead, predicts very smooth pressure change upon the cold gas arrival; and it predicts a slower arrival than experimentally recorded. The cold gas average drag enhancement is predicted by the code to be higher than the data suggests. It should be noted that higher spikes do exist on the data records. Only average ratio values obtained from the impulse data were used to plot Figure 24 from Table 5-C. It should be noted that the enhancement is about constant along the test section for a given driver pressure.

The second effect that changed the pressure-time waveform (and hence yield) is shown by the code results in Figure 20. Notice the very sharp cutoff of the positive phase and the relatively low, and extensive negative phase of the records. This effect shows up sooner on the data records and is more of a rarefaction decay than a discontinuous drop as the code suggests. Experimentally, the cold gas and recompression fan effects move back from the shock front with travel along the test section. The data show that Station 70 (7 dia.) cannot be used with a cold driver operation above, perhaps, 100 kPa side-on overpressure at the station.

A shorter driver, and shorter duration record, ought to minimize the cold gas/recompression fan effects. Figure 26 shows a comparison of records from the long, 288 cm, driver with those obtained from a short,

 The text is continued on page 65.

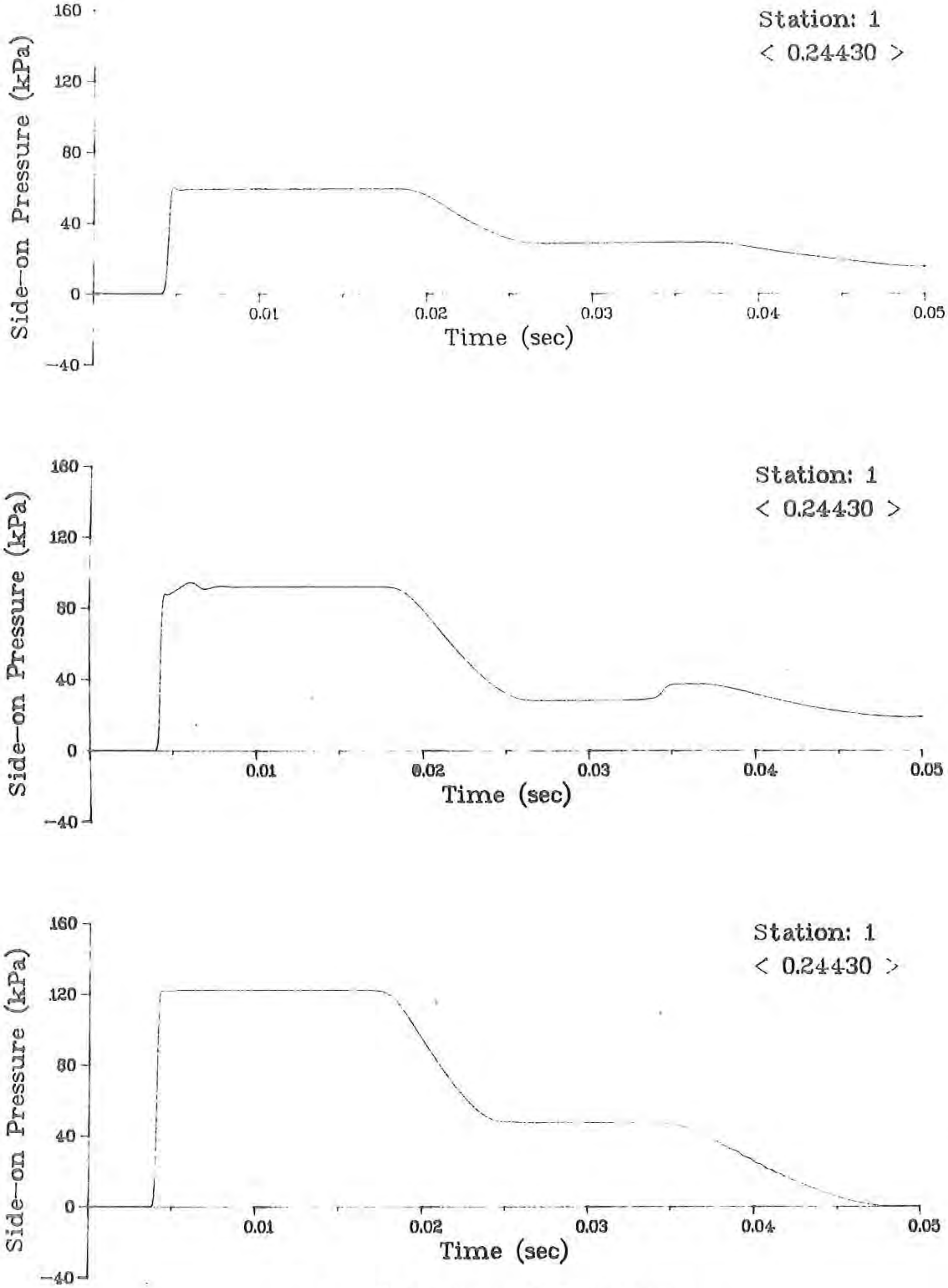

A. Station at 7 Diameters

Figure 18. Hydrocode Side-On Overpressure Predictions - Long Driver; 2034, 3103, and 4220 kPa.

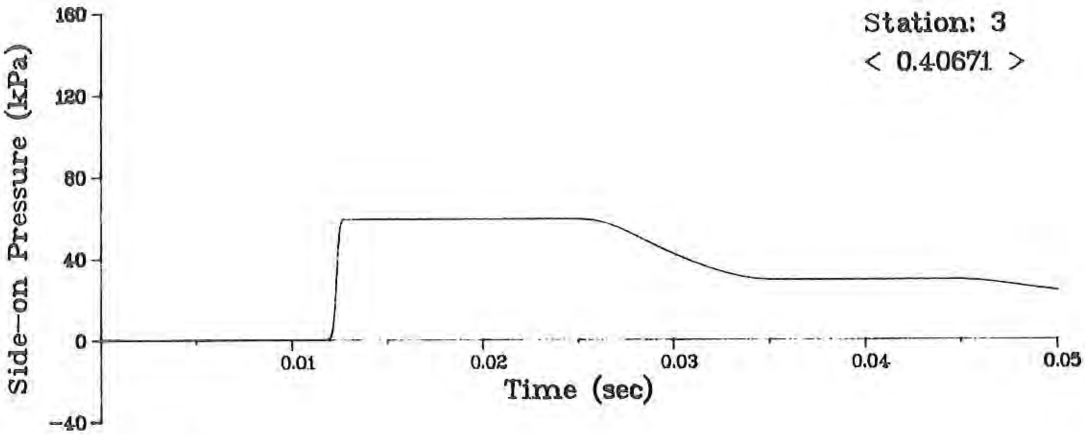

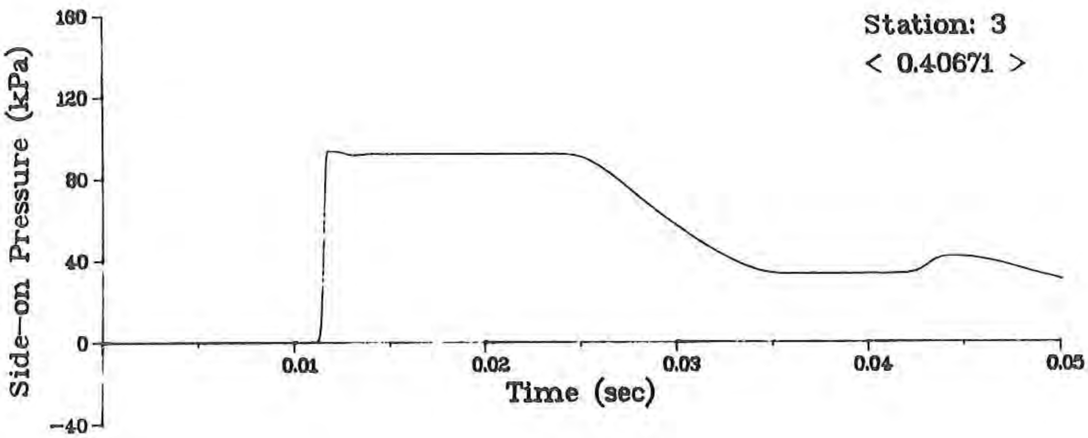

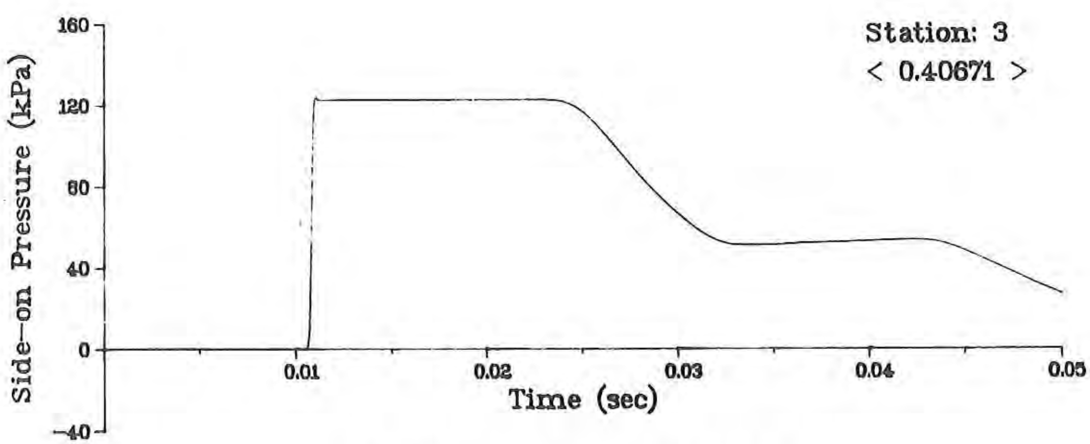

B. Station at 20 Diameters

Figure 18. Hydrocode Side-On Overpressure Predictions - Long Driver; 2034, 3103, and 4220 kPa (Cont'd).

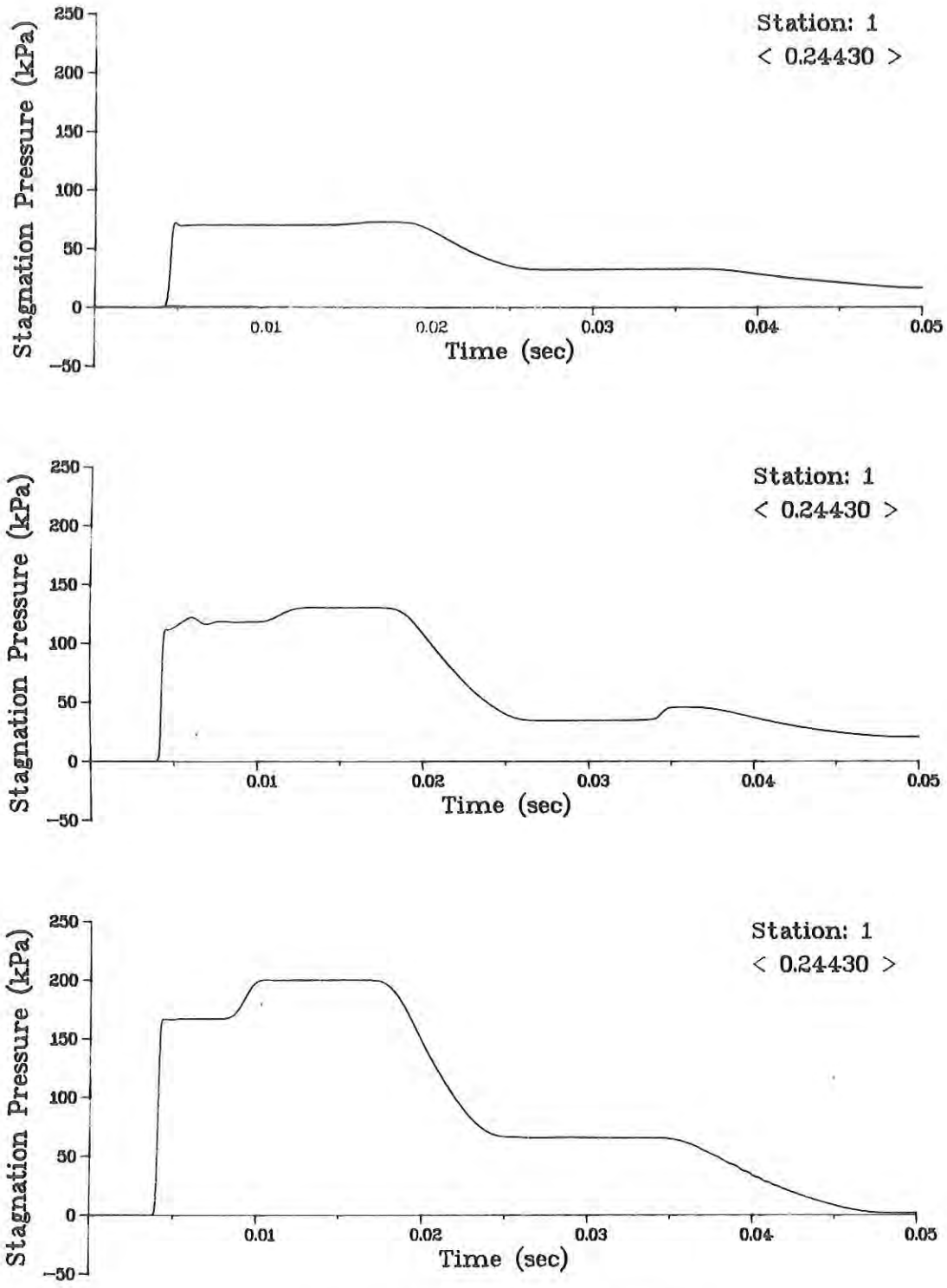

A. Station at 7 Diameters

Figure 19. Hydrocode Stagnation Overpressure Predictions - Long Driver; 2034, 3103, and 4220 kPa.

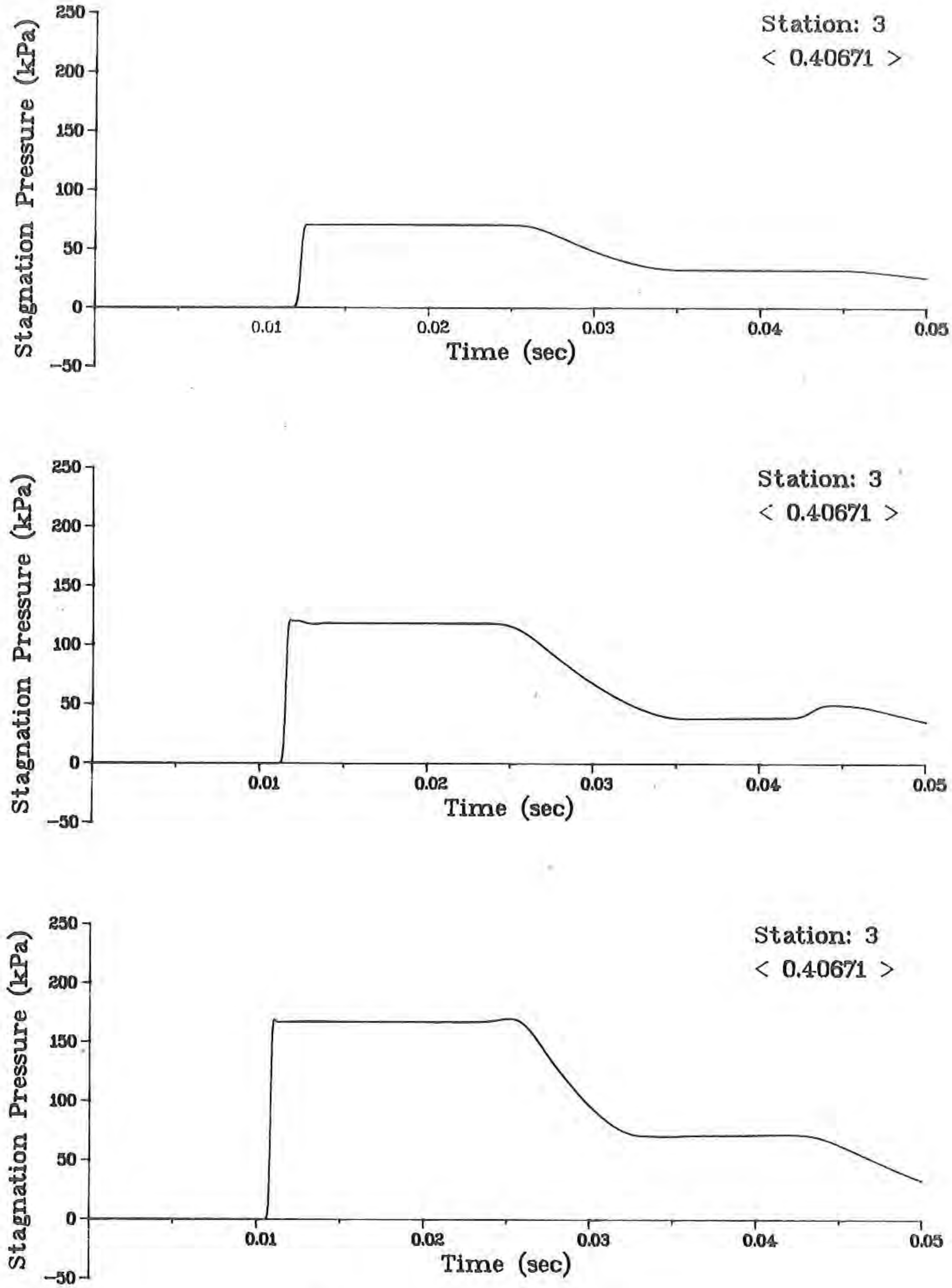

B. Station at 20 Diameters

Figure 19. Hydrocode Stagnation Overpressure Predictions - Long Driver; 2034, 3103, and 4220 kPa (Cont'd).

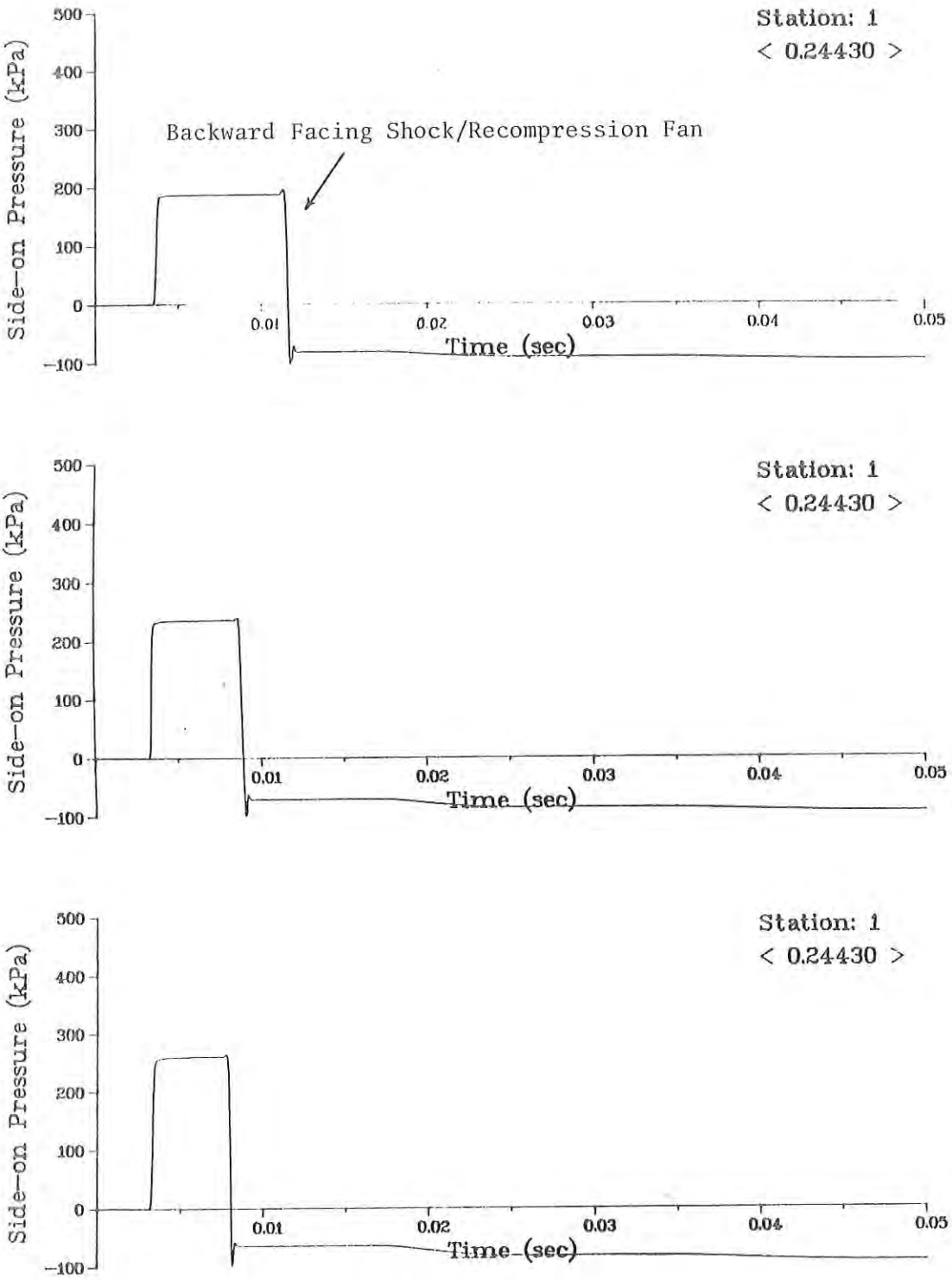

A. Station at 7 Diameters

Figure 20. Hydrocode Side-On Overpressure Predictions - Long Driver; 7480, 10963, and 13169 kPa.

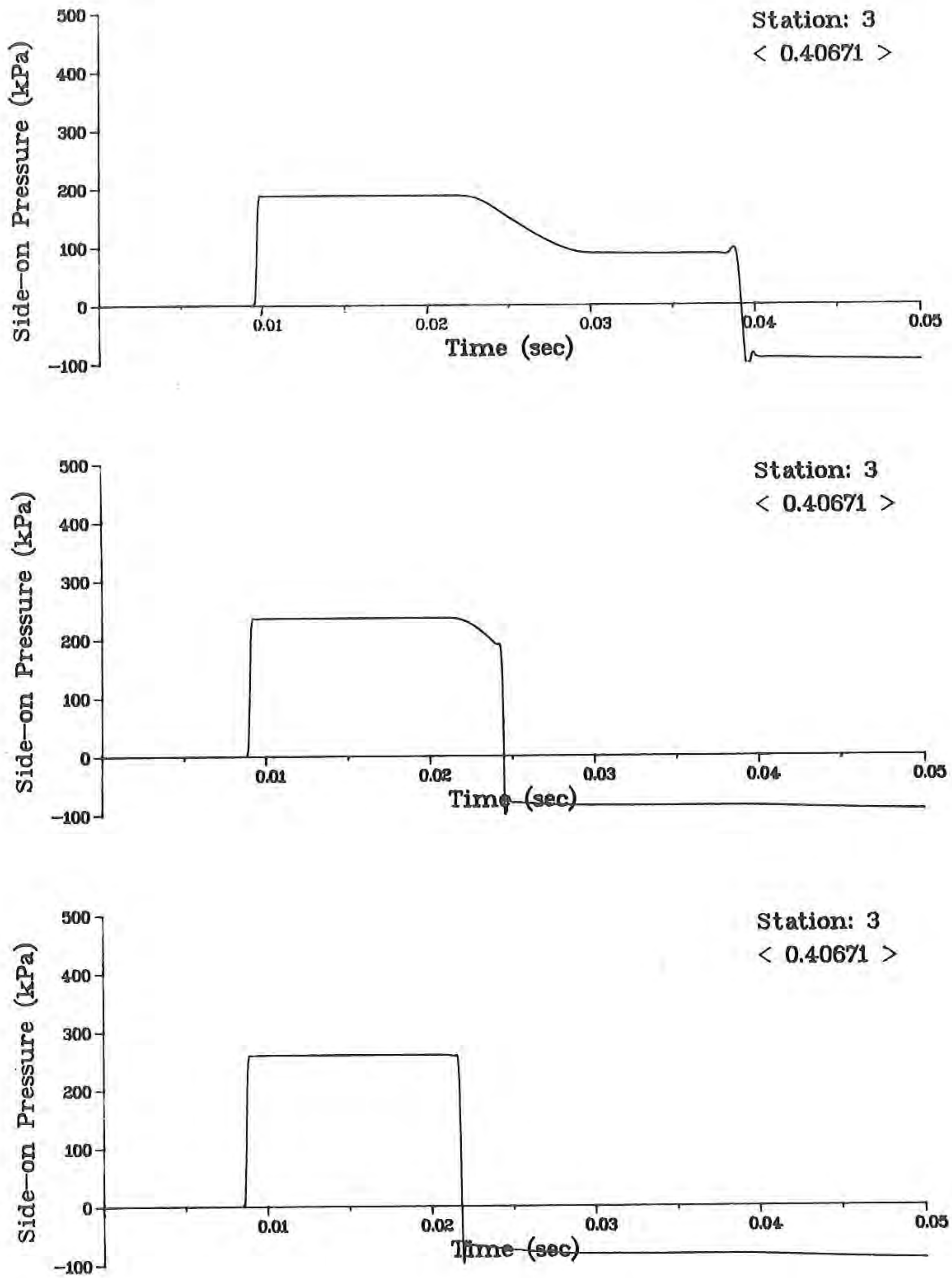

B. Station at 20 Diameters

Figure 20. Hydrocode Side-On Overpressure Predictions - Long Driver; 7480, 10963, and 13169 kPa (Cont'd).

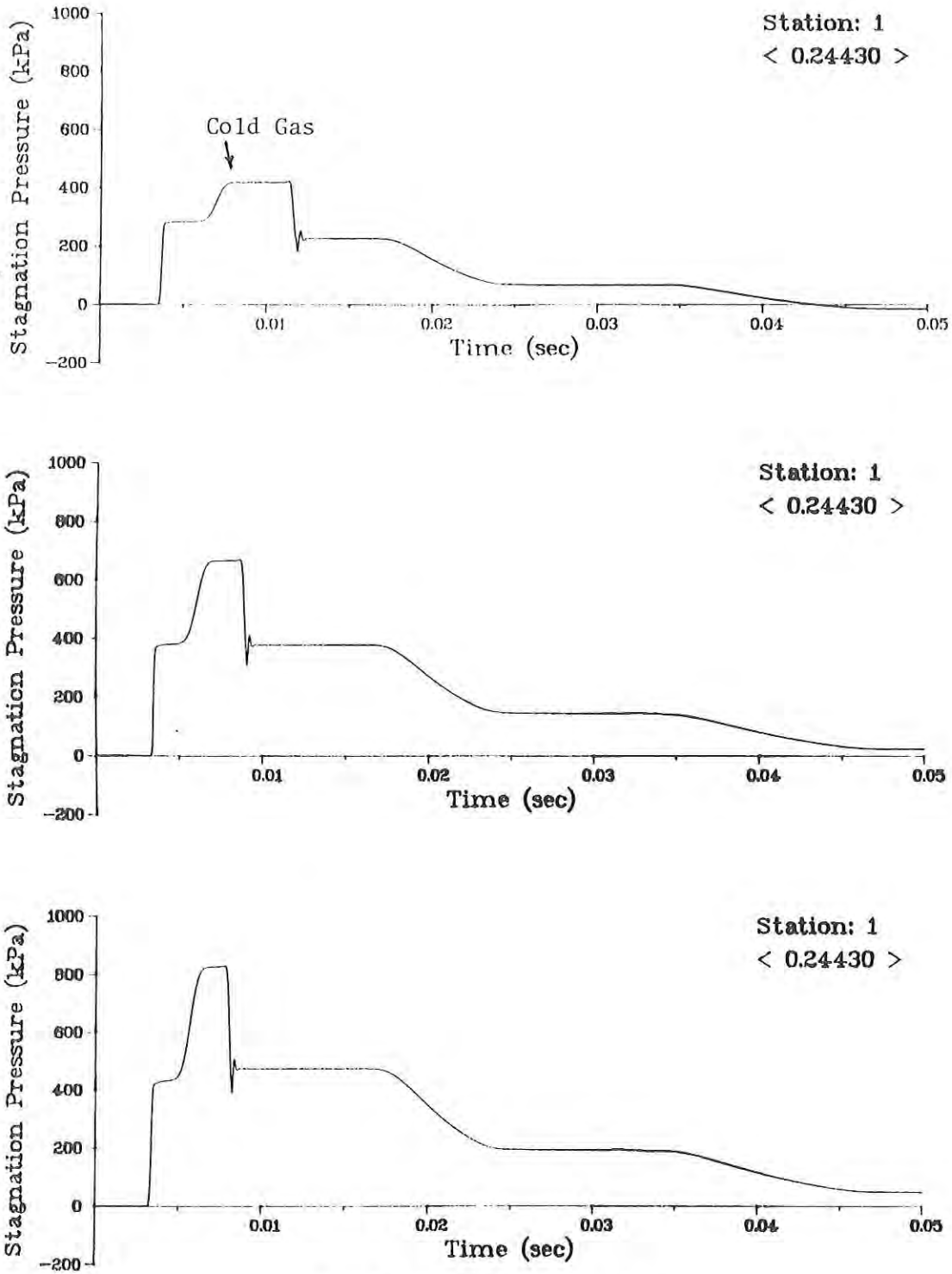

A. Station at 7 Diameters

Figure 21. Hydrocode Stagnation Overpressure Predictions - Long Driver; 7480, 10963, and 13169 kPa.

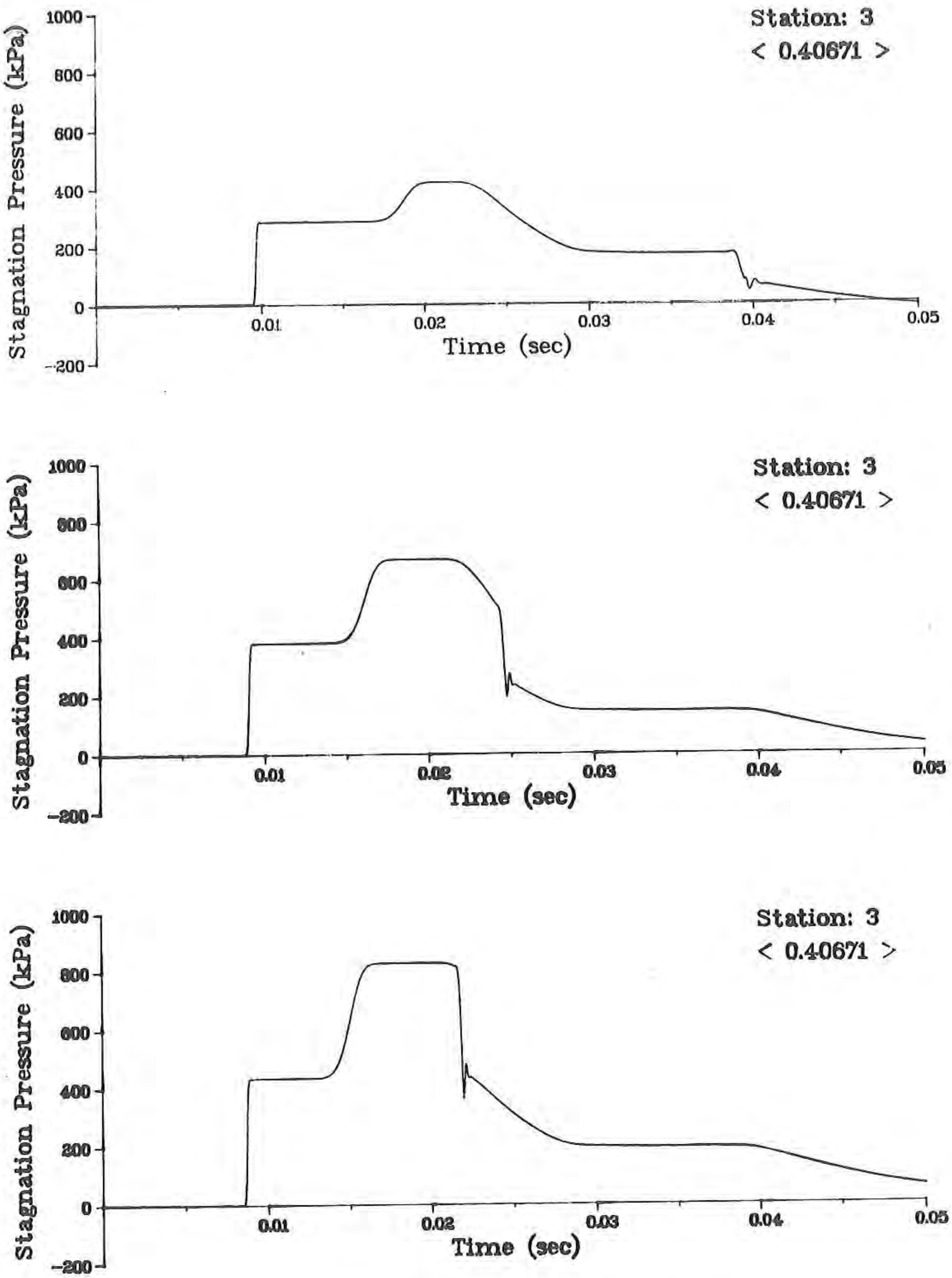

B. Station at 20 Diameters

Figure 21. Hydrocode Stagnation Overpressure Predictions - Long Driver; 7480, 10963, and 13169 kPa (Cont'd).

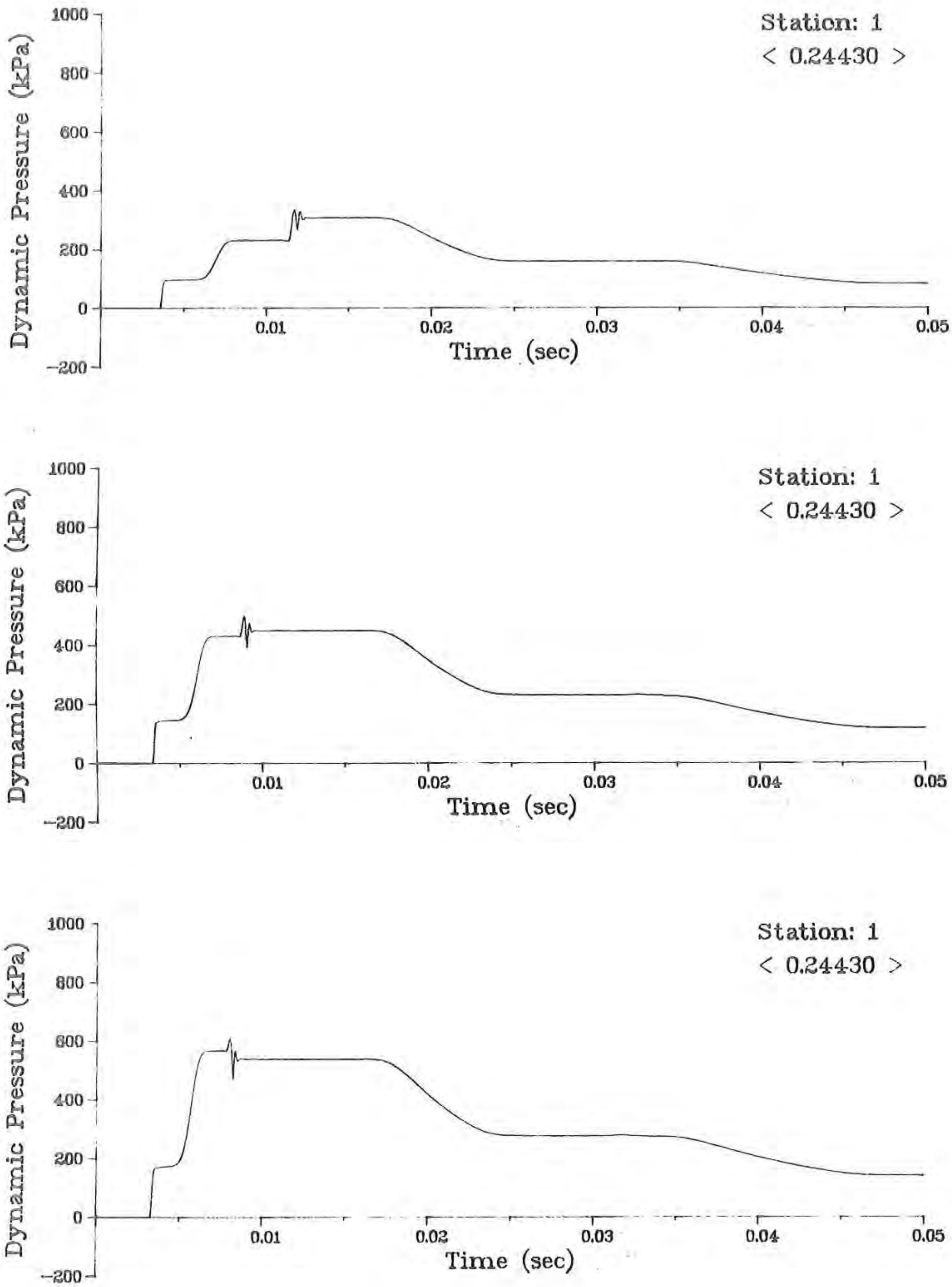

A. Station at 7 Diameters

Figure 22. Hydrocode Dynamic Overpressure Predictions - Long Driver; 7480, 10963, and 13169 kPa.

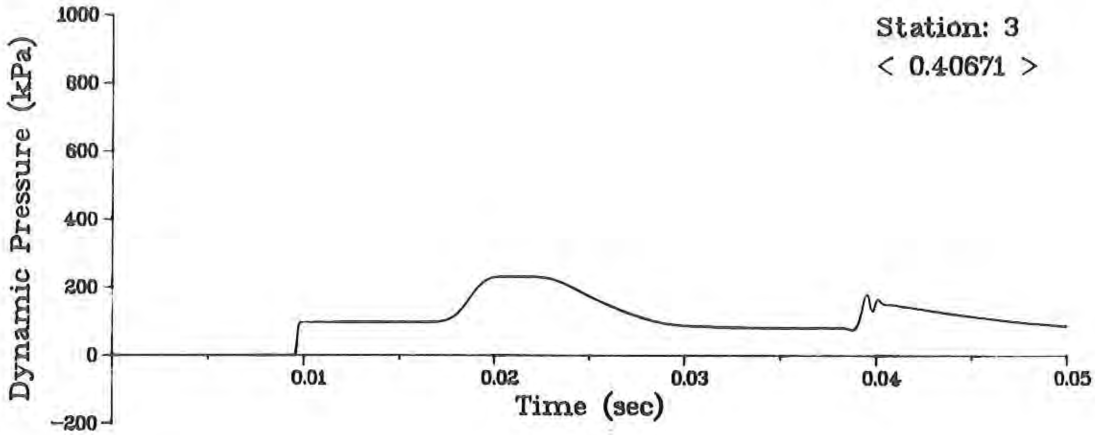

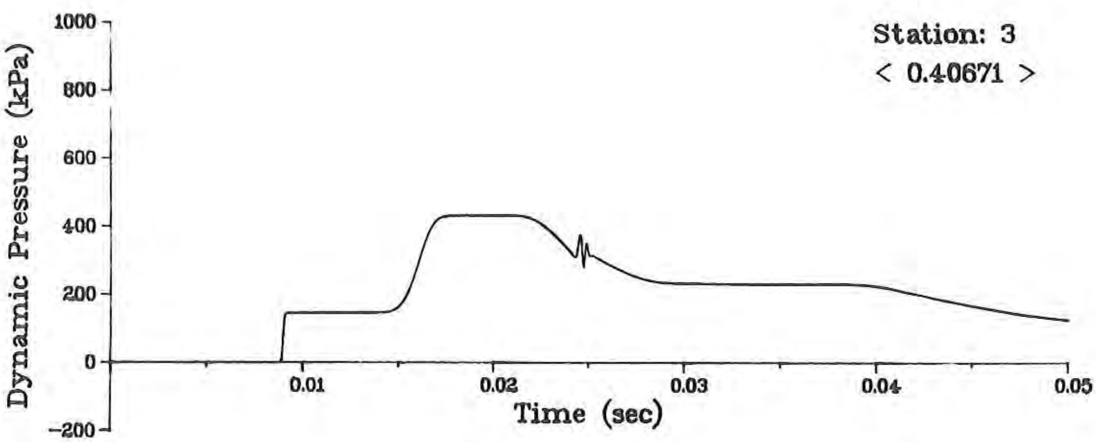

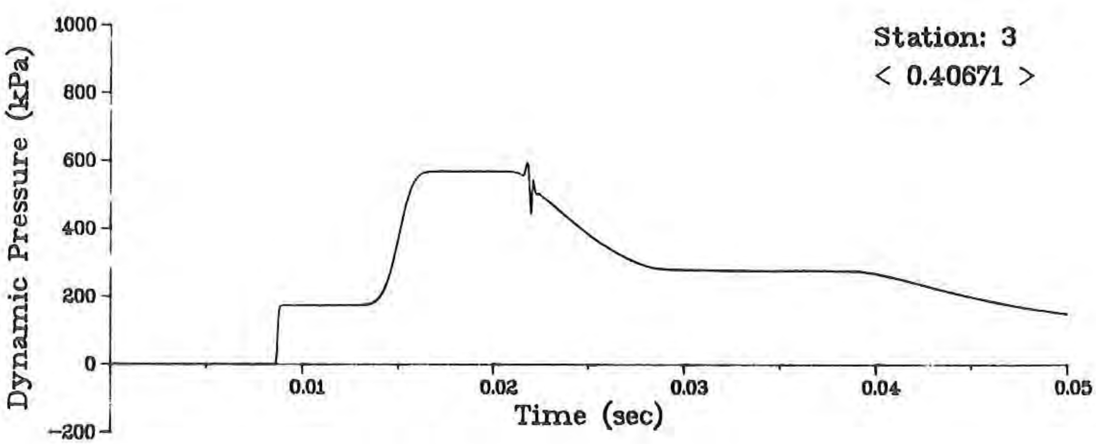

B. Station at 20 Diameters

Figure 22. Hydrocode Dynamic Overpressure Predictions - Long Driver; 7480, 10963, and 13169 kPa (Cont'd).

TABLE 5. COMPARISON OF COMPUTER CODE SIMULATION WITH MEASURED PARAMETERS; 288 CM DRIVER, 16:1 THROAT RATIO

A. Shock Front Overpressure, kPa

Shot Number	Driver Pressure kPa	BRL-Q1D Code Station 70	150	200	240	280	Experiment Station 70	150	200	240	280
18	300	13.1		Same			13.8	---	13.2	13.3	13.0
17	603	24.4		Same			23.5	22.8	23.2	23.0	22.0
19	1138	35.6		Same			38.0	38.3	38.0	37.6	37.0
20	2034	57.5		Same			60.4	60.0	61.2	60.4	57.0
16	3103	92.5		Same			88.0	85.0	86.5	82.5	82.5
21	4220	120.0		Same			106.5	100.0	100.0	100.0	93.0
14	5171			No Run			131.5	122.5	120.5	111.8	110.0
15	7480	180.8		Same			155.0	156.0	153.8	155.0	150.0
22	10963	238.5		Same			193.0	193.0	190.0	191.0	177.5
23	13169	257.7		Same			215.0	212.0	212.0	210.0	203.0

B. Cold Gas Arrival After Shock Front, ms

20	2034	10.1	---	---	---	---	---	---	---	---	---
16	3103	5.7	---	---	---	---	5.0	---	---	---	---
21	4220	4.2	9.2	12.8	---	---	4.2	---	---	---	---
14	5171			No Run			2.8	7.3	10.4	---	---
15	7480	2.6	6.3	8.4	9.7	11.6	2.2	6.1	8.5	10.7	---
22	10963	1.7	4.0	5.1	6.8	8.0	1.8	4.7	6.0	7.6	8.8
23	13169	1.6	3.7	4.7	5.5	6.6	1.7	4.3	5.2	6.6	7.5

TABLE 5. COMPARISON OF COMPUTER CODE SIMULATION WITH MEASURED PARAMETERS; 288 CM DRIVER, 16:1 THROAT RATIO (CONT'D)

C. Cold Gas Drag Enhancement Ratio

Shot Number	Driver Pressure kPa	BRL-Q1D Code Station 70	150	200	240	280	Experiment Station 70	150	200	240	280
20	2034	1.33	---	---	---	---	---	---	---	---	---
16	3103	1.51	---	---	---	---	---	---	---	---	---
21	4220	1.75	1.77	---	---	---	---	---	---	---	---
14	5171			No Run			---	1.32	1.20	1.15	1.06
15	7480	2.42	2.27	2.27	2.22	---	---	1.48	1.50	1.50	1.26
22	10963	3.04	2.95	2.95	2.90	2.92	---	1.58	1.60	1.60	1.63
23	13169	3.33	3.48	3.45	3.45	3.36	---	1.80	1.90	1.90	1.90

D. Recompression Fan Arrival After Shock Front, ms

21	4220	---	---	---	---	---	4.2	---	---	---	---
14	5171			No Run			3.5	---	---	---	---
15	7480	8.0	17.6	29.5	---	---	3.5	14.0	---	---	---
22	10963	5.3	11.3	15.5	20.0	25.2	3.2	10.0	---	---	---
23	13169	4.5	9.8	12.6	16.0	19.7	3.8	10.1	12.9	18.0	---

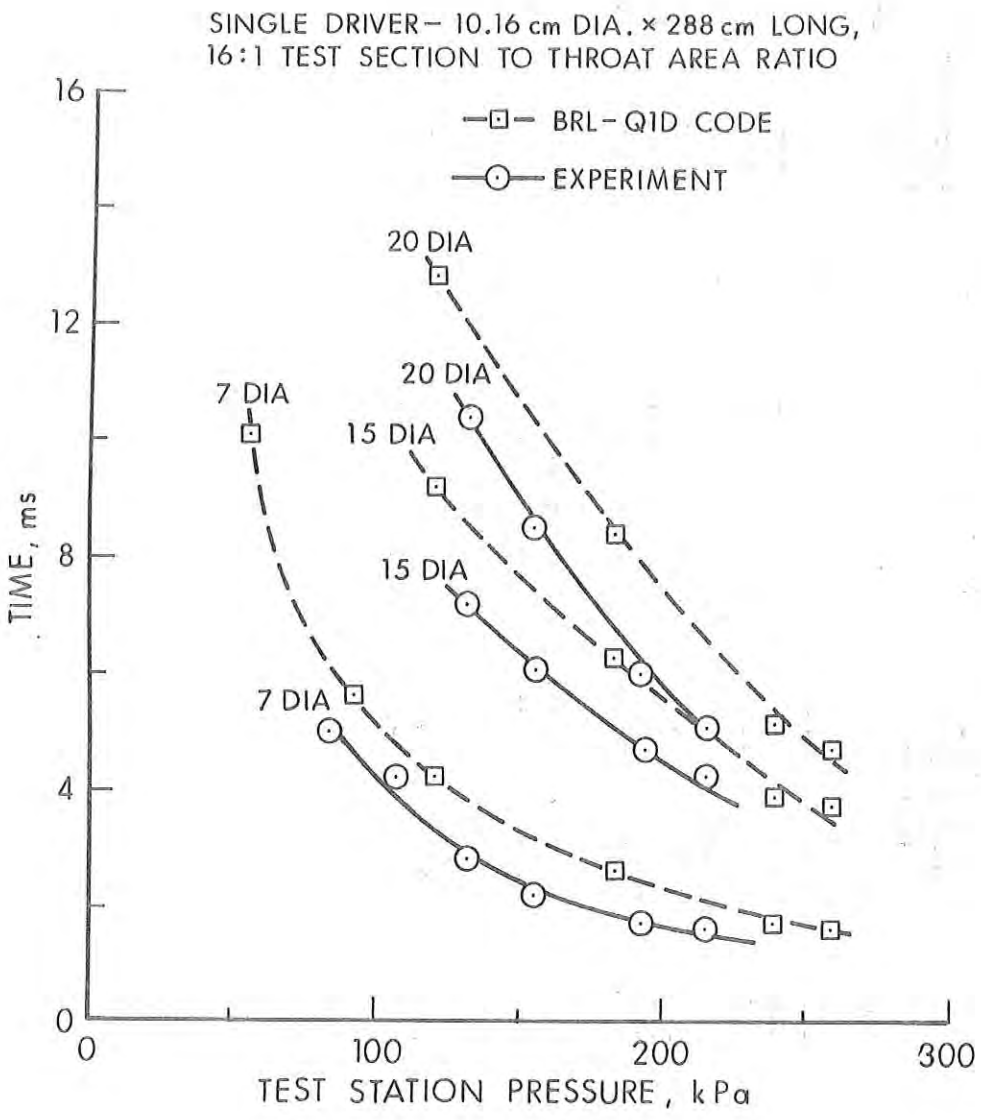

Figure 23. Arrival Time of Cold Gas after Shock Front Arrival at Test Station.

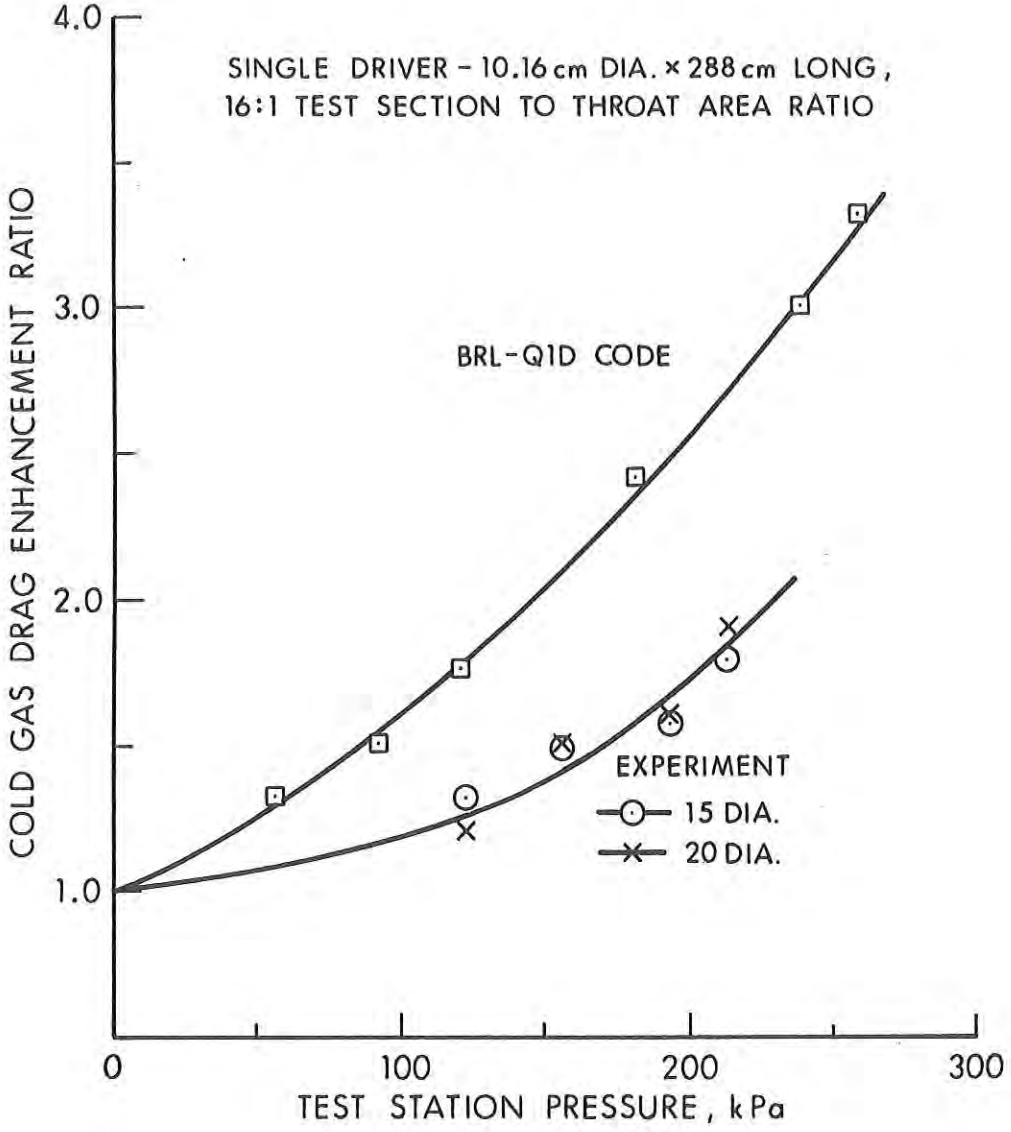

Figure 24. Drag Enhancement Ratio - Caused by Cold Gas Arrival at Test Station.

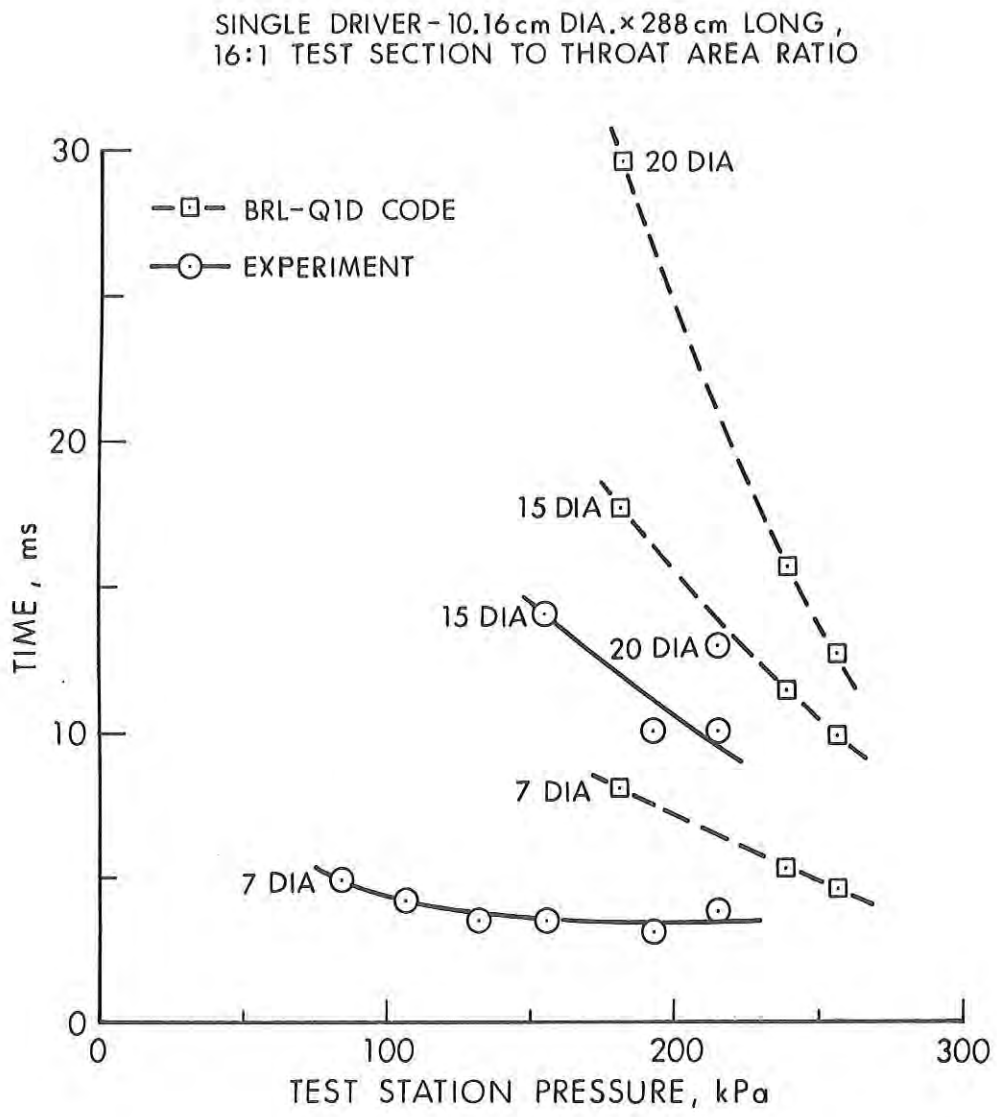

Figure 25. Arrival Time of Recompression Fan after Shock Front Arrival at Test Station.

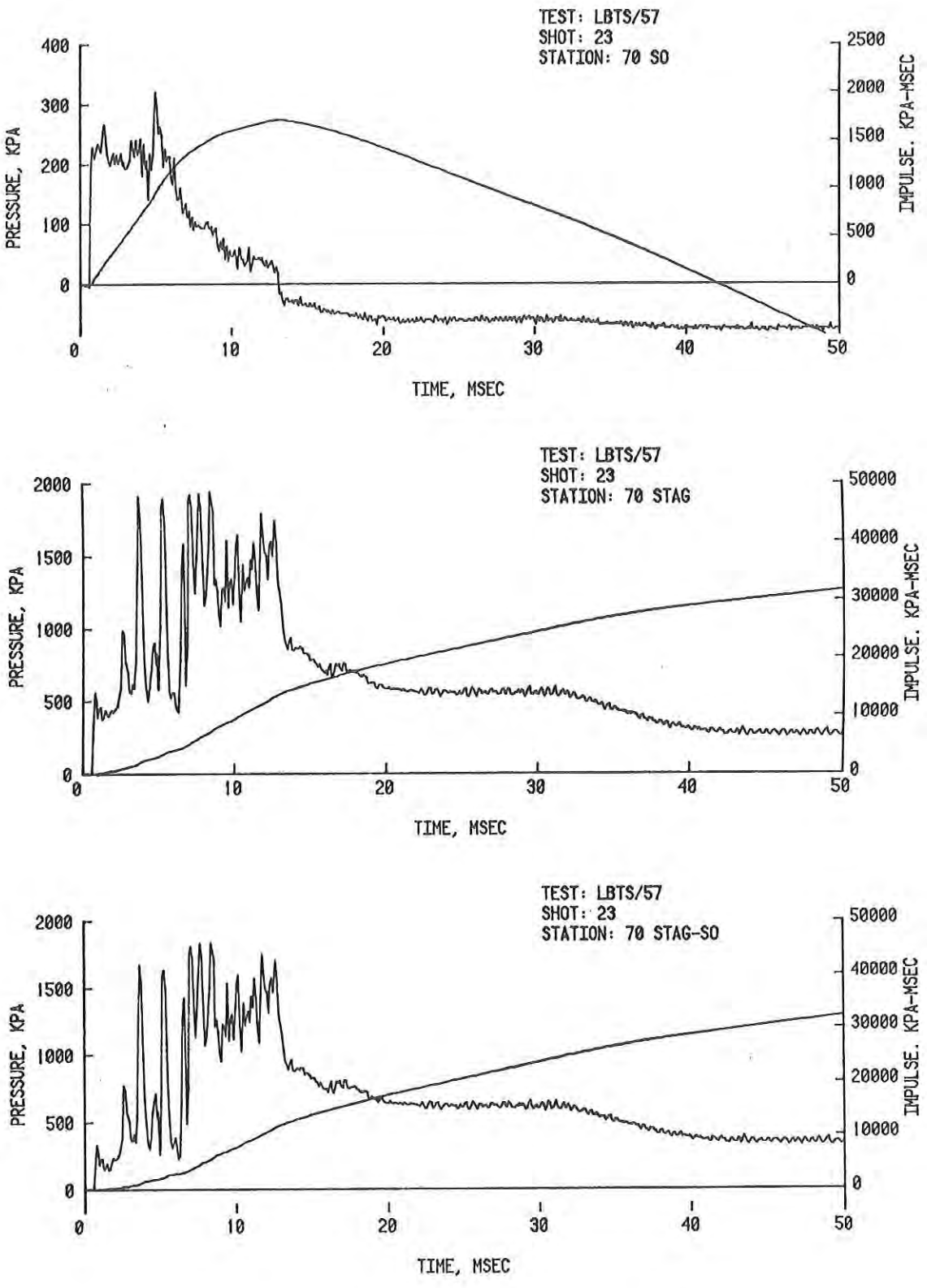

A. Long Driver - Station 70, 16:1 Throat Ratio

Figure 26. Comparison of Cold Gas Effects for Different Driver Configurations.

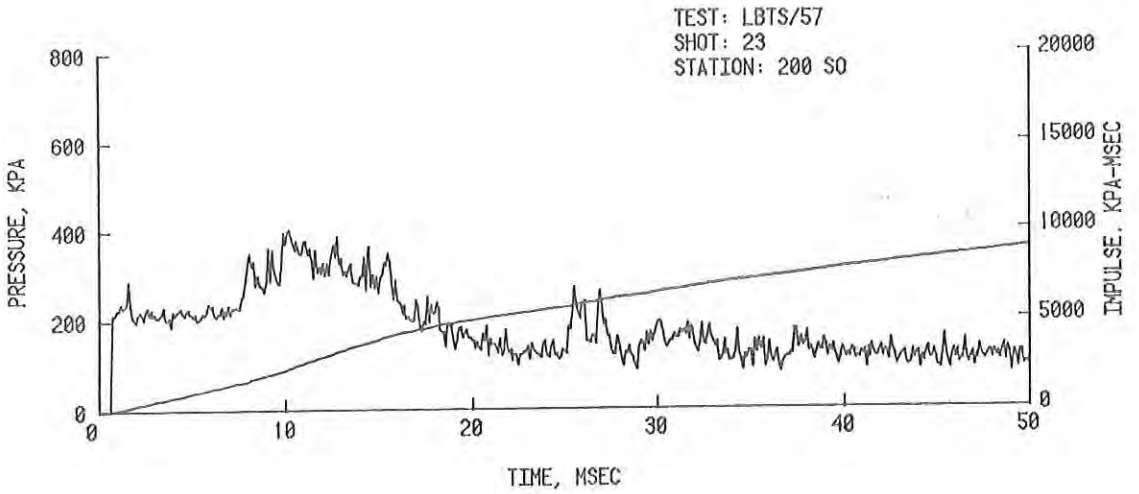

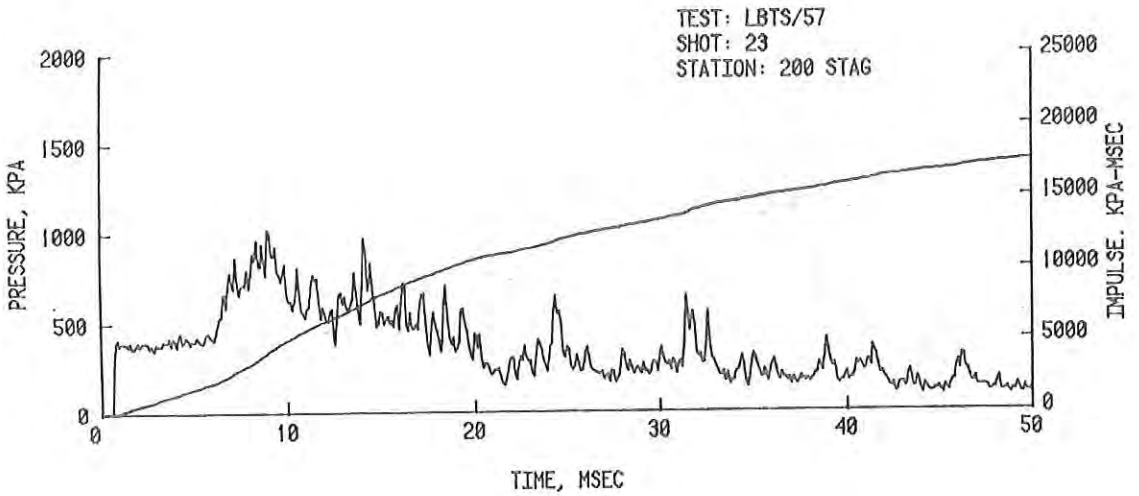

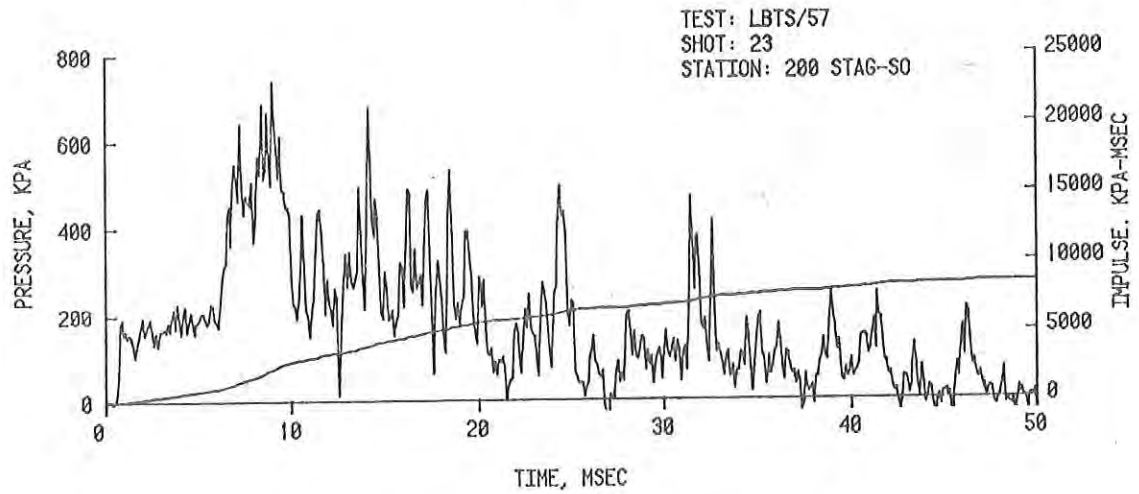

B. Long Driver -- Station 200, 16:1 Throat Ratio

Figure 26. Comparison of Cold Gas Effects for Different Driver Configurations (Cont'd).

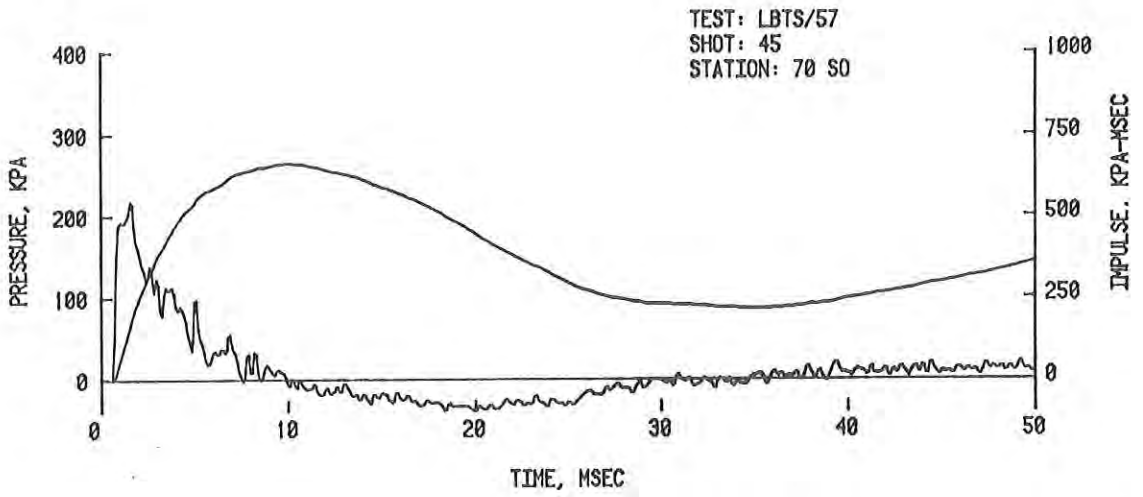

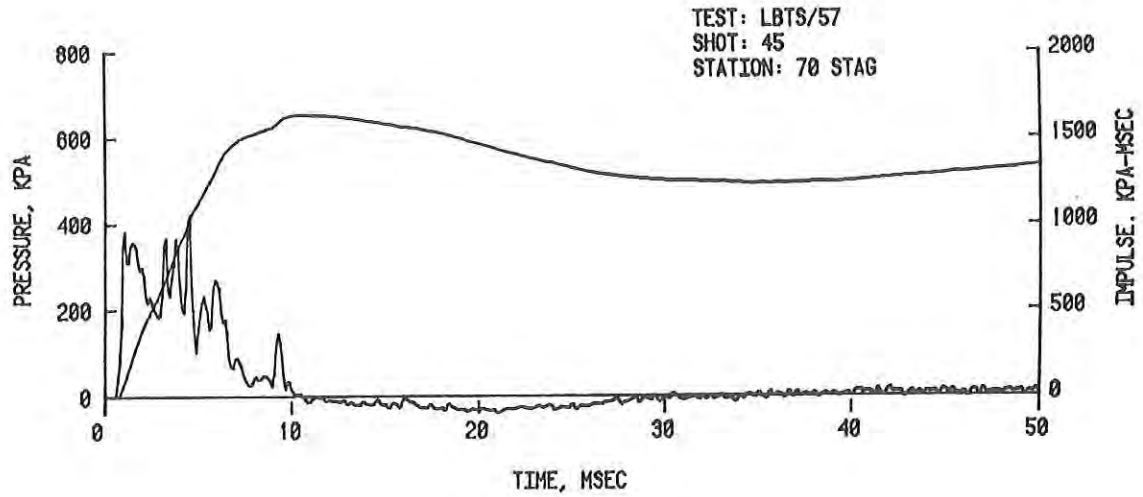

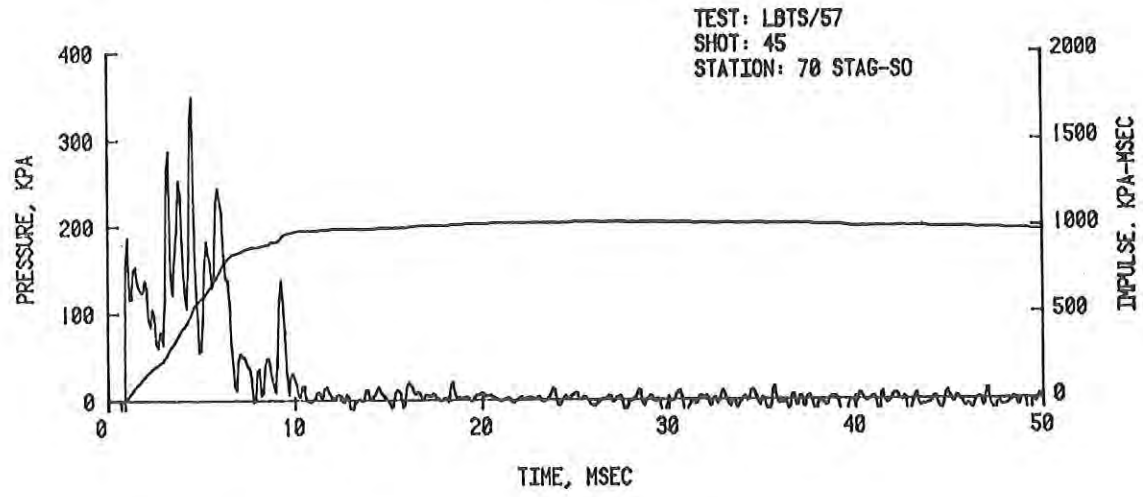

C. Short Driver - Station 70, 16:1 Throat Ratio

Figure 26. Comparison of Cold Gas Effects for Different Driver Configurations (Cont'd).

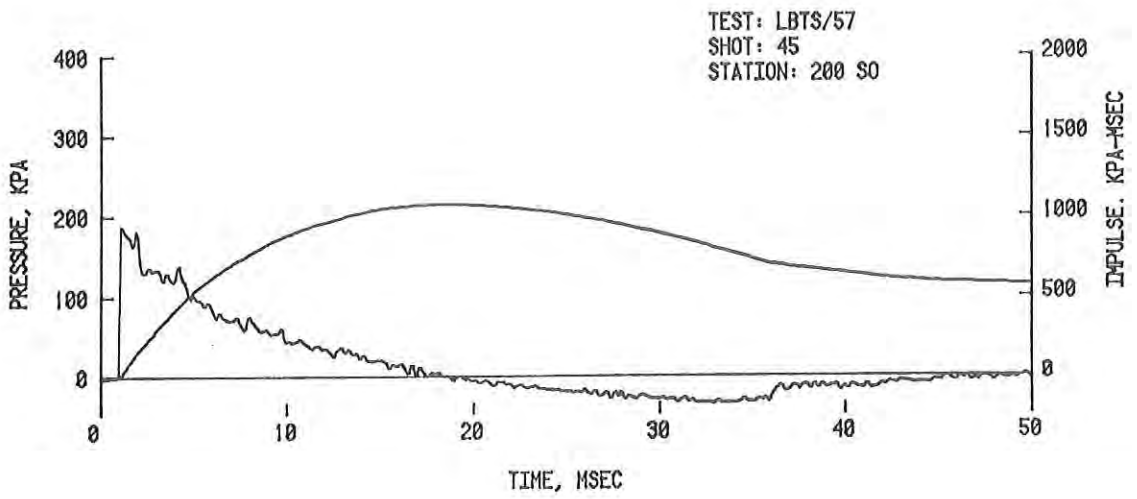

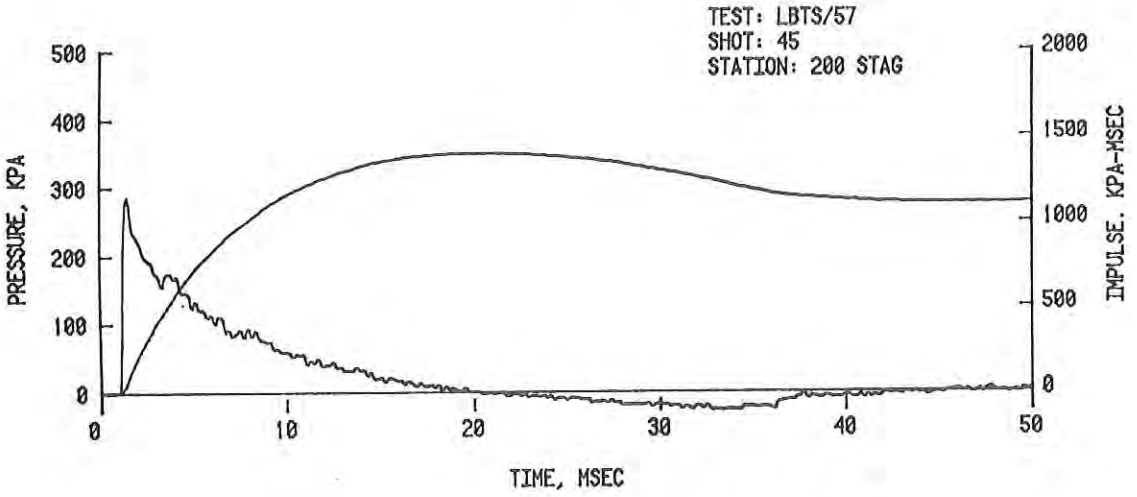

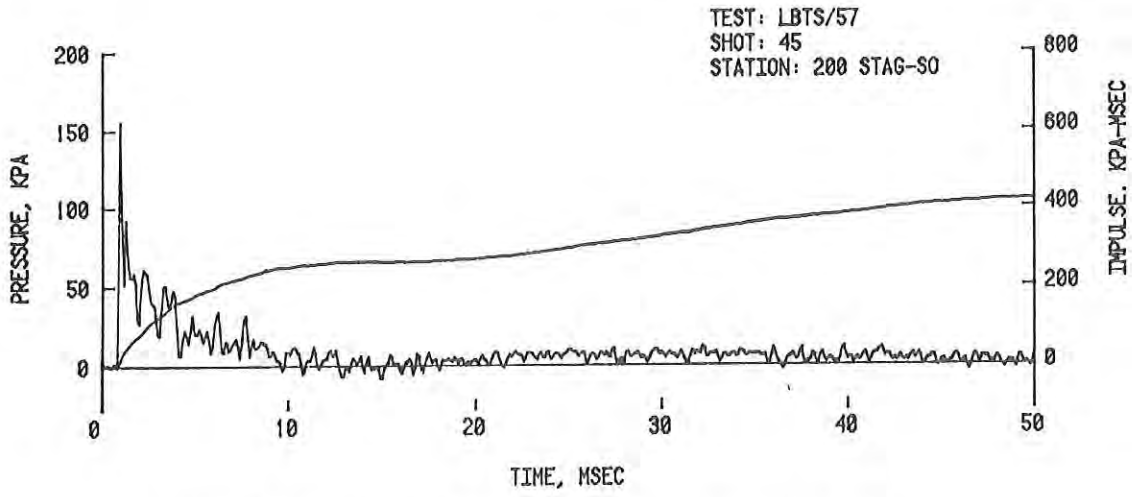

D. Short Driver - Station 200, 16:1 Throat Ratio

Figure 26. Comparison of Cold Gas Effects for Different Driver Configurations (Cont'd).

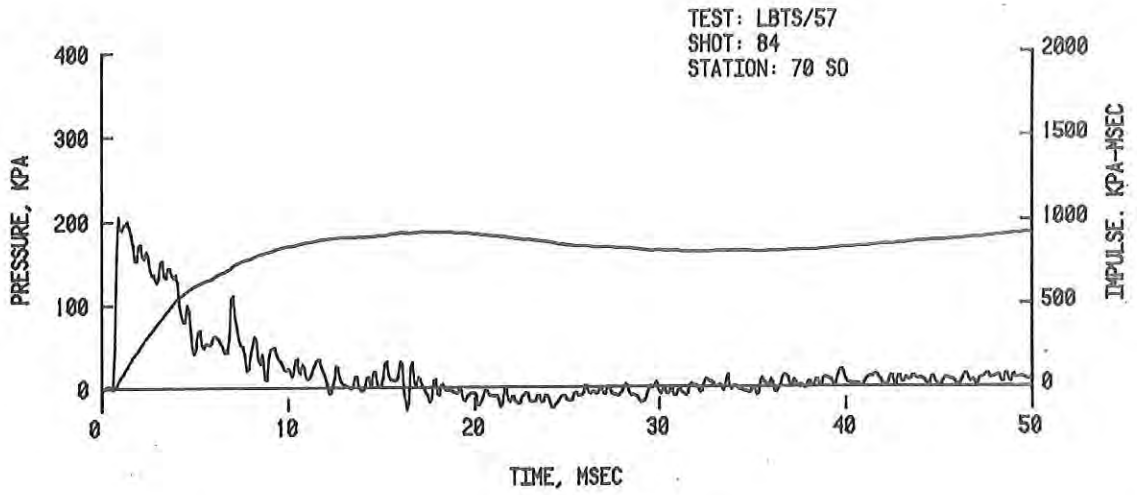

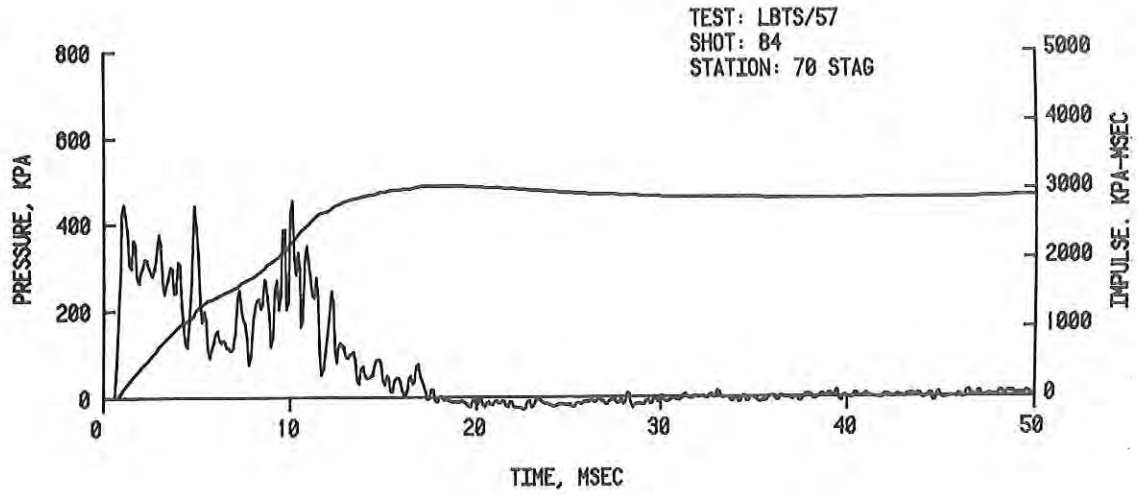

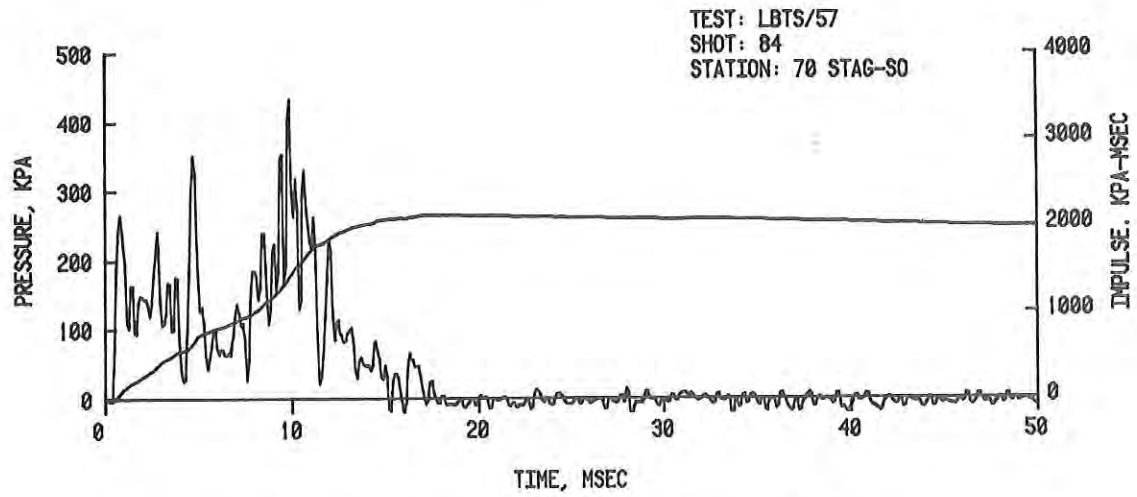

E. Short Driver - Station 70, 33:1 Throat Ratio

Figure 26. Comparison of Cold Gas Effects for Different Driver Configurations (Cont'd).

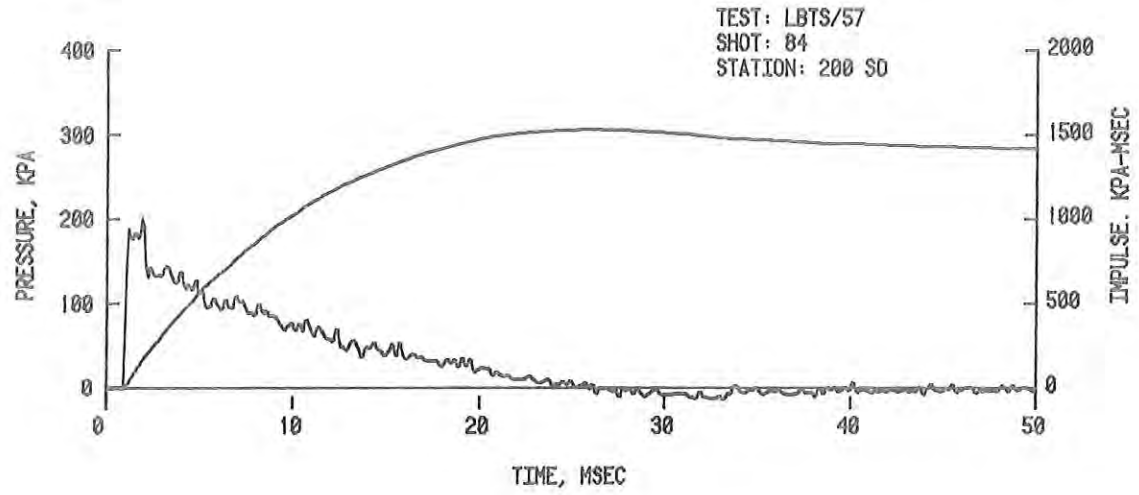

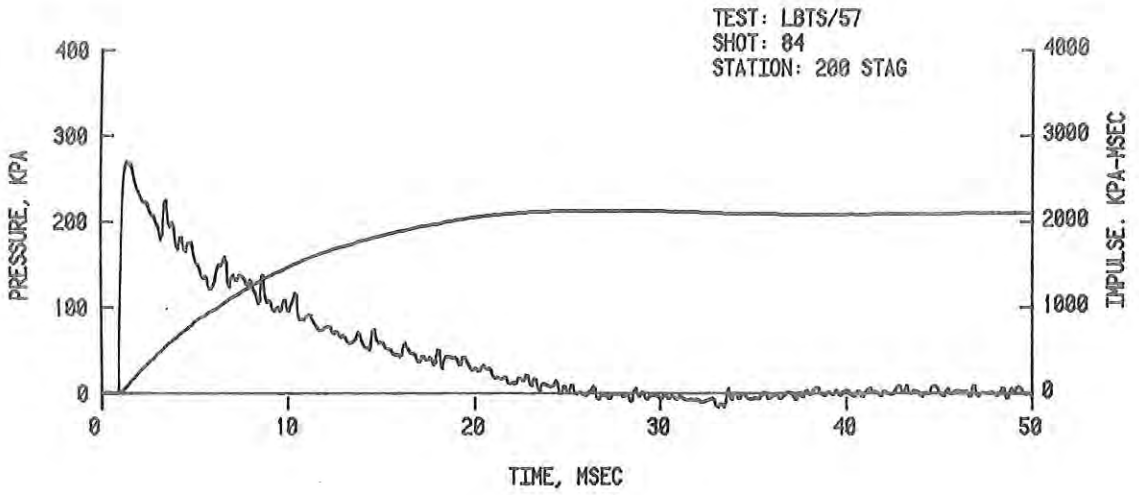

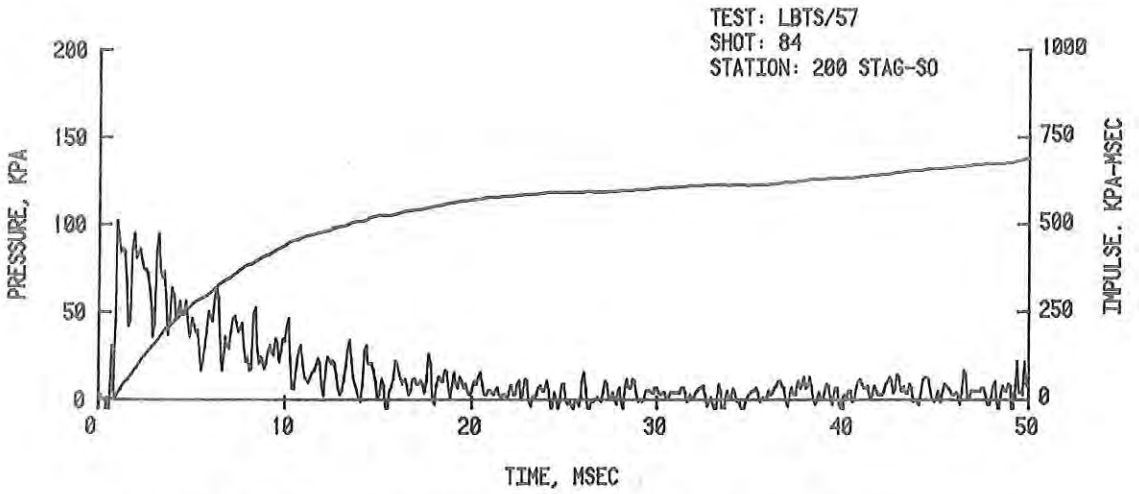

F. Short Driver - Station 200, 33:1 Throat Ratio

Figure 26. Comparison of Cold Gas Effects for Different Driver Configurations (Cont'd).

11.13 cm, driver. Indeed, the shorter driver does show the lesser effects on the records but are still unacceptable for a correct simulation of field yields at this pressure level if taken at 7 diameters. Station 200 (20 dia.) does show an improvement with acceptable records as seen in Figure 26-D and 26-F.

Accordingly, the full-size predictions for a single, cold gas driver simulator as presented in the next section are generally for the 20 diameter station.

4. ANALYSIS

The analysis includes a discussion of the full-size simulator yield predictions as calculated from side-on overpressure impulse scaled from Reference 8 data, and the effects of changing the throat baffle ratio at the diaphragm section.

4.1 Yield Predictions as a Function of Driver Configurations. As shown in the Test Matrix of Table 1, a series of drivers from 6.05 cm to 288 cm was used on the model for a driver pressure range of about 300 kPa to 1800 kPa. Side-on overpressures at 7 diameters varied from about 10 kPa to 225 kPa.

Reference 9 presents scaling laws relating the blast parameters between explosive yields. The treatment of yield here will consider ground bursts and the impulse available at a given overpressure from a certain yield in kilotons (kt).

The calculations of predicted yield for the full-size simulator were made by first scaling up the impulse from the model experiments, by multiplying by the scale factor of 57. At the same time, driver configurations were scaled in the same way. Table 6 lists the full-size predicted peak overpressure and impulse as a function of driver pressure and configuration. Predicted records of pressure versus time and impulse versus time for stations at 7 to 20 diameters for the full-size simulator are shown in Figures 27 and 28. Figures 29 and 30 summarize the full-scale impulse as a function of driver parameters. Driver lengths and volumes are noted on each curve.

Values of full-scale impulse from Table 6 were then compared to the values given in Figure 31. This figure is a plot of data taken from the Defense Nuclear Agency (DNA) blast program listed in Reference 8. The yields were then found from Equation 1.

$$I_1/I_2 = (W_1/W_2)^{1/3}, \qquad (1)$$

where I_1 is the impulse for a given reference yield, W_1, (in this case, 1 kt) and I_2 is the impulse at the same pressure level for the predicted yield, W_2. Impulse is given in kPa-s and yield in kt for simulation of nuclear explosions.

It should be noted that for other field scenerios, other yields may be calculated for height-of-bursts (HOB), or for dynamic overpressure impulse,

The text is continued on page 79.

TABLE 6. PREDICTED YIELD FOR FULL-SIZE FROM EXPERIMENTAL SIDE-ON OVERPRESSURE IMPULSE

Shot Number-Station	Driver Pressure kPa	Driver Length m	Driver Volume m^3	Throat Baffle Ratio	Side-on Overpressure kPa	Impulse kPa-ms	Yield kt
4-200	314	6.34	166.9	16:1	17.0	1.30	0.1
47-200	317	19.37	510.0		18.6	3.20	1.9
53-200	338	51.22	1348.6		14.0	7.47	34.0
55-200	359	101.93	2683.8		13.0	15.55	365.0
57-200	352	135.19	3559.5		13.0	18.66	632.0
6-200	1124	6.34	166.9		34.1	4.41	1.3
49-200	1096	19.37	510.0		49.1	9.62	7.6
79-200	1124	41.09	1081.9		42.5	20.50	91.0
78-200	1117	62.81	1653.8		40.5	28.84	178.0
80-200	1145	83.07	2187.2		45.0	41.04	677.0
8-200	3137	6.34	166.9		66.7	10.57	6.3
69-200	3137	19.37	510.0		94.6	24.02	49.0
70-200	5171	19.37	510.0		127.0	36.54	132.0
75-200	3137	41.09	1081.9		94.0	48.88	411.0
77-200	3123	62.81	1653.8		99.0	72.66	1275.0
11-200	8274	6.34	166.9		113.4	23.95	44.0
71-200	8486	19.37	510.0		172.4	56.68	419.0
72-200	11549	19.37	510.0		202.5	75.09	882.0
13-200	14479	6.34	166.9		155.8	40.52	67.0
66-200	13962	10.68	281.2		192.0	60.00	466.0
65-70	17582	3.44	90.6		200.0	25.98	37.0
65-200	17582	3.44	90.6		141.0	30.78	74.0

TABLE 6. PREDICTED YIELD FOR FULL-SIZE FROM EXPERIMENTAL SIDE-ON OVERPRESSURE IMPULSE (CONT.)

Shot Number-Station	Driver Pressure kPa	Driver Length m	Driver Volume m^3	Throat Baffle Ratio	Side-on Overpressure kPa	Impulse kPa-ms	Yield kt
81-200	483	19.37	510.0	33:1	15.7	4.81	7.3
85-200	483	38.19	1005.5		15.7	9.09	51.0
89-200	496	54.12	1425.0		13.5	11.51	138.0
91-200	545	83.07	2187.2		15.0	20.69	641.0
35-200	2027	6.34	166.9		39.0	6.84	4.0
82-200	1827	19.37	510.0		39.3	16.74	58.0
86-200	1827	38.19	1005.5		40.6	31.35	356.0
90-200	1834	54.12	1425.0		39.8	41.04	771.0
37-200	5192	6.34	166.9		83.4	15.45	14.9
83-200	5199	19.37	510.0		88.9	37.60	198.0
87-200	5240	38.19	1005.5		94.9	74.10	1415.0
40-70	14479	6.34	166.9		195.3	32.37	72.0
40-200	14479	6.34	166.9		142.4	36.28	121.0
84-200	14789	19.37	510.0		200.0	86.96	1386.0
94-200	903	42.54	1120.1	64:1	13.0	18.80	681.0

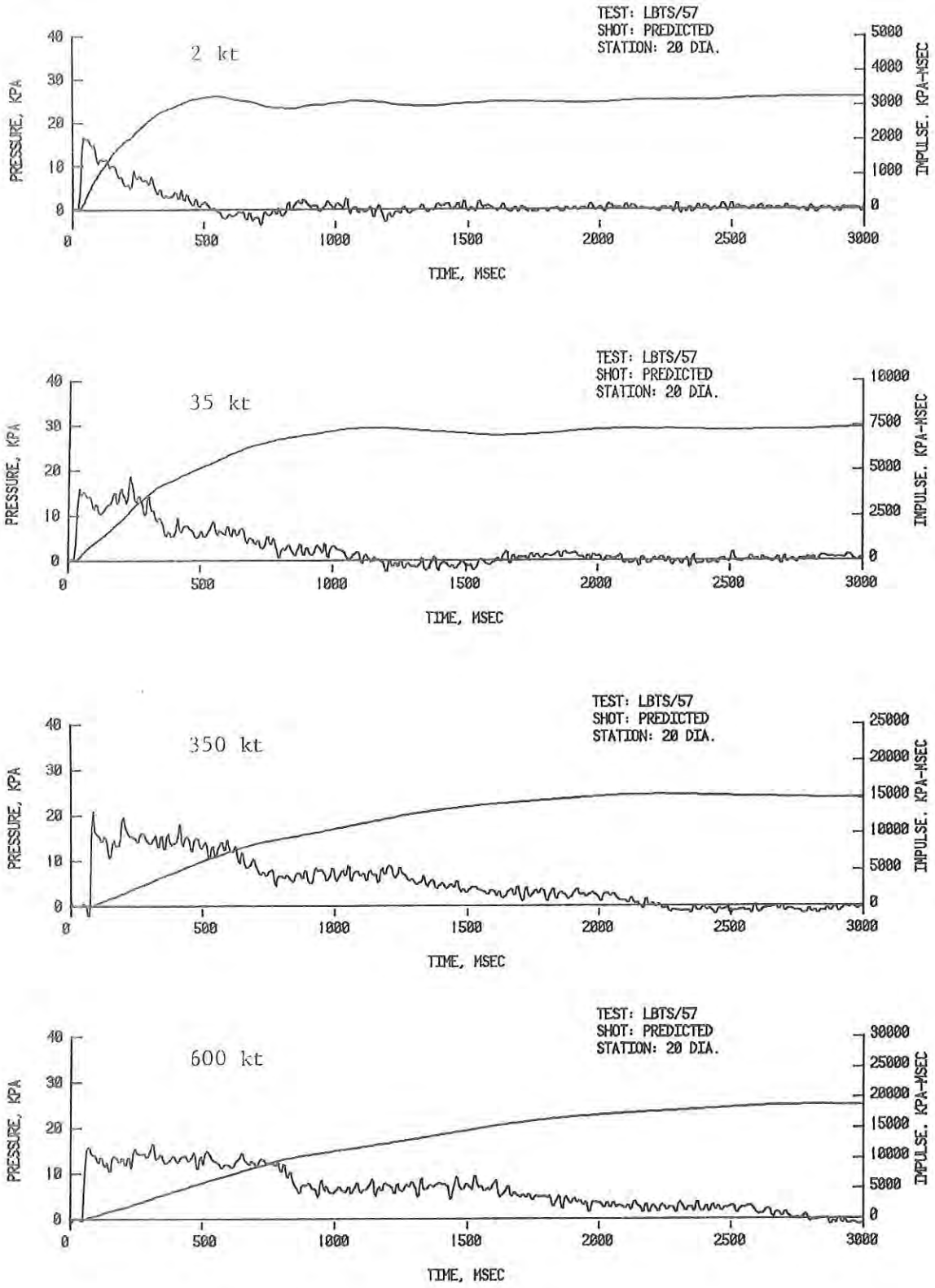

A. 15 kPa

Figure 27. Experimental Results Scaled to Full-Size; Yields for Station at 20 Diameters - 16:1 Throat Ratio.

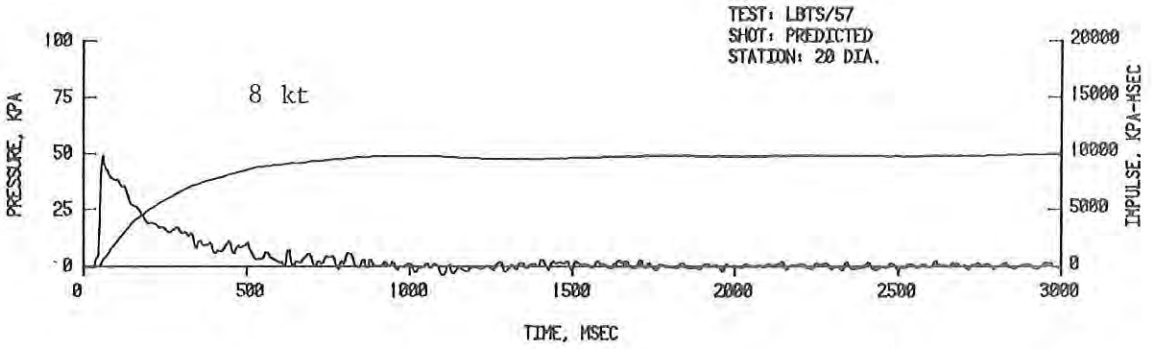

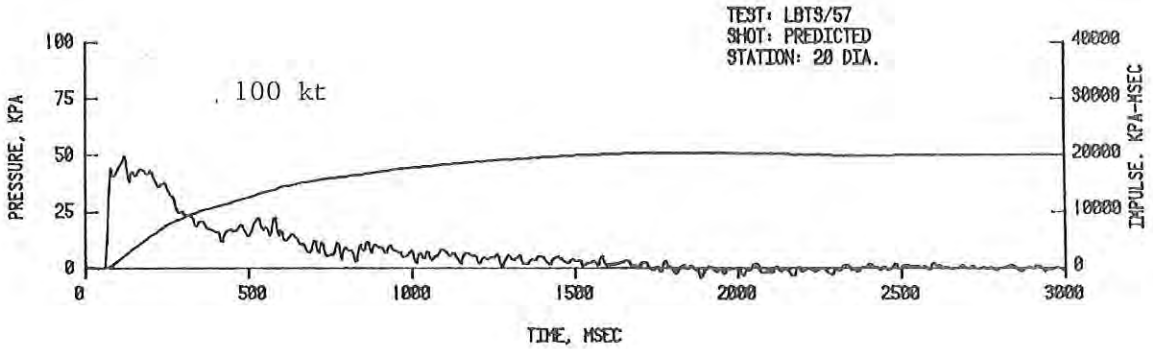

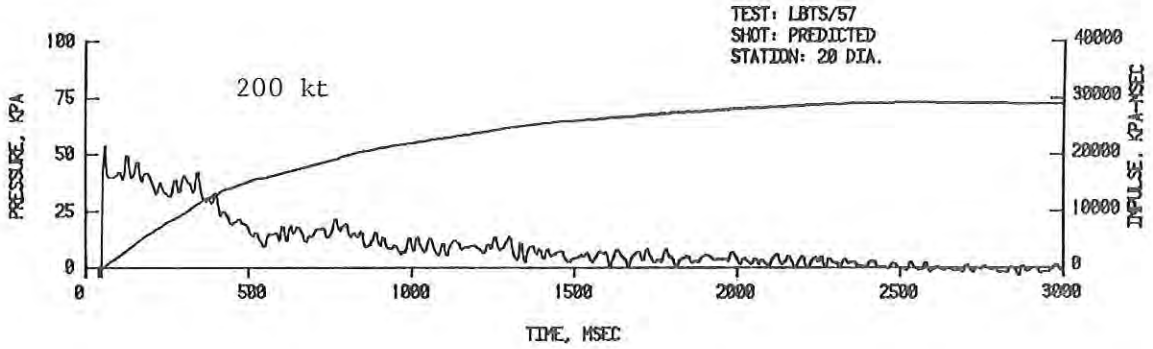

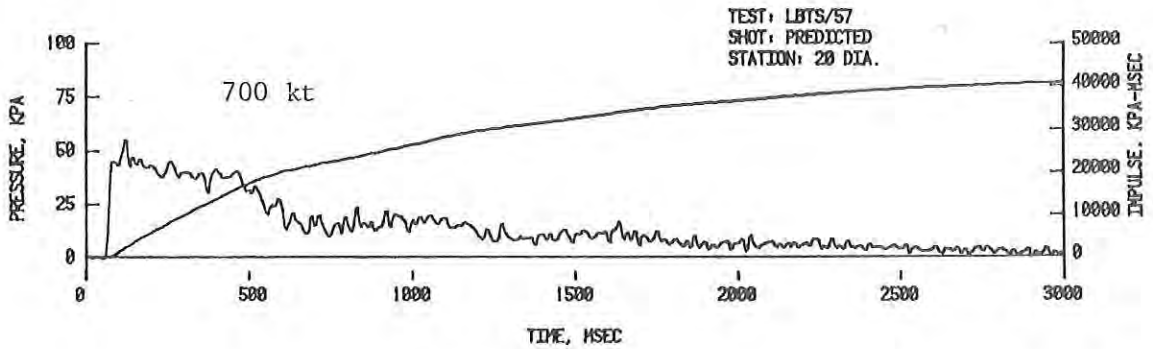

B. 45 kPa

Figure 27. Experimental Results Scaled to Full-Size; Yields for Station at 20 Diameters - 16:1 Throat Ratio (Cont'd).

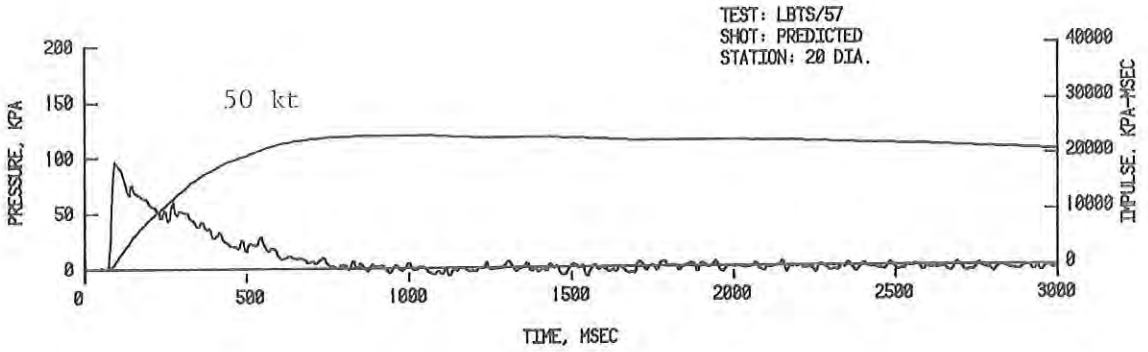

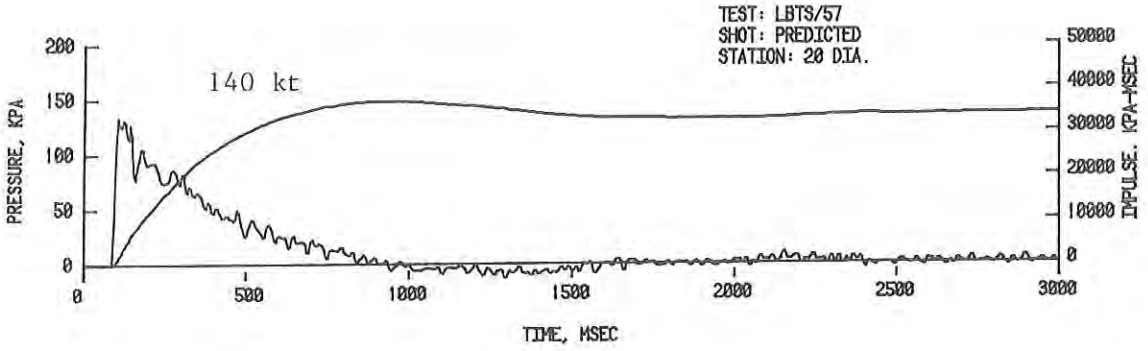

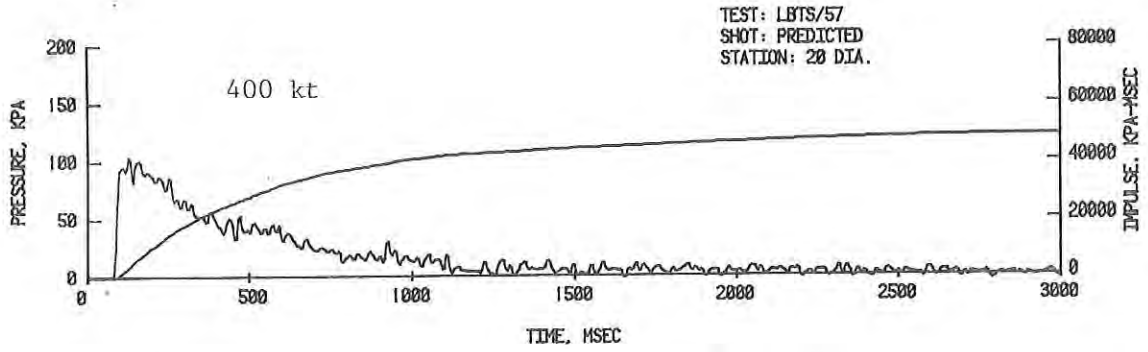

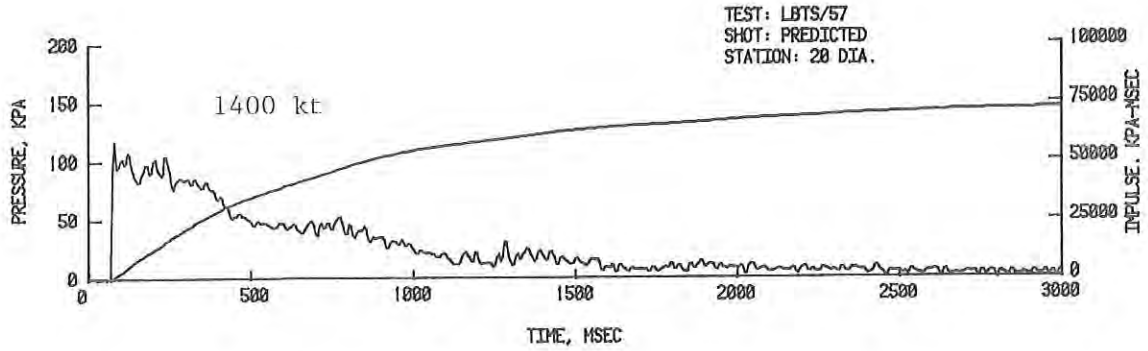

C. 100 kPa

Figure 27. Experimental Results Scaled to Full-Size; Yields for Station at 20 Diameters - 16:1 Throat Ratio (Cont'd).

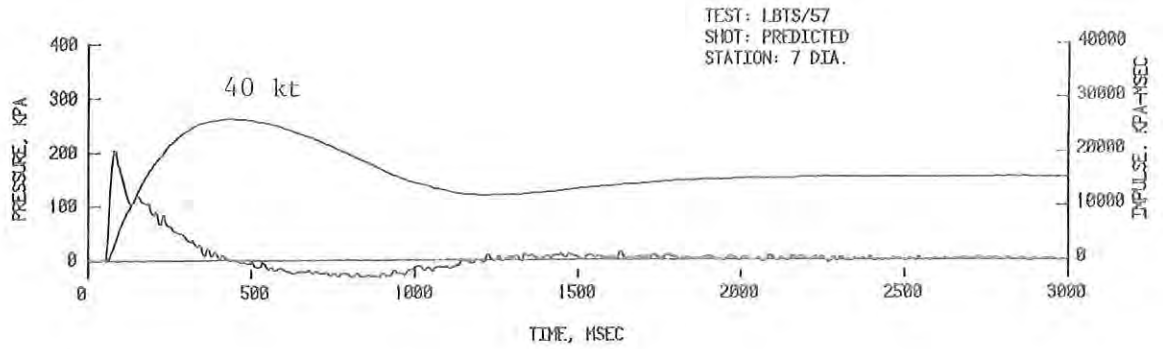

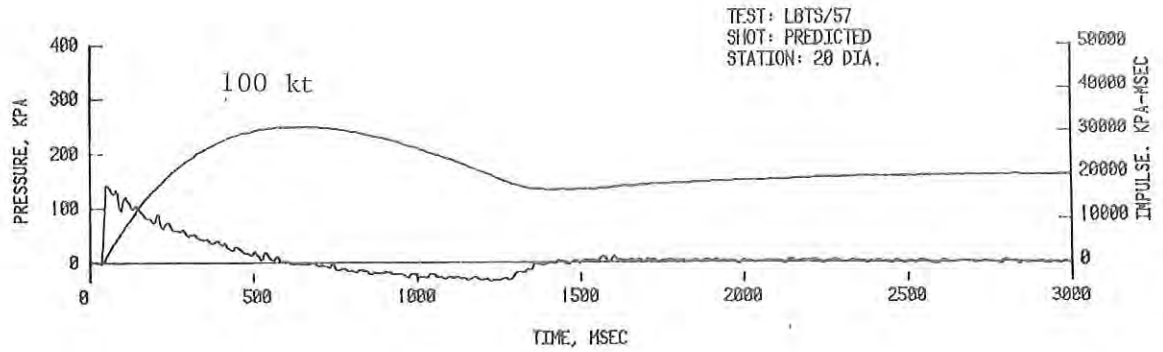

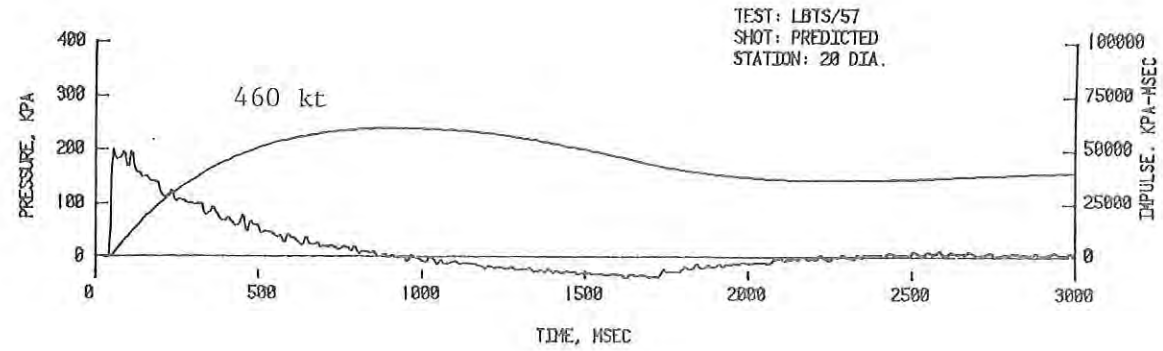

D. 140-200 kPa

Figure 27. Experimental Results Scaled to Full-Size; Yields for Station at 20 Diameters - 16:1 Throat Ratio (Cont'd).

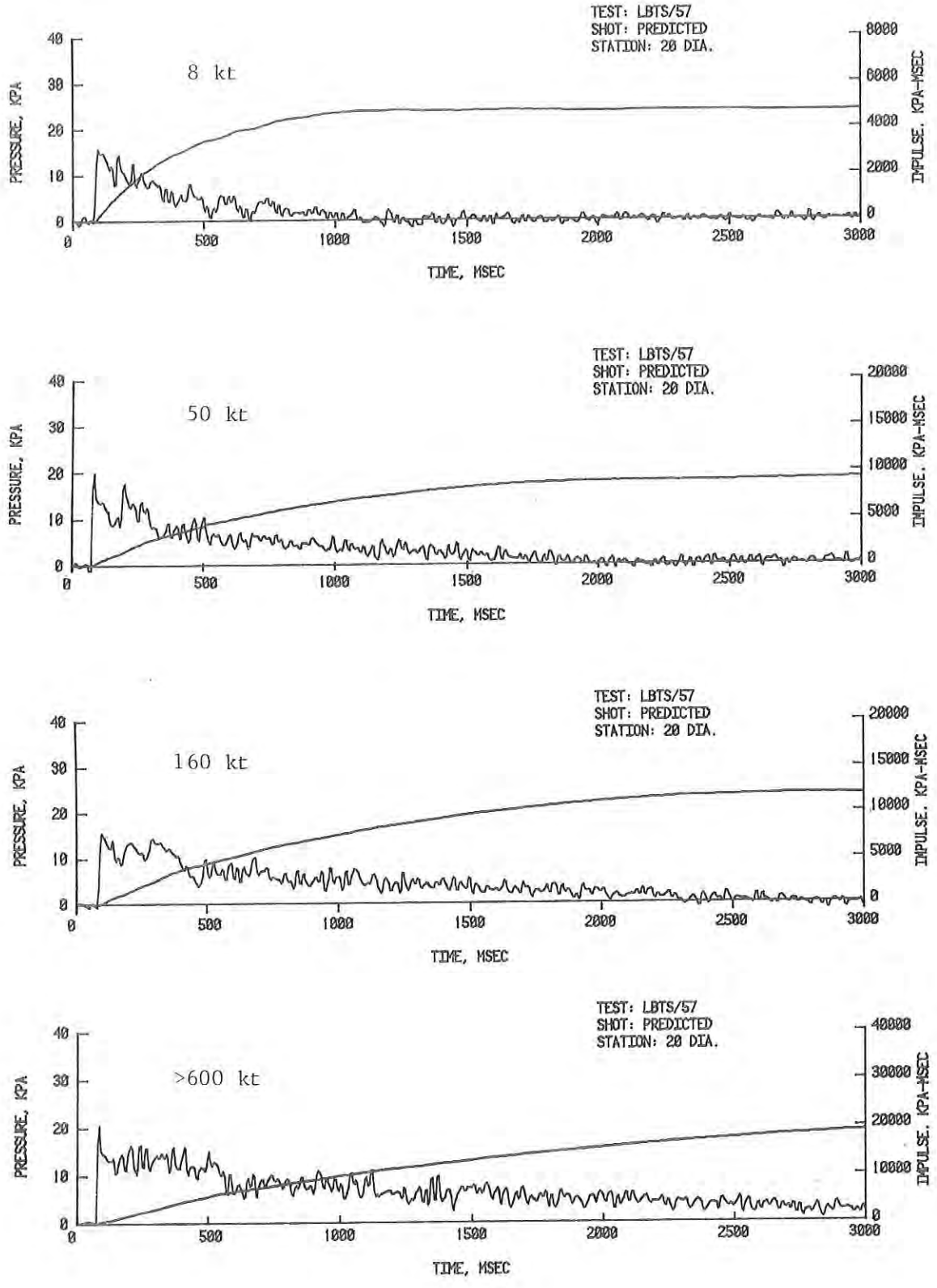

A. 15 kPa

Figure 28. Experimental Results Scaled to Full-Size; Yields for Stations at 7 or 20 Diameters - 33:1 Throat Ratio.

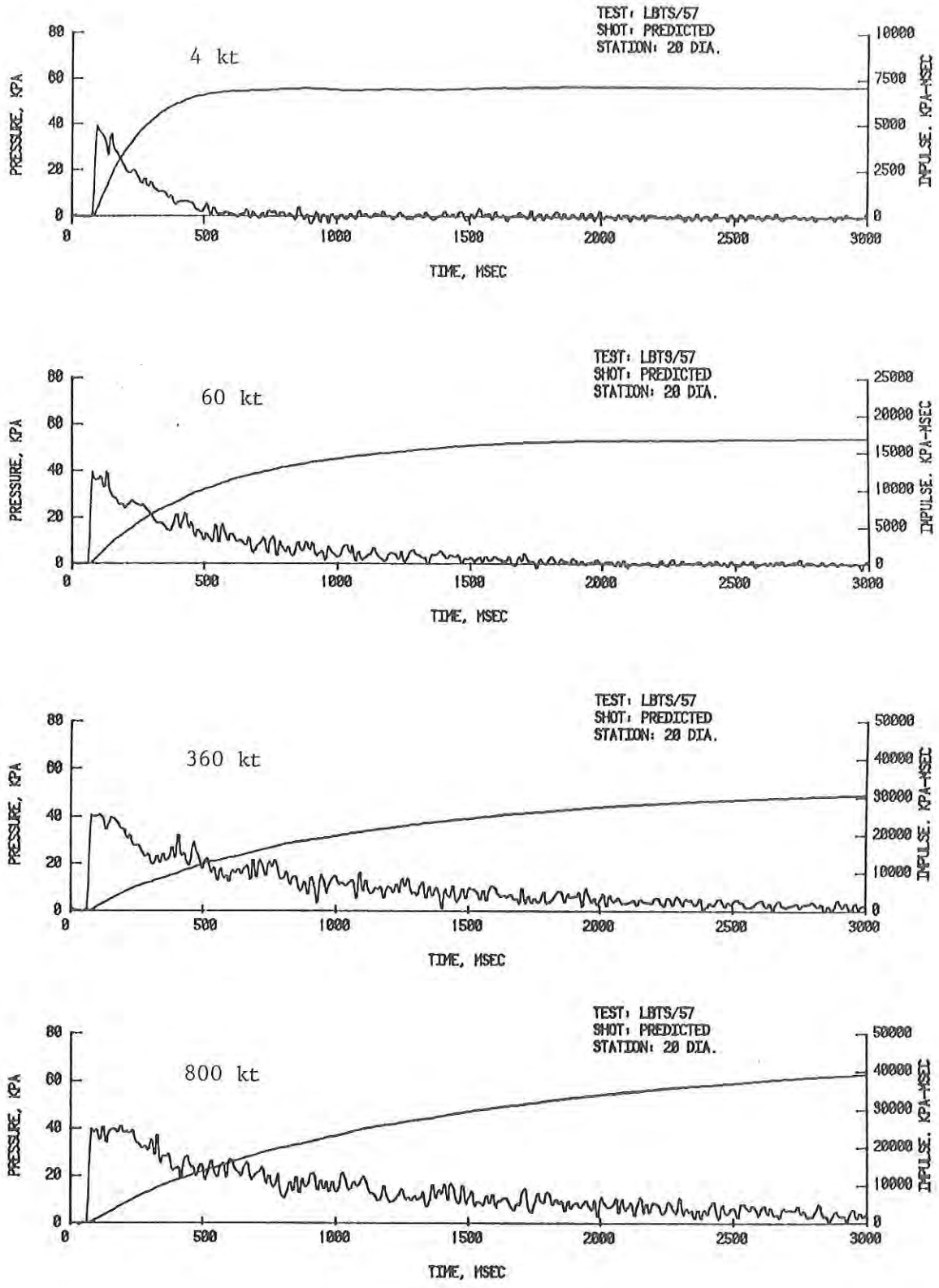

B. 40 kPa

Figure 28. Experimental Results Scaled to Full-Size; Yields for Stations at 7 or 20 Diameters - 33:1 Throat Ratio (Cont'd).

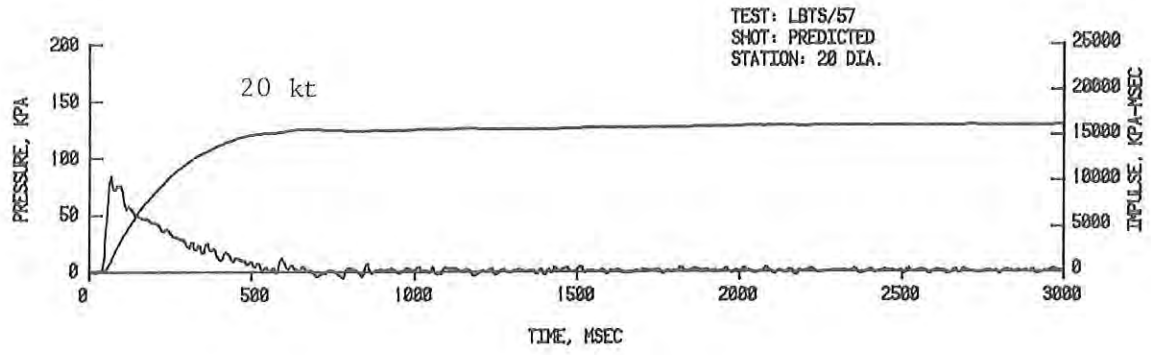

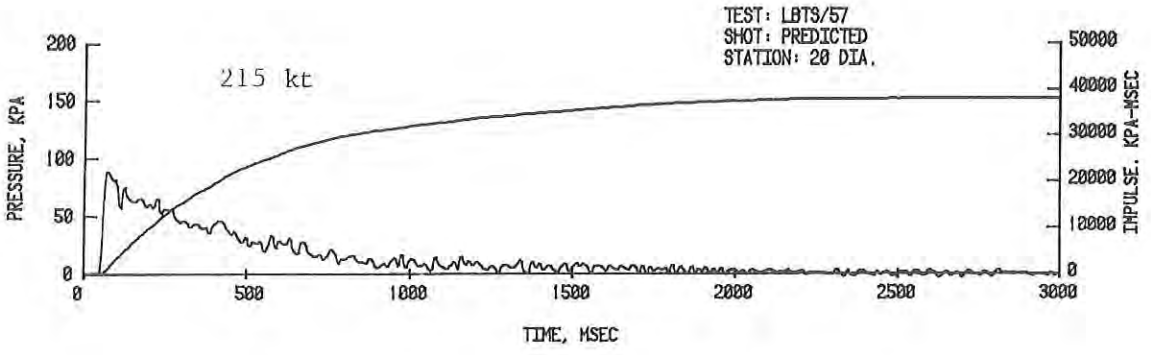

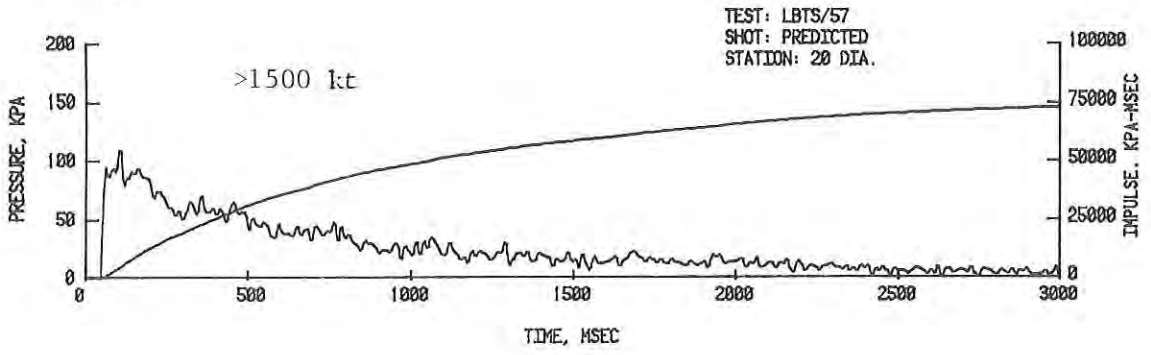

C. 90 kPa

Figure 28. Experimental Results Scaled to Full-Size; Yields for Stations at 7 or 20 Diameters - 33:1 Throat Ratio (Cont'd).

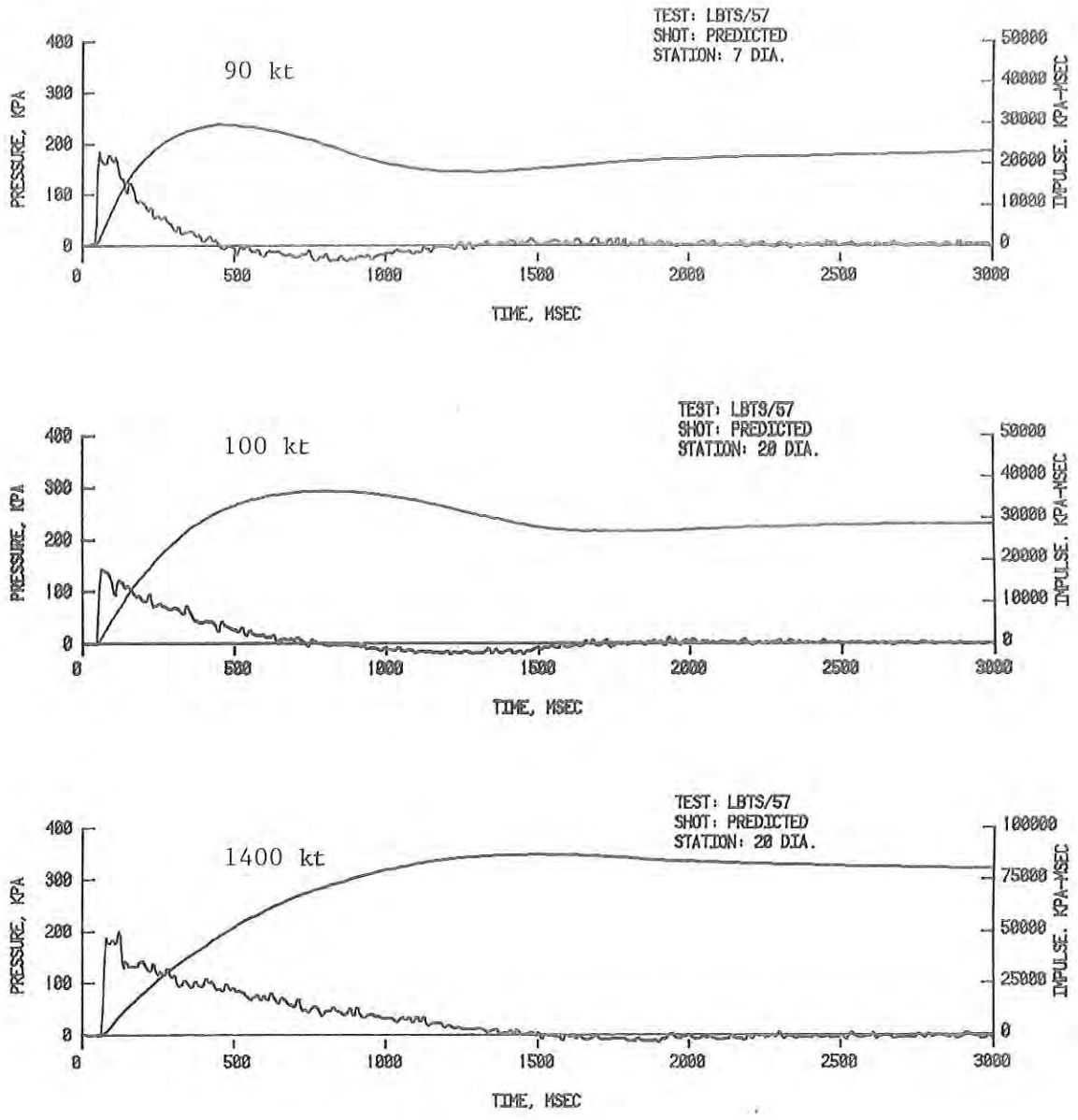

D. 140-200 kPa

Figure 28. Experimental Results Scaled to Full-Size; Yields for Stations at 7 or 20 Diameters - 33:1 Throat Ratio (Cont'd).

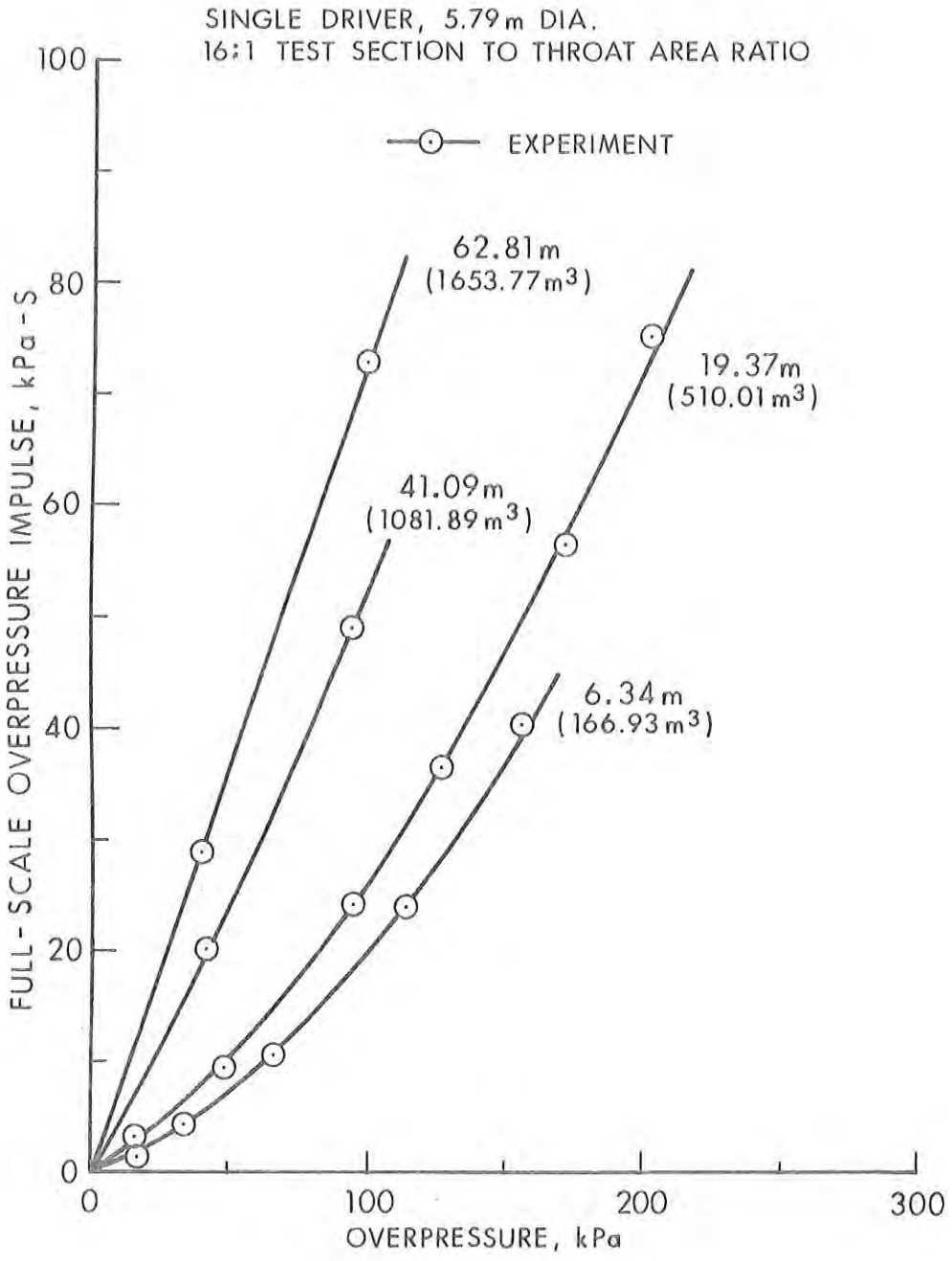

Figure 29. Full-Scale Impulse vs Side-On Overpressure at 20 Diameters; for Different Driver Lengths, 16:1 Throat Ratio.

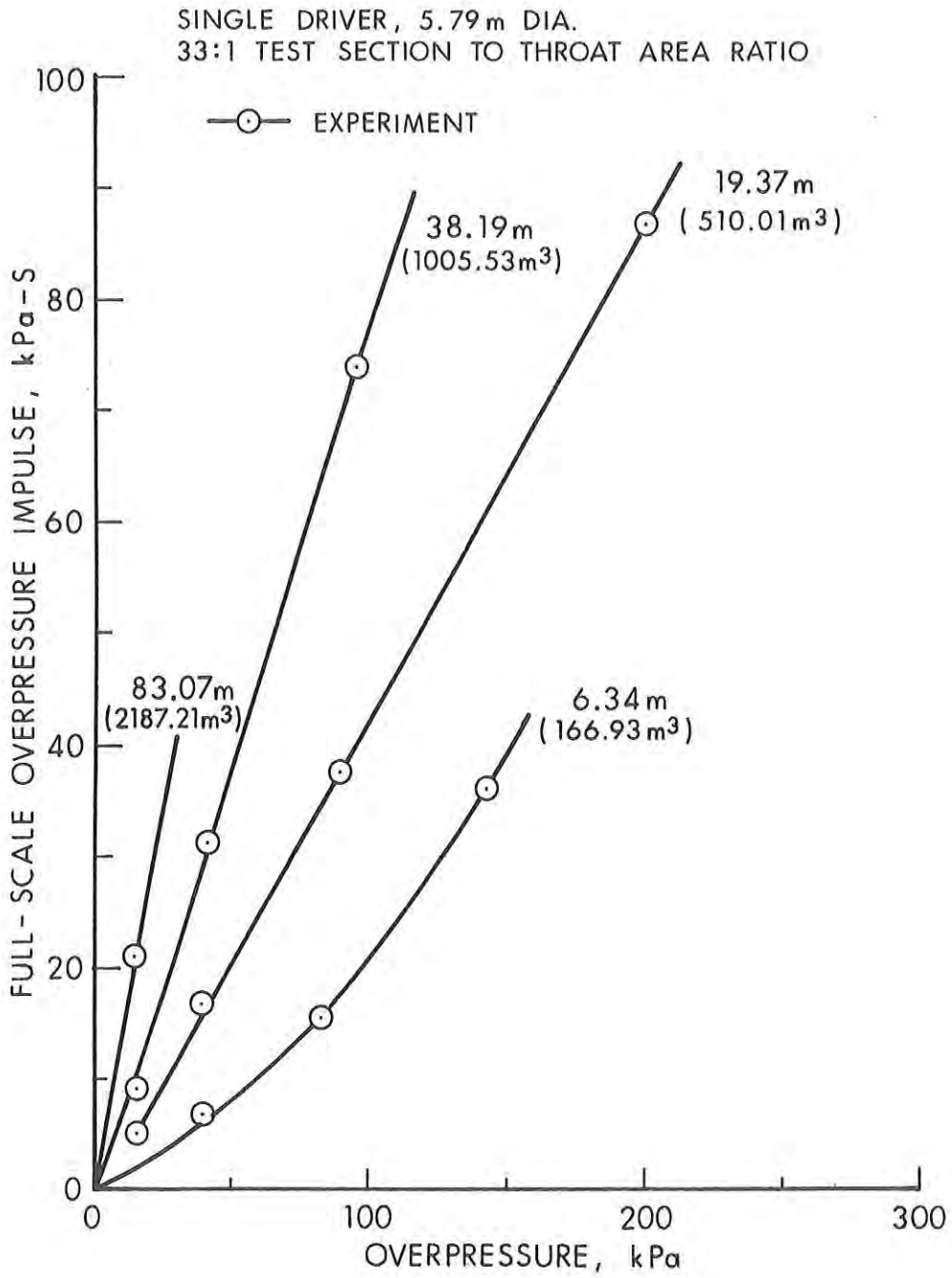

Figure 30. Full-Scale Impulse vs Side-On Overpressure at 20 Diameters; for Different Driver Lengths, 33:1 Throat Ratio.

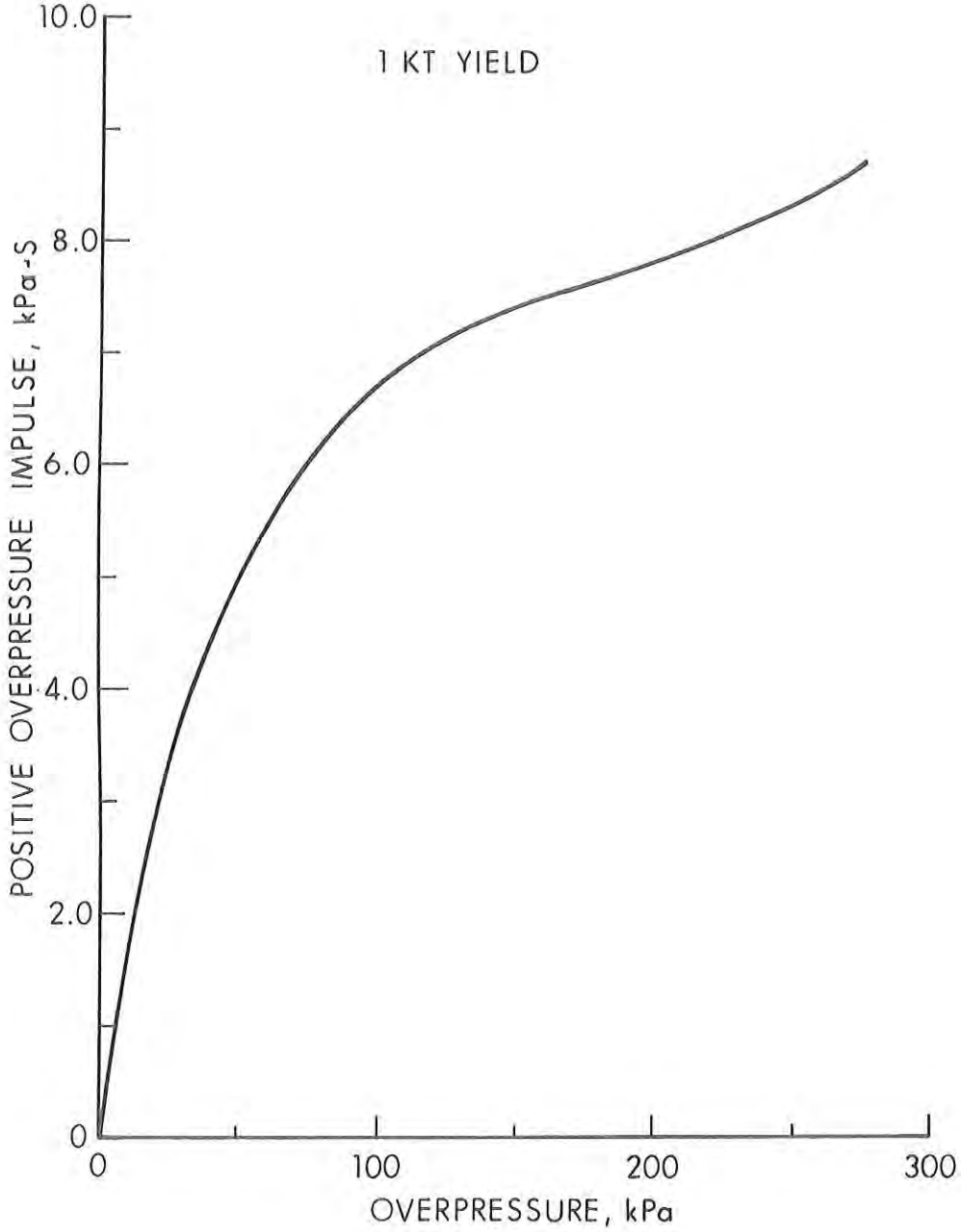

Figure 31. Impulse vs Side-On Overpressure for 1 kt Surface Burst.

if desired. The method of yield calculation would be the same, but impulses would be compared to another impulse-yield curve instead of Figure 31.

The yields as a function of side-on overpressure and driver/throat ratio configuration are presented in Figures 32 and 33. Data are plotted from both Tables 3 and 6 in order to compare Stations 7 and 20. These curves are ordered very well except for points on the 223 kPa set at the high yield end. There, the recompression fan has shortened the positive wave duration and the corresponding yield for a particular driver configuration. As a result, the curve turns away from the left axis to the right - indicating a longer driver is needed.

Table 6, above, lists the calculated full-size yields in the last column, as a function of the various test station pressure levels and the driver configurations used in the tests. The table illustrates the range of yields available for a single, cold gas driver design. Most are adequate except at low yields (below 50 kt) for test station pressures above 200 kPa. The decay rate caused by the relatively short positive durations needed, will be substantial. The driver pressure then would have to be increased to achieve the desired test station pressure level. This would add additional expensive material design constraints on the driver. A heated driver design would probably be a better trade-off for a large simulator than designing for the expected increased driver pressure needed.

4.2 Throat Baffle Effects. A major element in the design of the driver configuration is the test section to throat baffle area ratio (baffle ratio). As noted in the tables and graphs, throat ratios of 16:1, 33:1, and 64:1 were listed for this set of experiments. The throat baffle size is most important when designing for large yields (600 kt/at low test pressures (13-15 kPa in these tests)). Values from Table 6 show the effect of the change in throat baffle ratio. Figure 34 illustrates the similarity of waveforms obtained by varying the driver length, the driver pressure, and the baffles ratio. To summarize, the increasing baffle ratio (smaller area baffle) restricts the driver flow to add more duration to a waveform produced by a given driver length. The peak overpressure produced becomes a smaller value at the same time.

Figure 34 illustrates the results of three baffle ratios used. The maximum driver length needed at the 13-15 kPa overpressure was 42.5 m (full-size) when it was used with the 64:1 baffle ratio; whereas, a 135 meter length is needed for the 16:1 baffle ratio. A penalty in increased driver pressure must be paid, however, for the shortened driver as is seen from Figure 35. The driver pressure (noted in parenthesis) must be roughly doubled for a throat ratio increase of two times if the test section pressure is to be maintained. At low driver pressures, the smaller length driver probably will still be a cost effective design for the full-size simulator.

5. SUMMARY AND CONCLUSIONS

Experimental data have been obtained and compared with BRL-Q1D hydrocode predictions of blast effects obtained for a 1:57 scale shock tube model of a single cold air driver for large blast thermal simulator.

The text is continued on page 84.

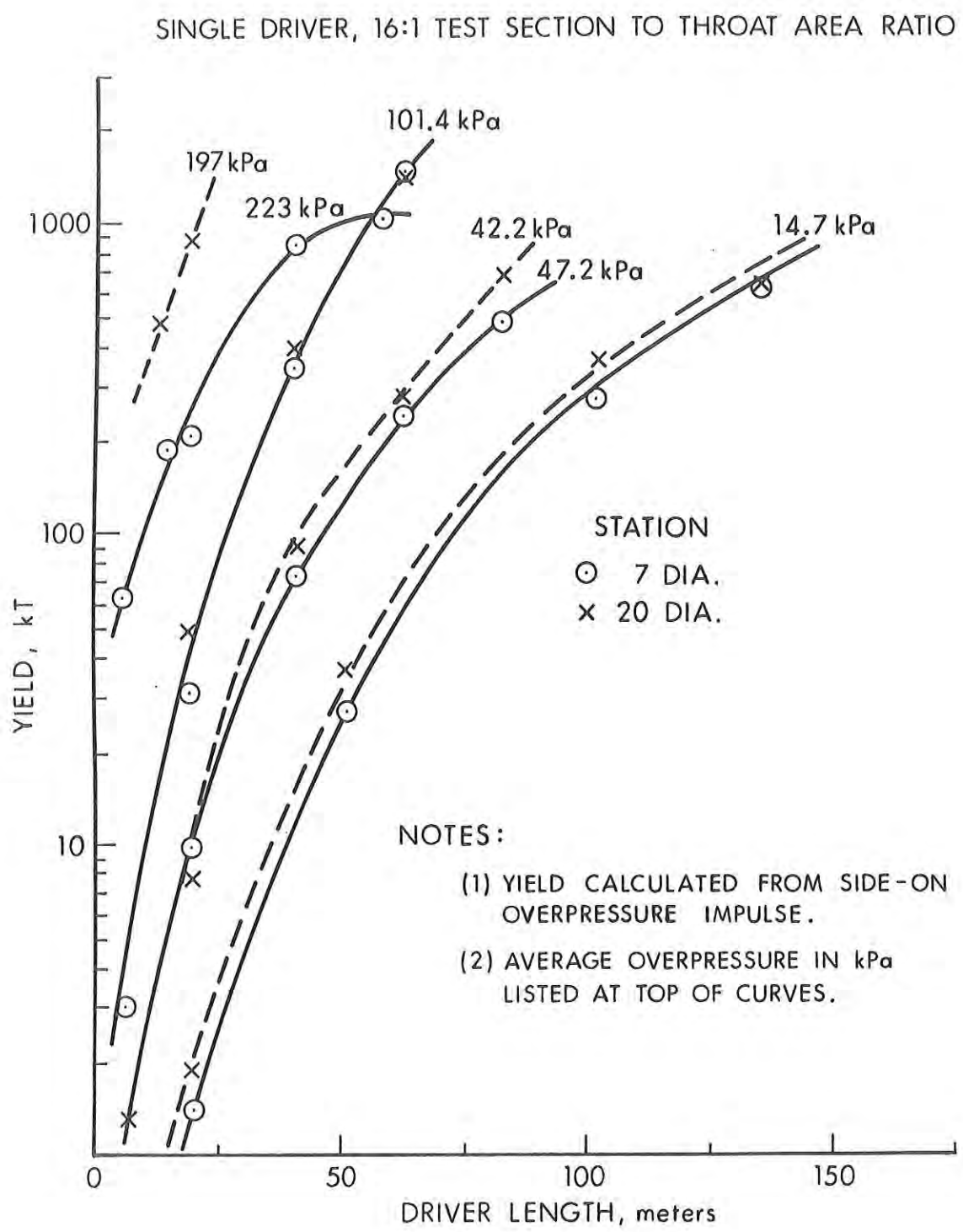

Figure 32. Predicted Yield as a Function of Driver Length, 16:1 Throat Ratio.

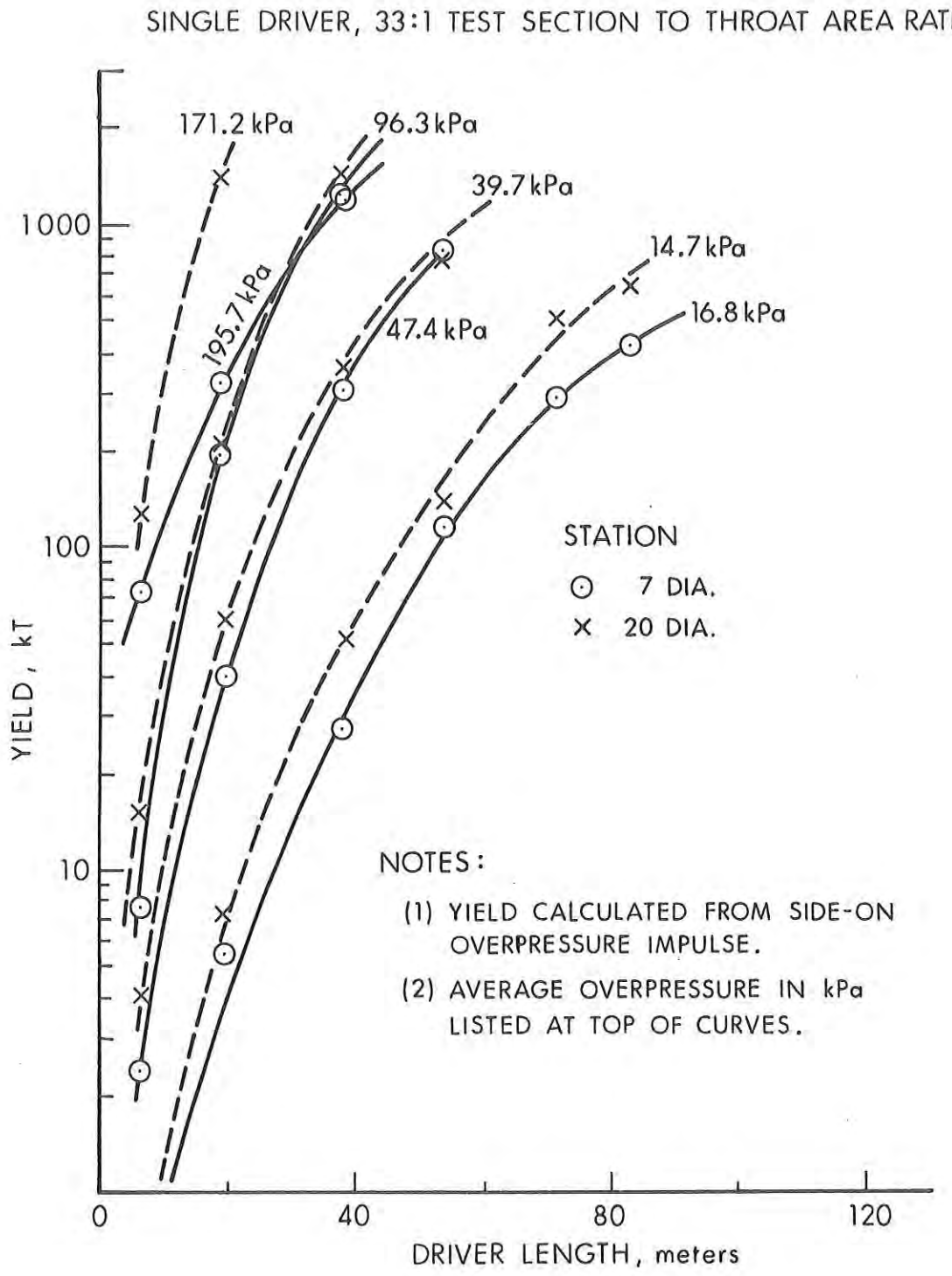

Figure 33. Predicted Yield as a Function of Driver Length, 33:1 Throat Ratio.

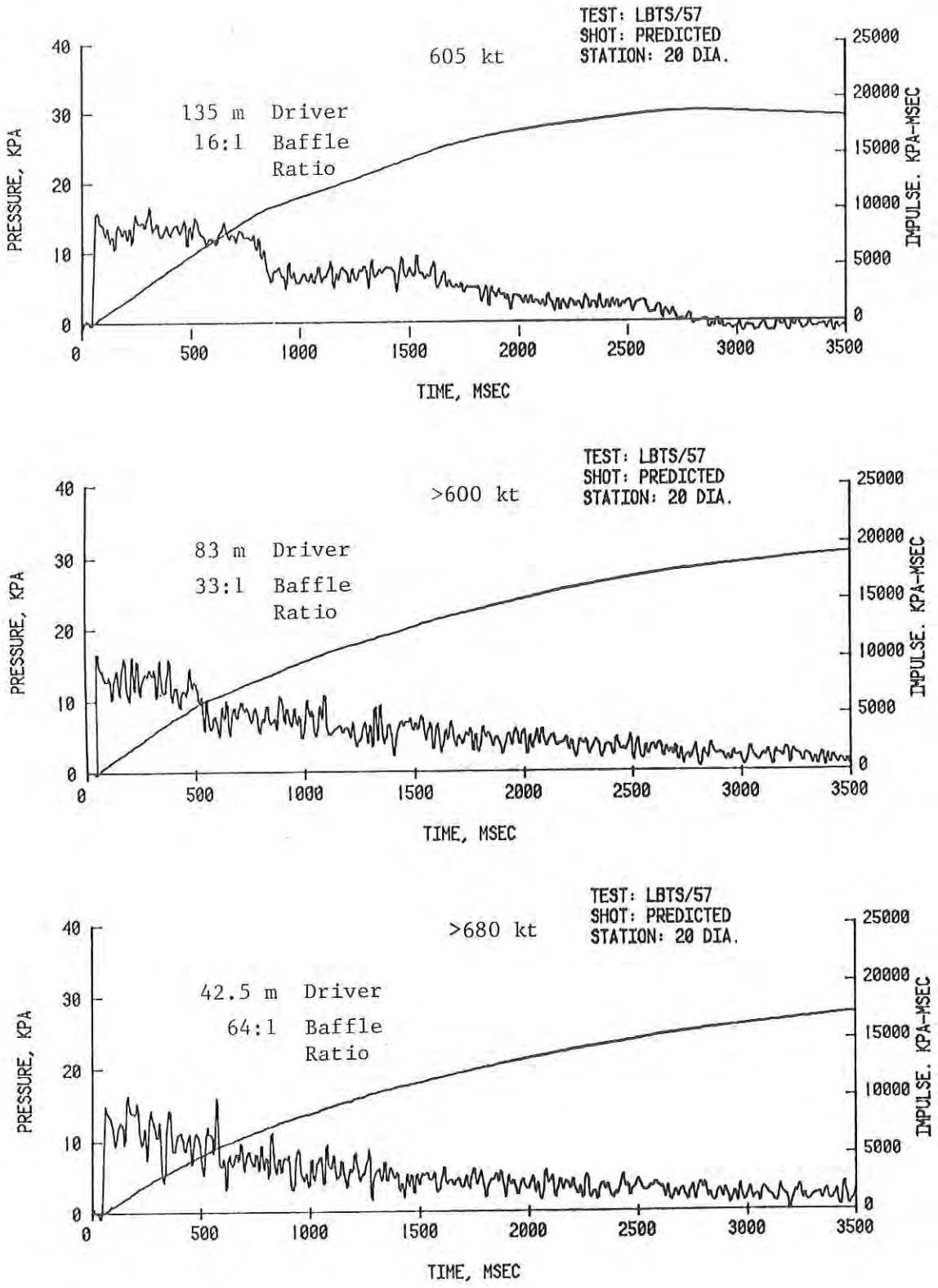

Figure 34. Experimental Baffle Effects Scaled to Full-Size.

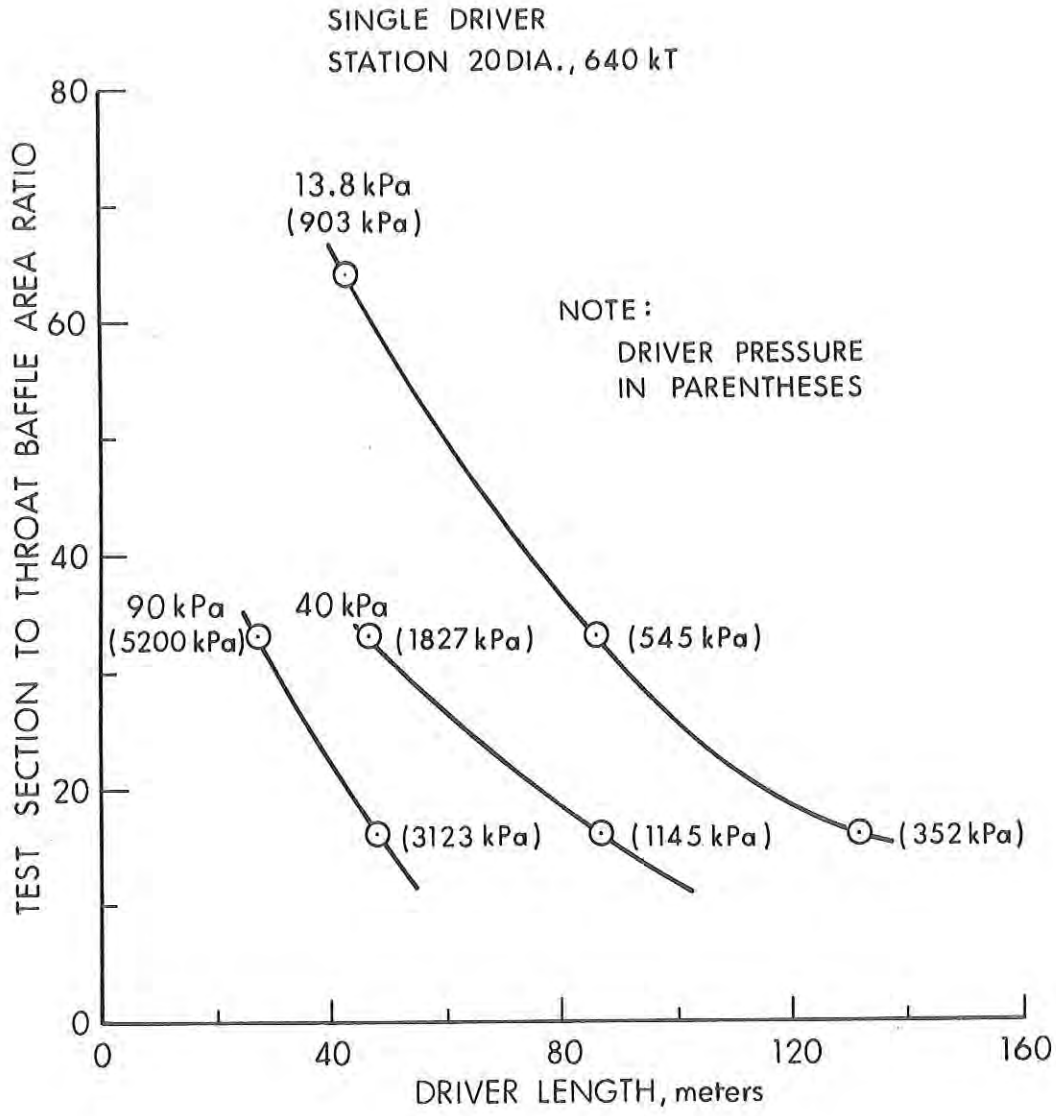

Figure 35. Effect of Throat Baffle on Driver Length.

Thermal effects were not a part of this study. BRL has the task of preparing a design for the Army of a large simulator capable of full-size multiservice equipment tests to simulate the blast and thermal effects from nuclear events. The experiments and code comparisons reported here were designed to give insight into a number of blast parameters fundamental to the design of such a simulator.

Parameters studied were: blast wave decay, overpressure in the test section as a function of driver pressure, blast wave duration and impulse as a function of driver/throat baffle configuration, and effects of the cold air driver gas/recompression fan arrival at a particular test station.

It was concluded that a station at 20 test section diameters was needed to minimize the cold gas/recompression fan effects, at test station pressures of, and above, 100 kPa. A pressure decay problem was also evident above this pressure for low yields (short duration, blast waves). This could be corrected with the use of still higher driver pressures. The suggested preliminary large simulator design had not provided for these higher pressures.

A heated driver to replace the cold driver design should probably be considered. Nearer test stations might possibly be utilized in the heater driver design. Acceptable levels of recompression fan and peak pressure decay effects, hopefully, could be obtained with such a design. Cold gas effects would, of course, have been eliminated by the heated driver. Throat baffles would still be needed to minimize the driver length at the low pressure/high yield end of the simulator's operating range.

The BRL-Q1D code was quite helpful in predicting the general waveforms for the various driver/baffle configurations tested. The predicted enhancement of the drag because of cold gas/recompression fan effects from the code were higher than actually measured. Also, the code predicted more test time to be available before the cold gas or recompression fan arrived at a given test station. The Q1D code did furnish some helpful guidelines for a very complicated blast parameter study; it did it efficiently and at a low cost. Further computations utilizing two-dimensional hydrocodes, accounting for the real gas effects present experimentally, would of course, provide better experimental agreement. This would be done at greater costs in both computing time and effort, however.

LIST OF REFERENCES

1. Crosnier, J. R. and Monsac, J. B. G., "Large Diameter High Performanc Blast Simulator," Seventh MABS, Medicine Hat, Alberta, Canada, 13-17 July 1981.

2. Kingery, Charles N. and Coulter, George A., "Rarefaction Wave Eliminator Concepts for a Large Blast/Thermal Simulator," BRL-TR-2634, Ballistic Research Laboratory, Aberdeen Proving Ground, MD, February 1985 (AD A153073).

3. Hisley, Dixie M., Gion, Edmund J., and Bertrand, Brian P., "Performance and Predictions for a Large Blast Simulator Model," BRL-TR-2647, Ballistic Research Laboratory, Aberdeen Proving Ground, MD, April 1985.

4. Opalka, Klaus O. and Mark, A., "The BRL-Q1D Code: A Tool for the Numerical Simulation of Flows in Shock Tubes with Variable Cross-Sectional Area," BRL-TR-2763, Ballistic Research Laboratory, Aberdeen Proving Ground, MD, October 1986.

5. Coulter, George A., Bulmash, Gerald, and Kingery, Charles, "Feasibility Study of Shock Wave Modification in the BRL 2.44 m Blast Simulator," ARBRL-MR-03339, Ballistic Research Laboratory, Aberdeen Proving Ground, MD, March 1984 (AD A139631).

6. "Quartz Sensors," Catalog 884, PCB Piezotronics, Inc., Depew, NY, 1984.

7. Coulter, George A., Bulmash, Gerald and Kingery, Charles N. "Experimental and Computational Mdoeling of Rarefaction Wave Eliminators Suitable for the BRL 2.44 m Shock Tube," ARBRL-TR-02503, Ballistic Research Laboratory, Aberdeen Proving Ground, MD, June 1983 (AD A131894).

8. Jordan, Douglas and Welsh, Leland M., "Blast Effects Program for the IBM PC and PC/XT, Version 2.1," Report No. DNA-EH-84-02-G, HTI-5DR-84-227, Defense Nuclear Agency, Washington, DC 20305-1000, December 7, 1984.

9. Gladstone, Samuel and Dolan, Philip J. - Editors, "The Effects of Nuclear Weapons," Department of Army Pamphlet No. 50-3, HQ, Department of Army, March 1977.

DISTRIBUTION LIST

No. of Copies	Organization
12	Administrator Defense Technical Info Center ATTN: DTIC-FDAC Cameron Station Alexandria, VA 22304-6145
1	Office Secretary of Defense ADUSDRE (R/AT) (ET) ATTN: Mr. J. Persh, Staff Specialist, Materials and Structures Washington, DC 20301
1	Under Secretary of Defense for Research and Engineering Department of Defense Washington, DC 20301
1	Director of Defense Research and Engineering Washington, DC 20301
1	Assistant Secretary of Defense (Atomic Energy) ATTN: Document Control Washington DC 20301
1	Assistant Secretary of Defense (MRA&L) ATTN: EO&SP Washington, DC 20301
1	Director Defense Advanced Research Projects Agency 1400 Wilson Boulevard Arlington, VA 22209
1	Director Defense Intelligence Agency ATTN: DT-1B, Dr. J. Vorona Washington, DC 20301
2	Chairman Joint Chiefs of Staff ATTN: J-3, Operations J-5, Plans & Policy (R&D Division) Washington, DC 20301
4	Director Defense Nuclear Agency ATTN: SPTD, Mr. T.E.Kennedy DDST (E), Dr. E.Sevin OALG, Mr. T.P.Jeffers LEEE, Mr. J. Eddy Washington, DC 20305
1	Commander Field Command Defense Nuclear Agency ATTN: Tech Lib, FCWS-SC Kirtland AFB, NM 87115
1	Chairman Department of Defense Explosives Safety Board 2461 Eisenhower Avenue Alexandria, VA 22331
1	HQDA (DAMA-ART-M) Washington, DC 20310
1	HQDA (DAEN-ECE-T/ Mr. R. L. Wright) Washington, DC 20310
1	HQDA (DAEN-MCC-D, Mr. L. Foley) Washington, DC 20310
1	HQDA (DAEN-RDL, Mr. Simonini) Washington, DC 20310
1	HQDA (DAEN-RDZ-A, Dr. Choromokos) Washington, DC 20310
1	HQDA (DALO-SMA) ATTN: COL W. F. Paris II Washington, DC 20310
1	HQDA (DAMA-CSM-CA) Washington, DC 20310
1	HQDA (DAMA-AR; NCL Div) Washington, DC 20310

DISTRIBUTION LIST

No. of Copies	Organization
1	HQDA (DAMA-NCC, COL R. D. Orton) Washington, DC 20310
1	HQDA (DAPE-HRS) Washington, DC 20310
3	Director Institute for Defense Analyses ATTN: Dr. H. Menkes Dr. J. Bengston Tech Info Ofc 1801 Beauregard St. Alexandria, VA 22311
1	Commander US Army Ballistic Missile Defense Systems Command ATTN: J. Veeneman P. O. Box 1500, West Station Huntsville, AL 35807
1	Director US Army Ballistic Missile Defense Systems Command Advanced Technology Center ATTN: M. Whitfield P. O. Box 1500 Huntsville, AL 35807-3801
2	Director US Army Engineer Waterways Experimental Station ATTN: WESNP K. Davis P. O. Box 631 Vicksburg, MS 39180-0631
1	Commander US Army Materiel Command ATTN: AMCDRA-ST 5001 Eisenhower Avenue Alexandria, VA 22333-0001
1	Commander US Army Materiel Command ATTN: AMCSF 5001 Eisenhower avenue Alexandria, VA 22333-0001
2	Commander US Army Armament Material Readiness Command ATTN: Joint Army-Navy-Air Force Conventional Ammunition Prof Coord GP/El Jordan Rock Island, IL 61299
1	Commander US Army Armament Research, Development and Engineering Center ATTN: SMCAR-MSI Dover, NJ 07801-5001
2	Commander US Army Armament Research, Development and Engineering Center ATTN: SMCAR-TDC SMCAR-LCM-SPC Dover, NJ 07801-5001
1	Commander US Army Development and Employment Agency ATTN: MODE-ORO Fort Lewis, WA 98433-5000
1	Commander US Army Armament, Munitions and Chemical Command ATTN: AMSMC-IMP-L Rock Island, IL 61299-7300
1	Commander Pine Bluff Arsenal Pine Bluff, AR 71601

DISTRIBUTION LIST

No. of Copies	Organization
1	Commander US Army Rock Island Arsenal Rock Island, IL 61299
1	Commanding General US Army Armament Command ATTN: AMSAR-SA Rock Island Arsenal Rock Island, IL 61201
1	Commander US AMCCOM ARDEC CCAC Benet Weapons Laboratory ATTN: SMCAR-CCB-TL Watervliet, NY 12189-4050
1	Commander Indiana Army Ammunition Plant Charlestown, IN 47111
1	Commander Joliet Army Ammunition Plant Joliet, IL 60436
1	Commander Kansas Army Ammunition Plant Parsons, KS 67357
1	Commander Lone Star Army Ammunition Plant Texarkana, TX 75502
1	Commander Longhorn Army Ammunition Plant Marshall, TX 75671
1	Commander Louisiana Army Ammunition Plant Shreveport, LA 71102
1	Commander Milan Army Ammunition Plant Milan, TN 38358
1	Commander Radford Army Ammunition Plant Radford, VA 24141
1	Commander Ravenna Army Ammunition Plant Ravenna, OH 44266
1	Commander US Army Aviation Systems Command ATTN: AMSAV-ES 4300 Goodfellow Blvd St. Louis, MO 63120-1798
1	Director US Army Aviation Research and Technology Activity Ames Research Center Moffett Field, CA 94035-1099
2	Director Lewis Directorate US Army Air Mobility Research and Development Laboratory Lewis Research Center ATTN: Mail Stop 77-5 21000 Brookpark Road Cleveland, OH 44135
1	Commander US Army Communications - Electronics Command ATTN: AMSEL-ED Fort Monmouth, NJ 07703-5301
1	Commander CECOM R&D Technical Library ATTN: AMSEL-IM-L (Reports Section) B. 2700 Fort Monmouth, NJ 07703-5000
1	Commander US Army Harry Diamond Lab. ATTN: SLCHD-TI 2800 Powder Mill Road Adelphi, MD 20783-1197

DISTRIBUTION LIST

No. of Copies	Organization
1	Director AMC, ITC ATTN: Dr. Chiang Red River Depot Texarkana, TX 75501
1	Commander US Army Missile Command ATTN: AMSMI-R, Mr. Rob Cobb Redstone Arsenal, AL 35898
1	Commander US Army Missile Command Research, Development, and Engineering Center ATTN: AMSMI-RD Redstone Arsenal, AL 35898-5245
1	Commander US Army Missile Command ATTN: AMSMI-RR, Mr. L. Lively Redstone Arsenal, AL 38598
1	Commander US Army Missile Command ATTN: AMSMI-RX, M. W. Thauer Redstone Arsenal, AL 35898-5249
1	Director US Army Missile and Space Intelligence Center ATTN: AIAMS-YDL Redstone Arsenal, AL 35898-5500
1	Commander US Army Natick Research and Development Laboratories ATTN: AMDNA-D, Dr. D. Seiling Natick, MA 01760
1	Commander US Army Tank Automotive Command ATTN: AMSTA-TSL Warren, MI 48397-5000
1	Commander Dugway Proving Ground ATTN: STEDP-TO-H, Mr. Miller Dugway, UT 84022
1	Commander US Army Foreign Science and Technology Center ATTN: Research & Data Branch Federal Office Building 220-7th Street, NE Charlottesville, VA 22901
1	Commander US Army Laboratory Command Materials Technology Laboratory ATTN: AMXMR-ATL Watertown, MA 02172-0001
1	Commander US Army Research Office P. O. Box 12211 Research Triangle Park NC 27709-2211
1	Commander US Army Engineer Div. Europe ATTN: EUDED, Dr. Roger Crowson APO New York, NY 09757
1	Division Engineer US Army Engineer Division Fort Belvoir, VA 22060
1	US Army Engineer Division ATTN: Mr. Char P. O. Box 1600 Huntsville, AL 35807
1	Commandant US Army Engineer School ATTN: ATSE-CD Fort Belvoir, VA 22060

DISTRIBUTION LIST

No. of Copies	Organization
1	Commander US Army Construction Engineering Research Lab P. O. Box 4005 Champaign, IL 61820
1	Director US Army TRADOC System Analysis Activity ATTN: ATOR-TSL White Sands Missile Range, NM 88002-5502
1	Commandant US Army Infantry School ATTN: ATSH-CD-CS-OR Fort Benning, GA 31905-5400
3	Commander US Army Belvoir Research and Development Center ATTN: STRBE-NN Fort Belvoir, VA 22060-5606
1	Assistant Secretary of the Navy (Research and Development) Navy Development Washington, DC 20350
3	Chief of Naval Operation ATTN: OP-411, C. Ferraro, Jr. CPT R. L. Wernsman OP-41B Washington, DC 20350
1	Commander Naval Air Systems Command ATTN: AIR 532 Washington, DC 20360
1	Commander Naval Facilities Engineering Command ATTN: Code 04T5 Washington, DC 22360
1	Commander Naval Sea Systems Command ATTN: SEA-Q6H M. R. Van Slyke Washington, DC 20362
1	Commander Naval Sea Systems Command ATTN: SEA-0333 Washington, DC 20362
2	Commander David W. Taylor Naval Ship Research and Development Center ATTN: Mr. A. Wilner, Code 1747 Mr. W. W. Murray, Code 17 Bethesda, MD 20084-5000
1	Commander Naval Ship Research and Development Center ATTN: Mr. Lowell T. Butt Underwater Explosions Research Division Portsmouth, VA 23709
1	Commander Naval Surface Weapons Center Dahlgren Laboratory ATTN: E-23, Mr. J. J. Walsh Dahlgren, VA 22448
3	Commander Naval Surface Weapons Center ATTN: Dr. Leon Schindel Dr. Victor Dawson Dr. P. Huange Silver spring, MD 20902-5000
2	Commander Naval Surface Weapons Center White Oak Laboratory ATTN: R-15, Mr. M. M. Swisdak Mr. W. D. Smith III Silver Spring, MD 20902-5000

DISTRIBUTION LIST

No. of Copies	Organization
1	Commander Naval Weapons Center ATTN: Code 0632, Mr. G. Ostermann China Lake, CA 93555
1	Commanding Officer Naval Weapons Support Center (Code 502) Crane, IN 47522
1	Officer-in-Charge Naval EOD Facility ATTN: Code D, Mr. L. Dickenson Indian Head, MD 20640
1	Commander Naval Weapons Evaluation Facility ATTN: Document Control Kirtland AFB Albuquerque, NM 87117
1	Commander Naval Research Laboratory ATTN: Code 2027, Tech 11b Washington, DC 20375
1	Officer-in-Charge (Code L31) Civil Engineering Laboratory ATTN: Code L51, Mr. W. A. Keenan Naval Construction Battalion Center Port Hueneme, CA 93041
1	HO USAF (AFNIE-CA) Washington, DC 20330
3	HQ USAF (AFRIDQ; AFRODXM; AFRDPM) Washington, DC 20330
1	Air Force Systems Command ATTN: IGFG Andrews AFB Washington, DC 20334

No. of Copies	Organization
1	AFTAWC (OA) Eglin AFB, FL 32542
1	Air Force Armament Laboratory ATTN: AFATL/DOIL (Technical Information Center) Eglin AFB, FL 32542-5438
1	Commander Air Force Armament Laboratory ATTN: DLYV, Mr. R. L. McGuire Eglin AFB, FL 32542
1	AFRPL Edwards AFB, CA 93523
1	Ogden ALC/MMWRE ATTN: (Mr. Ted E. Comins) Hill AFB, UT 84056
1	AFWL/SUL Kirtland AFB, NM 87117
1	Director of Aerospace Safety HQ, USAF ATTN: JDG/AFISC (SEVV), COL J. E. McQueen Norton AFB, CA 92409
2	HQ, USAF ATTN: IDG/AFISC, (SEW) W. F. Gavitt, Jr. (SEV) Mr. K. R. Gopher Norton AFB, CA 92409
2	Director Joint Strategic Target Planning Staff ATTN: JLTW; TPTP OFFUTT AFB Omaha, NE 68113
1	HQ AFESC/RDC Walter Buckholtz Tyndall AFB, FL 32403

DISTRIBUTION LIST

No. of Copies	Organization
1	AFESC/RDC Tyndall AFB, FL 32403
3	AFML (LNN, Dr. T. Nicholas; MAS; MBC, Mr. D. Schmidt) Wright-Patterson AFB, OH 45433
1	AFWAL Wright-Patterson AFB, OH 45433
2	AFLC (MMWM/CPT D. Rideout; IGYE/K. Shopker) Wright-Patterson AFB, OH 45433
1	FTD (ETD) Wright-Patterson AFB, OH 45433
1	Headquarters Department of Energy Office of Military Application Washington, DC 20545
1	Director Office of Operational and Environmental Safety US Department of Energy Washington, DC 20545
1	Albuquerque Operations Office US Department of Energy ATTN: Div. of Operational Safety P. O. Box 5400 Albuquerque, NM 87115
1	Director AMC Field Safety Activity ATTN: AMXOS-OES Charlestown, IN 47111-9669
1	Mr. Richard W. Watson Director, Pittsburgh Mining & Safety Research Center Bureau of Mine, Dept of the Interior 4800 Forbes Avenue Pittsburgh, PA 15213
1	Director Lawrence Livermore Laboratory Technical Information Division P. O. Box 808 Livermore, CA 94550
1	Director Los Alamos Scientific Lab ATTN: Dr. J. Taylor P. O. Box 1663 Los Alamos, NM 87544
2	Director Sandia National Laboratories ATTN: Info Dist Div Dr. W. A. von Riesemann (Div 6442) Albuquerque, NM 87115
1	Director National Aeronautics and Space Administration George C. Marshall Space Flight Center Huntsville, AL 35812
2	Director National Aeronautics and Space Administrtion Aerospace Safety Research and Data Institute 21000 Brook Park Road Lewis Research Center Cleveland, OH 44135

DISTRIBUTION LIST

No. of Copies	Organization
1	Director National Aeronautics and Space Administration Scientific and Technical Information Facility P. O. Box 8757 Baltimore/Washington International Airport, MD 21240
1	National Academy of Science ATTN: Mr. D. G. Groves 2101 Constitution Avenue, NW Washington, DC 20418
10	Central Intelligence Agency OIR/DB/Standard GE47 HQ Washington, DC 20505
1	DNA Information and Analysis Center Kaman Tempo ATTN: DASIAC 816 State Street P.O. Drawer QQ Santa Barbara, CA 93102
1	Institute of Makers of Explosives ATTN: Mr. F. P. Smith, Jr., Executive Director 1575 Eve St., N.W., Suite 550 Washington, DC 20005
1	Aberdeen Research Center ATTN: Mr. John Keefer 30 Diamond St. P. O. Box 548 Aberdeen, MD 21001
1	Agbabian Associates ATTN: Dr. D. P. Reddy 250 N. Nash Street El Segundo, CA 90245
1	Ammann & Whitney ATTN: Mr. N. Dobbs Suit 1700 Two World Trade Center New York, NY 10048
1	Black & Veatch Consulting Engineers ATTN: Mr. H. L. Callahan 1500 Meadow Lake Parkway Kansas City, MO 64114
1	Dr. Wilfred E. Baker Wilfred Baker Engineering P. O. Box 6477 San Antonio, TX 78209
1	Aeronautical Research Associates of Princeton, Inc. ATTN: Dr. C. Donaldson 50 Washington Road, P.O.Box 2229 Princeton, NJ 08540
1	Applied Research Associates, Inc. ATTN: Mr. J. L. Drake 1204 Openwood Street Vicksburg, MS 39180
1	J. G. Engineering Research Associates 3831 Menlo Drive Baltimore, MD 21215
2	Kaman-AviDyne ATTN: Dr. N.P.Hobbs Mr. S. Criscione Northwest Industrial Park 83 Second Avenue Burlington, MA 01803
3	Kaman-Nuclear ATTN: Dr. F. H. Shelton Dr. D. Sachs Dr. R. Keffe 1500 Garden of the Gods Road Colorado Springs, CO

DISTRIBUTION LIST

No. of Copies	Organization
1	Knolls Atomic Power Laboratory ATTN: Dr. R. A. Powell Schenectady, NY 12309
1	McDonnell Douglas Astronautics Western Division ATTN: Dr. Lea Cohen 5301 Bosla Avenue Huntington Beach, CA 92647
1	Physics International 2700 Merced Street San Leandro, CA 94577
1	R&D Associates ATTN: Mr. John Lewis P. O. Box 9695 Marina del Rey, CA 90291
1	R&D Associates ATTN: G. P. Ganong P. O. Box 9335 Albuquerque, NM 87119
2	The Boeing Company Aerospace Division ATTN: Dr. Peter Grafton Dr. D. Strome Mail Stop 8C-68 P. O. Box 3707 Seattle, WA 98124
2	AVCO Corporation Structures and Mechanics Dept. ATTN: Dr. William Broding Dr. J. Gilmore 201 Lowell Street Wilmington, MA 01887
1	Aerospace Corporation P.O. Box 92957 Los Angeles, CA 90009
1	General American Transportation Corp. General American Research Div. ATTN: Dr. J. C. Shang 7449 N. Natchez Avenue Niles, IL 60648
1	Hercules, Inc. ATTN: Billings Brown Box 93 Magna, UT 84044
1	Mason & Hanger-Silas Mason Co., Inc. Plantex Plant P. O. Box 647 Amarillo, TX 79117
1	Lovelace Research Institute ATTN: Dr. E. R. Fletcher P. O. Box 5890 Albuquerque, NM 87115
1	Massachusetts Institute of Technology Aeroelastic and Structures Research Laboratory ATTN: Dr. E. A. Witmar Cambridge, MA 02139
1	Monsanto Research Corporation Mound Laboratory ATTN: Frank Neff Miamisburg, OH 45342
1	Science Applications, Inc. Suite 310 1216 Jefferson Davis Highway Arlington, VA 22202
2	Battelle Memorial Institute ATTN: Dr. L. E. Hulbert Mr. J. E. Backofen, Jr. 505 King Avenue Columbus, OH 43201
1	Georgia Institute of Tech ATTN: Dr. S. Atluri 225 North Avenue, NW Atlanta, GA 30332
1	IIT Research Institute ATTN: Mrs. H. Napadensky 10 West 35 Street Chicago, IL 60616

DISTRIBUTION LIST

No. of Copies	Organization
2	Southwest Research Institute ATTN: Dr. H. N. Abramson Dr. U. S. Lindholm 8500 Culebra Road San Antonio, TX 78228
1	Brown University Division of Engineering ATTN: Prof. R. Clifton Providence, RI 02912
1	Florida Atlantic University Dept. of Ocean Engineering ATTN: Prof. K. K. Stevens Boca Raton, FL 33432
1	Texas A&M University Department of Aerospace Engineering ATTN: Dr. James A. Stricklin College Station, TX 77843
1	University of Alabama ATTN: Dr. T. L. Cost P. O. Box 2908 University, AL 35486
1	University of Delaware Department of Mechanical and Aerospace Engineering ATTN: Prof. J. R. Vinson Newark, DE 19711

Aberdeen Proving Ground

Dir, USAMSAA
ATTN: AMXSY-D
AMXSY-MP, H. Cohen
Cdr, USATECOM
ATTN: AMSTE-SI-F
Cdr, CRDC, AMCCOM
ATTN: SMCCR-RSP-A
SMCCR-MU
SMCCR-SPS-IL
Cdr, US Army Toxic and Hazardous Materials Agency
ATTN: AMXTH-TE

USER EVALUATION SHEET/CHANGE OF ADDRESS

This Laboratory undertakes a continuing effort to improve the quality of the reports it publishes. Your comments/answers to the items/questions below will aid us in our efforts.

1. BRL Report Number _____ Date of Report _____

2. Date Report Received _____

3. Does this report satisfy a need? (Comment on purpose, related project, or other area of interest for which the report will be used.) _____

_____

_____

4. How specifically, is the report being used? (Information source, design data, procedure, source of ideas, etc.) _____

_____

_____

5. Has the information in this report led to any quantitative savings as far as man-hours or dollars saved, operating costs avoided or efficiencies achieved, etc? If so, please elaborate. _____

_____

_____

6. General Comments. What do you think should be changed to improve future reports? (Indicate changes to organization, technical content, format, etc.)

_____

_____

_____

CURRENT ADDRESS

_____
Name

_____
Organization

_____
Address

_____
City, State, Zip

7. If indicating a Change of Address or Address Correction, please provide the New or Correct Address in Block 6 above and the Old or Incorrect address below.

OLD ADDRESS

_____
Name

_____
Organization

_____
Address

_____
City, State, Zip

(Remove this sheet, fold as indicated, staple or tape closed, and mail.)

FOLD HERE

Director
US Army Ballistic Research Laboratory
ATTN: DRXBR-OD-ST
Aberdeen Proving Ground, MD 21005-5066

NO POSTAGE
NECESSARY
IF MAILED
IN THE
UNITED STATES

OFFICIAL BUSINESS
PENALTY FOR PRIVATE USE, $300

BUSINESS REPLY MAIL
FIRST CLASS PERMIT NO 12062 WASHINGTON, DC
POSTAGE WILL BE PAID BY DEPARTMENT OF THE ARMY

Director
US Army Ballistic Research Laboratory
ATTN: DRXBR-OD-ST
Aberdeen Proving Ground, MD 21005-9989

FOLD HERE